uOttawa

L'Université canadienne
Canada's university

FACULTÉ DES ÉTUDES SUPÉRIEURES ET POSTOCTORALES

uOttawa

L'Université canadienne
Canada's university

FACULTY OF GRADUATE AND POSDOCTORAL STUDIES

Rida Al Osman

AUTEUR DE LA THÈSE / AUTHOR OF THESIS

M.Sc. (Systems Science)

GRADE / DEGREE

Systems Science

FACULTÉ, ÉCOLE, DÉPARTEMENT / FACULTY, SCHOOL, DEPARTMENT

Development of "AlarmLocator" A Computerized Model for Predicting Optimum Number, Location, and Power Level of Acoustic Warning Devices in Noisy Work Plants

TITRE DE LA THÈSE / TITLE OF THESIS

Professor Christian Giguère

DIRECTEUR (DIRECTRICE) DE LA THÈSE / THESIS SUPERVISOR

Professor Chantal Laroche

CO-DIRECTEUR (CO-DIRECTRICE) DE LA THÈSE / THESIS CO-SUPERVISOR

EXAMINATEURS (EXAMINATRICES) DE LA THÈSE / THESIS EXAMINERS

Professor T. Aboulnasr

Professor M. Bouchard

Gary W. Slater

Le Doyen de la Faculté des études supérieures et postdoctorales / Dean of the Faculty of Graduate and Postdoctoral Studies

Development of "AlarmLocator" –

A Computerized Model for Predicting the Optimum Number, Location, and Power Level of Acoustic Warning Devices in Noisy Work Plants

Rida Al Osman

A THESIS SUBMITTED TO THE FACULTY OF
GRADUATE AND POSTDOCTORAL STUDIES IN
PARTIAL FULFILMENT OF THE REQUIREMENTS
FOR THE DEGREE OF
MASTER OF SCIENCE SYSTEMS SCIENCE
UNIVERSITY OF OTTAWA

Supervised by:

Dr. Christian Giguère
Associate Professor
Audiology/Speech Language Pathology Program, School of Rehabilitation Sciences, University of Ottawa

Dr. Chantal Laroche
Associate Professor
Audiology/Speech Language Pathology Program, School of Rehabilitation Sciences, University of Ottawa

Your file Votre référence
ISBN: 978-0-494-32431-8
Our file Notre référence
ISBN: 978-0-494-32431-8

Acknowledgements

I would like to express my sincere appreciation to my thesis supervisors, Dr. Christian Giguère and Dr. Chantal Laroche, for their generous guidance and great support throughout my research project.

I would also like to thank my parents, my brothers, Hussein and Firas, for their moral support.

Table of Contents

Abstract

Acoustic warning signals are necessary to promptly alert workers of events which can compromise safety. Failure to react to warning signals can increase the risk of accidents in the workplace. Unfortunately, the use of warning signals in industry is poorly regulated and submitted to intuitive installation practices, often with little regard to the many factors contributing to an efficient use. This research presents the development of a new software tool called "AlarmLocator" to automate the process of installing auditory warning devices in a given setting, in terms of the characteristics of the devices to use and their optimal location in the plant. The software tool, when use in combination with psychoacoustic model "Detectsound" (Zheng et al., 2006), produces a solution to two practical installation problems: (1) selecting a suitable number of warning devices and acoustic power for a given work area, and (2) specifying the location of the devices in the plant in such a way that the signals emitted are clearly audible by all workers at all workstations. Thus, a solution to the problem of installing warning devices is provided in a format that can be easily understood and used in the workplace. A simple hybrid method, combining the mirror image technique and the classical room acoustics theory was used in this research to compute the sound pressure level generated by acoustic alarm devices. The former technique accounts for wall-placement directivity effects by using a relatively low order of virtual sources to simulate early reverberation. The classical theory of room acoustics is used for late reverberation. The method only requires specification of the overall room dimensions and the estimated or measured reverberation time; however it is currently limited to rectangular-shaped rooms. It was validated in a classroom at the University of Ottawa to verify that sound pressure level predictions by "AlarmLocator" would provide realistic solutions of optimal installation of acoustic warning devices in the workplace. The validation was carried out over 125 arrangements (source, receiver, frequency) and average errors of 0.15 and 2.2 dB were noted for estimated and measured reverberation time conditions. This is well within the design range (13 dB) for the warning sound level window under "Detectsound".

[Work funded by a research grant provided by the Workplace Safety and Insurance Board (Ontario)].

Chapter 1. Introduction

Acoustic warning devices and alarms have been in existence since the dawn of mankind. For example, bell ringing and drum beating were used during early military operations to alert troops or units of danger. With technological advancement and the industrial revolution, acoustic signaling has been used in numerous fields to serve different purposes, including police and ambulance sirens, railway crossings, car alarms, fire alarms and various workplace warning devices.

In the workplace, acoustic warning devices are essential to promptly alert workers of imminent danger (Wilkins & Acton, 1982; Zheng et al., 2006). However, the installation of warning devices in noisy settings poses particular challenges for optimal detection and recognition of acoustics signals (Giguère et al., 2003), such as the use of adequate sound levels. A low level warning signal can easily be masked by the background noise, thereby leading to potential accidents caused by a failure for workers to detect the warning signal (Wilkins & Acton, 1982; Suter, 2002; Zheng et al., 2006). In contrast, excessively loud warning signals may elicit startle reflex for the workers, impede verbal communication in the critical moments following the onset of the alarm and cause hearing damage.

Warning signals in the workplace should allow workers to hear and promptly react to the intended signal (ISO 7731, 2003). The optimal design and installation of warning devices in a noisy environment often requires complex calculations taking many critical parameters into consideration (Zheng et al., 2006). A software tool, "AlarmLocator", was developed to provide an outline for improvements on health and safety of workers in noisy industrial workplaces by allowing its users to predict the optimal number, location and sound power of warning devices in the workplace, thereby providing huge benefits in industrial settings. Combined with the psychoacoustic tool "Detectsound" (Zheng, 2003; Zheng et al., 2006), it is hoped that this new tool can not only help decrease the risk of accidents caused by failure to react to weak warning signals, but also assist in protecting workers from hearing damage caused by excessively loud warning signals.

1.1 Noise and workplace safety

Noise is considered as one of the main hazardous factors in the workplace. Exposure to excessive noise may not only cause hearing loss; but can also result in several

psychological and physiological problems, as documented in the literature (Ward et al., 2000; Berglund et al., 2000). Indeed, noise-induced hearing loss is often accompanied by other long-term auditory effects in exposed workers, such as tinnitus (ringing in the ears), hyperacusis (increased sensitivity to loud noise) and reduced frequency selectivity (decreased ability to hear sounds in background noise) (Laroche et al., 1992; Hétu and Tran Quoc, 1994; Suter, 2002).

Ensuring safety in noisy workplaces is quite challenging. For instance, all workers must be able to hear, in the presence of background noise, acoustic signals warning them of an emergency, the presence of hazardous events or other circumstances requiring their immediate attention. Employees must also be able to communicate orally with other personnel during the course of dangerous events in order to react appropriately. In addition, such tasks must be carried out by workers wearing hearing protectors and those suffering hearing loss.

1.2 Audibility of warning sounds

The audibility of warning signals is dependent on the individual's hearing status (auditory thresholds, frequency selectivity), the noise field (level, spectrum) in the work area, the frequency and temporal characteristics of the warning sounds, as well as the attenuation provided by hearing protectors. Although hearing protectors can minimize the adverse effects of background noise in the workplace, they can also compromise the audibility of acoustic warning signals (Wilkins & Acton, 1982; Suter, 1989). Indeed, hearing protector standards, such as CSA Z94.2-02, warn against the potential problem of overprotection when fitting hearing protector devices (HPDs) to prevent disrupting speech communication between workers and the audibility of warning sounds. However, only broad recommendations are provided and it is not possible to make detailed analyses for specific situations.

Acoustic standard ISO 7731 (Danger signals for public and work areas) presents a set of guidelines to determine the sound level an alarm should produce at a given workstation. A software tool, "Detectsound", was also previously developed to determine whether the sound pressure level and spectrum of an acoustic warning signal satisfy the constraints for optimal detection and recognition by attending workers at any given workstation

(Zheng et al., 2006). This tool takes into consideration the effects of HPD as well as the workers' hearing status. "Detectsound" is particularly useful when assessing the suitability of existing alarm systems, where the alarm's sound level can be measured at each workstation. Unfortunately, these two tools do not provide a specific method to guide installation of acoustic warning devices on walls or ceiling in the work plant.

1.3 Installation of auditory warning devices in the workplace

To date, the installation of auditory warning devices in workplaces has been submitted to random or intuitive practices without proper considerations of factors contributing to an efficient use. For instance, a review of 93 different conditions of use in steel plant (Tran Quoc et al., 1992), revealed that in 40% of cases, the signals were not properly adjusted to warn of danger. In some cases, the warning signals were intentionally set at very high levels, resulting in extremely annoying signals which disrupting speech communication.

One of the most challenging factors for installing acoustic warning devices in an enclosed area is to set the sound pressure level suitably for all the employees. Commonly, in noisy industrial locations, employees have different hearing status; some workers could possibly have hearing protectors or others might be located at stations with low or high background noise levels. It has been demonstrated that in certain situations such as when extensive range in hearing status exists between co-workers (especially for warning signal components at high frequencies), no adequate solution may be found (Zheng, 2003).

Given the complex interaction between noise characteristics, hearing protector attenuation and hearing status, perception of acoustic warning signals in a given workplace by an individual worker or group of workers is difficult or impossible to predict without a detailed quantitative analysis of underlying acoustic and psychoacoustics factors (Laroche et al., 1991b; Robinson and Casili, 2000; ISO 7731, 2003; Zheng, 2003). Typically, predictive methods are based on the concept of a masked threshold for the warning signal, defined as the sound pressure level required to just detect the signal in a background noise. The warning signal is then adjusted to a certain level above the masked threshold to ensure it attracts attention and is recognizable. This is the main concept behind "Detectsound" (Zheng, 2003; Zheng et al., 2006).

Acoustic warning devices, however, are not normally installed at each workstation within a work area or plant. They are installed on walls or on the ceiling at a certain distance from the targeted workstations. In order to design alarm systems for new plants or to modify existing systems, the sound transmission path from the warning devices to the workstations must also be considered. Some researchers (Nanthavanij & Yenrades, 1999) have recently attempted to solve this problem by providing a set of analytical methods for predicting the optimum number, location, and sound power level of auditory warning devices for manufacturing facilities. However, only the direct sound field propagation from alarm devices to workstations was taken into account; the effects of sound reflection from walls, ceilings, floors and solid obstacles in the work plant were ignored. In typical settings, this assumption is unrealistic once the distance between alarm devices and workers is greater than a few meters. In practice, industrial work plants are often very reverberant, so that reflected sound waves can contribute considerably to the overall sound level at the receiver. In addition, the methods developed by Nanthavanij & Yenrades (1999) do not directly account for the effects of hearing loss (or hearing status in general) or the use of hearing protectors.

Extension of the work of Nanthavanij & Yenrades (1999) to more realistic simulations of the workplace sound field would be possible by use of classical room acoustic statistical methods (Fischetti, 2003), standardized sound field correction procedures for wall and ceiling effects in rooms (CSA Z107.52-M1983) or more advanced mirror image or geometrical acoustical prediction techniques (Borish, 1984; L'Espérance, 2000).

1.4 Research goal and thesis contribution

This research project will contribute to advancing knowledge in the selection, installation and use of auditory warning signal devices in noisy industrial settings to ensure safety in the workplace. The main goal is to develop and validate a tool integrated with "Detectsound" to automate the process of installing auditory warning devices in a given setting, by determining the number of devices as well their optimal location and sound power characteristics.

The new tool, "AlarmLocator", accounts for the sound propagation of auditory warning signals from the physical device location (on walls or ceilings) to the position of

individual workers or workstations in the plant. Both the direct field from the alarm devices and the reverberant field due to walls, ceilings, floors and other reflective surfaces are considered. The solution is based only on knowledge of the room's layout, the acoustic absorption characteristics of the walls, ceilings and floors, the reverberation time, the sound power characteristics of warning devices, and the distance between each warning device to each workstation.

Figure 1.1 presents the general modeling framework for optimal installation of warning devices. The method consists of integration of two software tools, "AlarmLocator" and "Detectsound". "Detectsound" (Zheng, 2003; Zheng et al., 2006), represented on the right side of Figure 1.1, analyzes the noise field in the industrial room to specify the acoustical characteristics of optimal warning signals or targets (sound level L_p at each frequency) for each workstation. The optimal warning signal levels can be adapted to the needs of specific workers at each workstation or those of a given population of workers. "Detectsound" requires four input parameters:

(1) The noise field at the workstation;

(2) The attenuation provided by hearing protectors (if used);

(3) The absolute hearing thresholds of the individual worker attending the workstation;

(4) The frequency selectivity of the worker.

The last 2 inputs can be obtained through clinical measurements or by predictive tools within Detectsound.

The output of Detectsound is the predicted optimal range (Design window) of warning signal levels at each workstation for various frequencies. The minimum (TL_{min}) and maximum (TL_{max}) target levels are defined respectively as 12 and 25 dB above the detection thresholds for warning sound perception in the noise field at the workstation over a range of signal frequencies from 125 to 3150 Hz, with an upper limit of 105 dB SPL. The range of target levels at each workstation represents a constraint to be satisfied during the installation of warning devices in the plant.

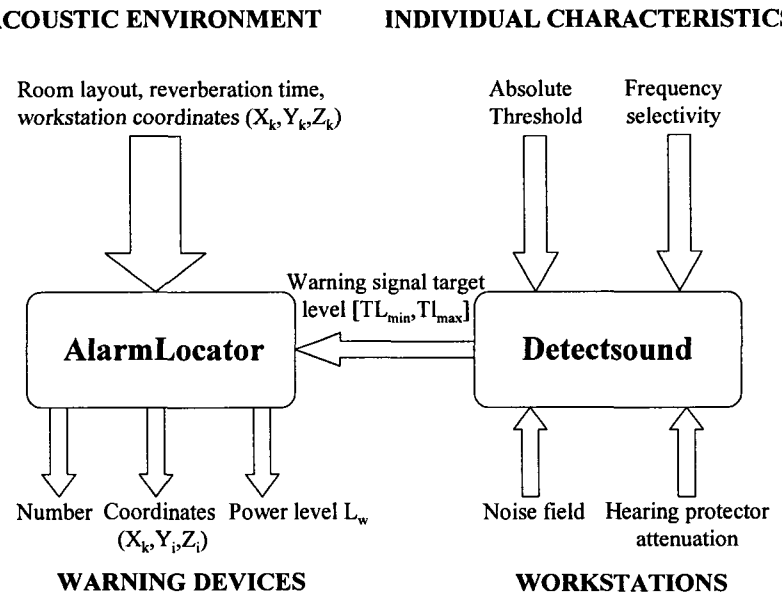

Fig. 1.1: Proposed solution to the problem of installing warning devices in the workplace involving the interaction of a psychoacoustic model of signal detection (Detectsound) and a model of acoustic propagation in rooms (AlarmLocator).

The "AlarmLocator" model of acoustic propagation in the work plant, developed in this research, presented in the left-hand side of Figure 1.1, has two sets of inputs:

(1) The target warning sound levels ([TL_{min}, TL_{max}]) at each workstation, as determined by "Detectsound";

(2) The characteristics of the work area (room layout, reverberation time or sound absorption, number and location of workstations in the room).

The goal of "AlarmLocator" is to search for warning device configurations that will satisfy the Detectsound warning sound level specifications at each workstation in the plant simultaneously. Specifically, the outputs of "AlarmLocator" include:

(1) The minimum required number of warning devices;

(2) The optimum spatial coordinates or location of the warning devices in the room;

(3) The optimum sound power level (i.e. volume level) of each warning device.

Together, these three outputs form a complete solution to the problem of installing acoustic warning devices provided in a format that can be easily understood and used in the workplace. The minimum number of devices and optimum power level specifications are required for purchasing purposes, whereas the optimal location of devices on walls and ceilings is required during installation.

1.5 Organization of the thesis

The work included in the thesis is structured in several chapters. Chapter 2 reviews the theoretical foundations of sound propagation, classical room acoustics theory, and the mirror image method of sound simulation in an enclosed space. Additionally, this chapter includes a hybrid method that combines the mirror image method with the classical room acoustics theory to compute the sound pressure level produced by sound sources, such as warning devices, that are located at the boundary surfaces of the room (e.g. walls, ceiling). Chapter 3 deals with the design and implementation of the "AlarmLocator" model. Simulated case studies are also depicted using this software. Chapter 4 presents an experimental validation for the "AlarmLocator" tool in a classroom at the University of Ottawa. Finally, a conclusion is presented in chapter 5 that summarizes the main findings from the present study and addresses some issues and improvements for future consideration.

Chapter 2. Theoretical foundations

An overview of the basic concepts in acoustics and the classical theory of room acoustics are presented below. Later in this chapter, a simple hybrid technique to compute the sound propagation from acoustic sources is established which combines the classical theory of room acoustics and the mirror image method.

2.1 Basic concepts and definitions

Absolute threshold: The absolute threshold corresponds to the minimum sound level perceived in the absence of any other external sounds. The absolute threshold is usually expressed in dB.

Masking: Masking occurs when more than one sound is presented. The weakest sound(s) cannot be detected by the human ear; therefore, they are masked by the strongest sound(s).

Masked threshold: The masked threshold of a sound is the level upon which it is just noticeable or detectable in the presence of the masker. The masker is any other sound present (i.e. background noise). It depends on the characteristics of the masking sound (level, frequency, temporal characteristics, etc.).

Anechoic room: The word anechoic comes from a Greek word signifying "without echoes". In an anechoic room, sound waves are free to propagate without any reflections.

Reverberant room: A reverberant room is the opposite of an anechoic room. The interior surfaces of the room are highly reflecting surfaces. Away for the source, the sound pressure level is more or less the same anywhere in the room.

Critical distance: In a typical room, there is a free propagation sound field near the source and a reverberant field far away from the source. The critical distance represents the boundary between the two conditions and is measured with respect to the source.

Sound power: A sound source radiates a measurable amount of acoustic energy per unit of time into the surrounding air, called sound power (Beranek & Ver, 1992). Sound power is measured in watts (W).

Sound power level: The sound power level describes the acoustical power radiated by a given source with respect to an international reference of 10^{-12} W (Irwin & Graf, 1979), and is defined as follows:

$$L_w = 10\log(W/W_{ref}) \quad [\text{dB}] \qquad (1)$$

where:

W = sound power in W
W_{ref} = reference sound power [10^{-12}W]

Sound intensity: The sound intensity is the continuous flow of power carried by a sound wave through a small area at a point in space (Beranek & Ver, 1992). Sound intensity is measured in W/m^2.

Sound intensity level: The sound intensity level describes the amount of sound intensity with respect to an international reference of 10^{-12} W/m^2 (Irwin & Graf, 1979), and is defined as follows:

$$L_I = 10\log(I/I_{ref}) \quad [\text{dB}] \qquad (2)$$

where:

I = sound intensity in W/m^2
I_{ref} = reference intensity [10^{-12} W/m^2]

Sound pressure: A fast variation in air pressure above and below atmospheric pressure is called sound pressure, measured in units of pascals (Pa) (Beranek & Ver, 1992).

Sound pressure level: The sound pressure level is the sound pressure measured with respect to an international reference of 20x10^{-6} Pa (Irwin & Graf, 1979), and is defined as follows:

$$L_p = 10\log(P^2/P^2_{ref}) \quad [\text{dB}] \qquad (3)$$

where:

P = root mean square sound pressure in Pa
P_{ref} = reference sound pressure [20x10^{-6} Pa]

Octave band: An octave band is the extent of the frequencies between f and 2f. Standardized values for the central frequencies of each octave band in audible range are 31.5, 63, 125, 250, 500, 1000, 2000, 4000, 8000, 16000 Hz (ANSI S1.6).

The lower and upper frequencies for each band are given by:

$$F_{lower} = \frac{F_{center}}{\sqrt{2}} \quad [\text{Hz}] \qquad (4)$$

$$F_{upper} = F_{center} * \sqrt{2} \quad [\text{Hz}] \qquad (5)$$

Third-octave band: This is the same as the octave band, but the analysis is carried out over frequency bands that are one-third of an octave band wide. The third octave band is used when finer frequency analysis is required. The one-third octave band centre frequencies in the audible range are: 25, 31.5, 40, 50, 63, 80, 100, 125, 160, 200, 250, 315, 400, 500, 630, 800, 1000, 1250, 1600, 2000, 2500, 3150, 4000, 5000, 6300, 8000, 1000, 12500, 16000, 20000 Hz (ANSI S1.6).

The lower and upper frequencies for each band are given by:

$$F_{lower} = \frac{F_{center}}{2^{1/6}} \quad [\text{Hz}] \qquad (6)$$

$$F_{upper} = F_{center} * 2^{1/6} \quad [\text{Hz}] \qquad (7)$$

2.2 Room acoustics

A typical room, such as an industrial work plant, is neither anechoic nor perfectly reverberant. In practice, two types of sound fields, a direct field from the source(s) and a multiple reflected or reverberant field co-exist. An overview of these two sound fields is presented in this section. Further details can be found in standards textbooks (Fischetti, 2003; Harris, 1979; Beranek & Ver, 1992; Irwin & Graf, 1979; Foreman, 1990).

2.2.1 Omnidirectional source

A source is considered to be omnidirectional or isotropic if it radiates the same amount of energy in all directions. In general, a source is considered omnidirectional if its dimensions are small with respect to the sound wavelength it produces (low frequency

case). Special sources are also designed to be omnidirectional (eg. Brüel & Kjaer 4292, 4295) over a wide range of frequencies.

2.2.2 Directivity

In most cases, the energy is not uniformly radiated around the source. Consequently, the source is considered directional. Acoustic sources are generally much more directional at high frequencies than at low frequencies (Fischetti, 2003).

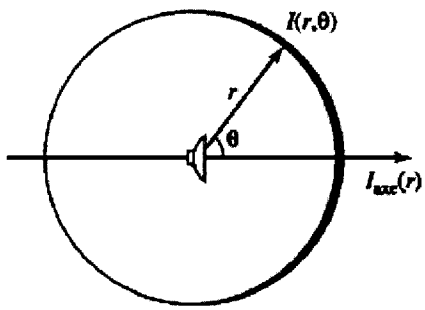

Fig. 2.1: Sound intensity around a directional source [From Fischetti (2003)].

The directivity of a source can be evaluated in an anechoic environment by measuring the sound intensity around the source as shown in Figure 2.1, where:

$I_{axis}(r)$: Intensity at a distance r from the source along the source axis (θ=0^0).

$I(r,\theta)$: Intensity at a distance r along the direction θ with respect to the source axis (θ=0^0).

$I_{avg}(r)$: Average intensity at a distance r from the source over all directions.

$I_{avg}(r)$ is calculated by averaging the intensities measured on all the points over a sphere of radius r centered on the source. $I_{avg}(r)$ is also equal to the intensity at a distance r in any direction from an omnidirectional source radiating a total sound power equal to that of the directional source. Consequently, $I_{avg}(r)$ is the total power W emitted by the source divided by the area of the sphere of radius r (Fischetti, 2003):

$$I_{avg}(r) = \frac{W}{4\pi r^2} \qquad [\mathrm{W/m^2}] \qquad (8)$$

2.2.2.1 Directivity factor

The source directivity factor Q_θ in a free space is defined as the ratio of the sound intensity $I(r,\theta)$ measured at angle θ and a distance r from the source to the average intensity $I_{avg}(r)$ at the same distance. Equivalently, Q_θ can be defined in terms of the mean square sound pressure as follows (Foreman, 1990):

$$Q_\theta = \frac{I(r,\theta)}{I_{avg}(r)} = \frac{P^2(r,\theta)}{P^2{}_s(r)} \qquad (9)$$

where:

$P(r,\theta)$ = root mean square sound pressure measured along direction θ at a distance r from a directional source emitting a total power of W watts into a free space [Pa].

$P_s(r)$ = root mean square sound pressure measured at a distance r from an omnidirectional source of power W radiating into a free space [Pa].

Along the source axis (θ=0^0), the directivity is:

$$Q = \frac{I(r,\theta = 0^0)}{I_{avg}(r)} = \frac{I_{axis}(r)}{I_{avg}(r)} = \frac{P^2{}_{axis}(r)}{P_s^{\,2}(r)} \qquad (10)$$

where:

$P_{axis}(r)$ = root mean square sound pressure measured at a distance r along the source axis (θ=0^0) for a source emitting a total power of W watts into a free space [Pa].

The directivity factor is dimensionless and does not depend on the distance from the source. Generally, Q increases with frequency (Fischetti, 2003).

As shown in Figure 2.2, the intensity along the source axis at a distance r is $I_{axis}(r) = \frac{W}{4\pi r^2}$ for an omnidirectional source, whereas the intensity along the source axis at a distance r is $I_{axis}(r) = \frac{WQ}{4\pi r^2}$ for a directional source.

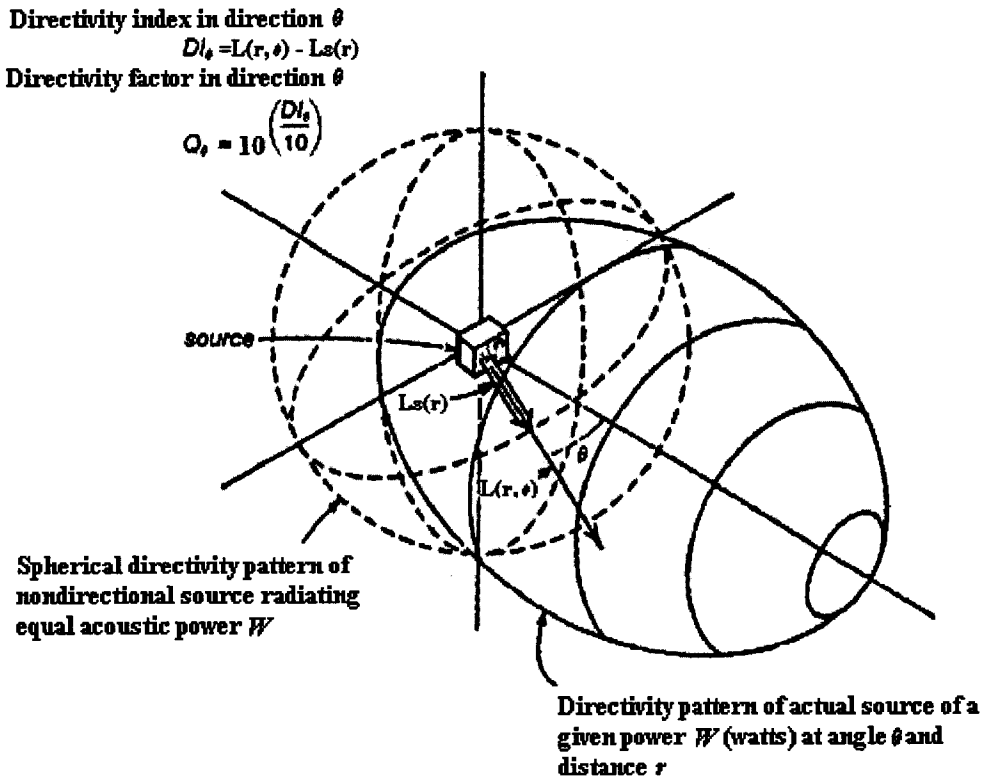

Fig. 2.2: Directivity pattern, directivity index, and directivity factor of a source radiating in a free space [From Foreman (1990)].

2.2.2.2 Directivity index

The directivity index DI_θ in free space is measured in dB and represents the difference between the sound intensity level of the source in a given direction θ and the average sound intensity level in all directions (Fischetti, 2003) as follows:

$$DI_\theta = 10\log(Q_\theta) = 10\log(\frac{I(r,\theta)}{I_{avg}(r)}) = 10\log(\frac{P^2(r,\theta)}{P^2{}_s(r)}) = L(r,\theta) - L_s(r) \quad (11)$$

where:

$$L(r,\theta) = 10\log\frac{P^2(r,\theta)}{P^2{}_{ref}} \quad (12)$$

$$L_s(r) = 10\log\frac{P^2{}_s(r)}{P_{ref}{}^2}. \quad (13)$$

For an omnidirectional source in free space, Q_θ=1 and DI_θ =0 dB by definition in all directions. When an omnidirectional sound source is placed over a perfectly reflecting surface (Figure 2.3), sound is radiating into a hemispherical space instead of a spherical

surface. Since the intensity at radius r is twice as large if the source radiates into a hemisphere as compared to a sphere (Foreman, 1990), the directivity factor Q for this arrangement is 2 and the directivity index DI is 3 dB. Similarly, if an omnidirectional source is placed at the intersection of two reflecting planes (e.g. at the corner of two walls in a room for instance), directivity factor Q would be equal to 4 and the directivity index DI would be 6 dB. If the omnidirectional source is located at a three plane intersection (on the upper or lower corner of the room for example), Q and DI would be equal to 8 and 9 dB respectively.

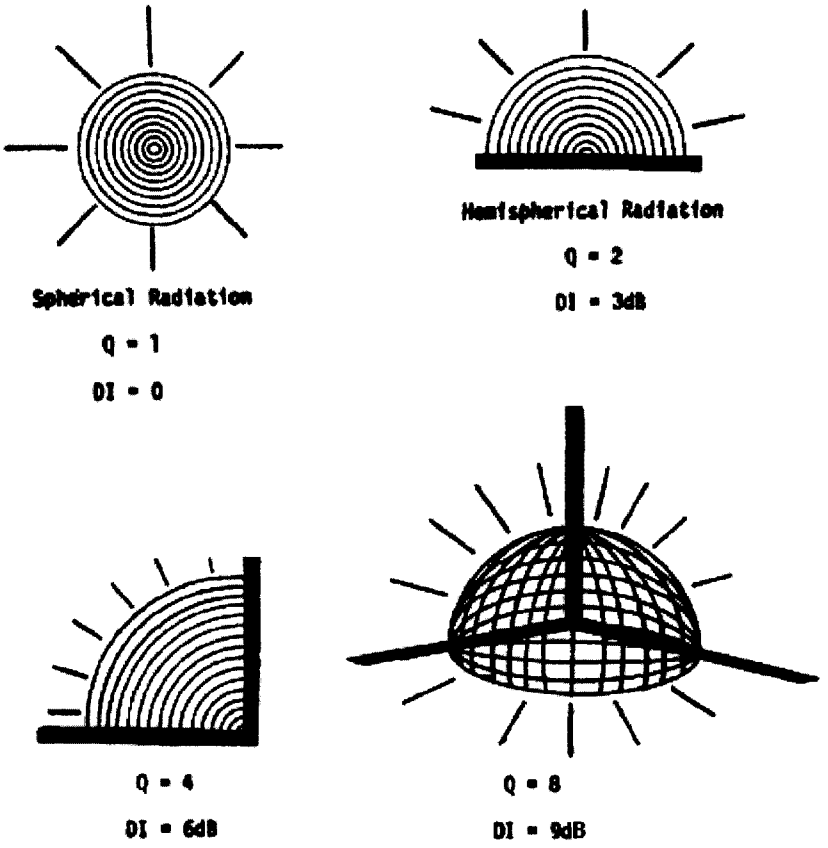

Fig. 2.3: Noise field directivity due to perfectly reflecting planes [From Ghering (1978)].

If a directional sound source is placed in an enclosed area or near reflecting planes, both its intrinsic directional characteristics and the directivity effects discussed above must be considered (Ostergaard, 2000).

2.2.3 Direct field

In the direct sound field near a source, well within the critical distance, the reflections from distant obstacles or walls have a negligible effect on the sound received. In these conditions, we can presume that the sound signal is transmitted from the source to the point under consideration (receiver) with no variation other than the attenuation due to the spherical spreading of the wave field or the atmospheric absorption (Irwin & Graf, 1979). The atmospheric absorption effects are normally considered when the distance between the transmitter and the receiver is greater than 20 m.

The sound pressure level along the source axis at a distance r is given by the following formula (geometrical spreading only):

$$L(r) = 10\log(\frac{I_{axis}(r)}{I_{ref}}) \qquad \text{[dB]} \qquad (14)$$

where: $I_{axis} = \frac{WQ}{4\pi r^2}$.

Hence:

$$L(r) = 10\log\frac{W}{W_{ref}} + 10\log\frac{Q}{4\pi r^2} \qquad \text{[dB].} \qquad (15)$$

$$L(r) = L_w + DI + 10\log\frac{1}{4\pi r^2}$$

The inverse square law implies that there is an attenuation of 6 decibels for each consecutive doubling of the distance from the source in the direct field, i.e.:

$$L(2r) = L(r) - 20\log 2 = L(r) - 6dB \qquad (16)$$

2.2.4 Reverberant field

Far from a source in a typical room, well beyond the critical distance, the contribution from the direct wave can become negligible compared to the aggregate of all reflection and diffraction effects from obstacles and room surfaces. This is referred to as the reverberant field.

2.2.4.1 Specular reflection

A specular reflection occurs when the sound wavelength is much smaller than the dimensions of the obstacle (Fischetti, 2003). In this case, the sound wave behaves as a ray

and obeys the laws of geometrical optics. Thus, the reflection's angle is equal to the incident's angle as shown in Figure 2.4a (Fischetti, 2003).

2.2.4.2 Diffuse reflection

A diffuse reflection occurs when the incident wave strikes a surface with irregularities whose dimensions are of the same order of magnitude as the wavelength of the incident wave (Fischetti, 2003). The reflected waves are dispersed along many directions. This is shown in Figure 2.4b.

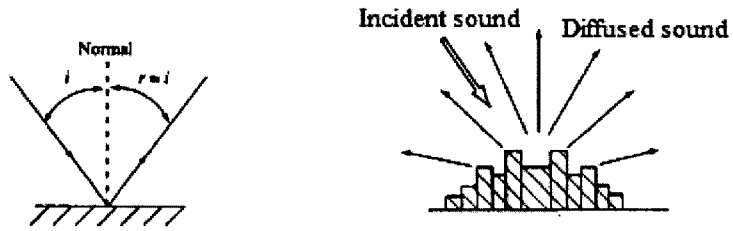

Fig. 2.4: Specular and diffuse reflection diagrams [From Fischetti (2003)]

2.2.4.3 Diffraction

This phenomenon occurs at low frequencies when the wavelength of the incident sound is much larger than the dimensions of the obstacle. In this case, the obstacle does not fully block sound propagation as shown in Figure 2.5a (Fischetti, 2003).

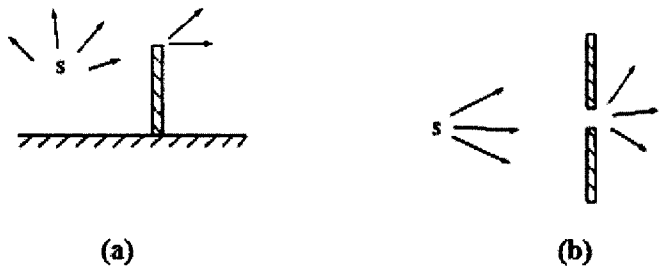

Fig. 2.5: Diffraction diagrams [From Fischetti (2003)]. The source is denoted by *S*.

The phenomenon of diffraction can also occur when the incident sound strikes a hole in a large obstacle if the sound wavelength is larger than the dimension of the hole (Fischetti, 2003). This is shown in Figure 2.5b.

2.2.4.4 Absorption

When a sound wave hits a large obstacle such a wall, part of the incident energy may also be absorbed, depending on the acoustical properties of the obstacle's material (Fischetti, 2003). The absorption properties of materials are usually expressed in terms of the absorption coefficient α, which is the proportion of incident energy absorbed by the surface. This coefficient α typically depends on the sound frequency and the angle of sound incidence on the material.

Different techniques exist to measure absorption coefficient of materials:

- Reverberation method (ISO 354, 2003)
- Impedance tube ISO (10534-1, 1996 & ISO 10534-2, 1998)
- Tone burst method (Brüel & Kjaer, 1988)

In room acoustics we usually consider the Reverberation method; only the frequency factor is considered (Fischetti, 2003). The angle of incidence is normally neglected by assuming that the sound field is diffuse and a strike at random incidence. Table 2.1 lists absorption coefficients for typical construction materials measured in reverberant room.

The amount of energy absorbed also depends on the surface area being struck. Given the material's acoustic absorption and the surface area, we can define the Sabine surface absorption for each surface element in a room using the following formula:

$$A_i = S_i \alpha_i \qquad [\mathrm{m}^2] \qquad (17)$$

where:

A_i = Sabine absorption for a surface S_i with coefficient α_i [m^2]

S_i = area of the i^{th} surface [m^2]

α_i = absorption coefficient of the i^{th} surface.

In a room constructed of N different surfaces S_i with different absorption coefficients α_i, the total absorption A in the room is the sum of the Sabine surface absorption over each interior surface within the room as follows:

$$A = \alpha_1 S_1 + \alpha_2 S_2 + \alpha_3 S_3 + ... + \alpha_N S_N = A_1 + A_2 + A_3 + ... + A_N \qquad [\mathrm{m}^2]. \quad (18)$$

We can then define the average absorption coefficient in the room $\bar{\alpha}$ as follows:

$$\bar{\alpha} = \frac{A}{S} = \frac{(\alpha_1 S_1 + \alpha_2 S_2 + \alpha_3 S_3 + ... + \alpha_N S_N)}{(S_1 + S_2 + S_3 + ... + S_N)} \quad \text{[unitless]} \quad (19)$$

where S is the total surface.

Construction Materials	Octave-Band Center Frequency (Hz)					
	125	250	500	1000	2000	4000
Brick, unglazed	0.03	0.03	0.03	0.04	0.05	0.07
Brick, unglazed, painted	0.01	0.01	0.02	0.02	0.02	0.03
Carpet on foam rubber	0.08	0.24	0.57	0.69	0.71	0.73
Carpet on concrete	0.02	0.06	0.14	0.37	0.6	0.65
Concrete block, coarse	0.36	0.44	0.31	0.29	0.39	0.25
Concrete block, painted	0.1	0.05	0.06	0.07	0.09	0.08
Floors, concrete or terrazzo	0.01	0.01	0.015	0.02	0.02	0.02
Floors, resilient flooring on concrete	0.02	0.03	0.03	0.03	0.03	0.02
Floors, hardwood	0.15	0.11	0.1	0.07	0.06	0.07
Glass, heavy plate	0.18	0.06	0.04	0.03	0.02	0.02
Glass, standard window	0.35	0.25	0.18	0.12	0.07	0.04
Gypsum, board, 1/2 in.	0.29	0.1	0.05	0.04	0.07	0.09
Panels, fiberglass, 11/2 in. thick	0.86	0.91	0.8	0.89	0.62	0.47
Panels, perforated metal, 4 in. thick	0.7	0.99	0.99	0.99	0.94	0.83
Panels, perforated metal with fiberglass insulation 2 in. thick	0.21	0.87	1.52	1.37	1.34	1.22
Panels, perforated metal with mineral fiber insulation 4 in. thick	0.89	1.2	1.16	1.09	1.01	1.03
Panels, plywood, 3/8 in	0.28	0.22	0.17	0.09	0.1	0.11
Plaster, gypsum or lime, rough finish on lash	0.02	0.03	0.04	0.05	0.04	0.03
Plaster, gypsum or lime, smooth finish on lash	0.02	0.02	0.03	0.04	0.04	0.03
Polyurethane foam, 1 in. thick	0.16	0.25	0.45	0.84	0.97	0.87
Tile, ceiling, mineral fiber	0.18	0.45	0.81	0.97	0.93	0.82
Tile, marble or glazed	0.01	0.01	0.01	0.01	0.02	0.02
Wood, solid, 2 in. thick	0.01	0.05	0.05	0.04	0.04	0.04

Table 2.1: Average absorption coefficient α for construction materials as a function of frequency [From Irwin & Graf (1979)].

2.2.4.5 Reverberation time

Because room surfaces are not perfectly absorptive in a typical room, sound will persist for a given time once a source is stopped, until all reflections are attenuated. The reverberation time (*RT*) in an enclosed space, also known as the Sound Decay Process, is the amount of time it takes for a stationary sound field to decay by 60 decibels once the source has been stopped (Beranek, 2002). This is illustrated in Figure 2.6. The sound

source is turned on at $t = 0$ and then cut off at $t = t_1$. Three phases of reverberation can be observed (Fischetti, 2003).

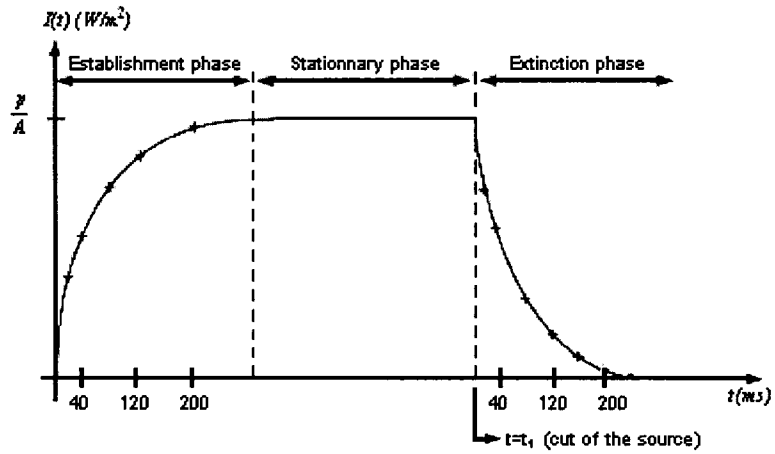

Fig. 2.6: The three phases of the reverberant field [From Fischetti (2003)].

In the establishment phase, sound waves are reflected back and forth many times between the walls, floor and ceiling. This will cause some loss of energy produced by the absorption at each single reflection; but since the sound source is operating continuously, the level of sound energy of the reflected waves will increase. The sound level keeps on increasing until attaining a certain level where it stays stationary. This level is determined when the rate of energy loss, due to absorption of the room surfaces, equals the rate at which the sound energy is provided by the source (Fischetti, 2003). When the source is stopped (at $t=t_1$ as shown in Figure 2.6), the intensity of the reverberant sound starts to decay; the amount of time it takes for the reverberant sound to decay by 60 dB is defined as the reverberation time or T_{60}.

In practice, it is not necessary to measure the time needed for the sound energy to decay by 60 dB to obtain the reverberation time since statistically it decays at a linear rate in dB/s. Two typical measures, T_{20} and T_{30}, give information on the diffuse sound decay and are derived from the decay curve segments between 5 dB and 25 dB or between 5 and 35 dB, respectively, below the stationary level as shown in Figure 2.7 (Brüel & Kjaer 7841). From the corresponding slope, T_{20} and T_{30} are calculated as the times needed to decay by 60 dB (Brüel & Kjaer 7841). A 5 dB margin below the stationary level is used to exclude

early sound reflections, which are not considered part of the diffuse sound decay process (Beranek, 2002).

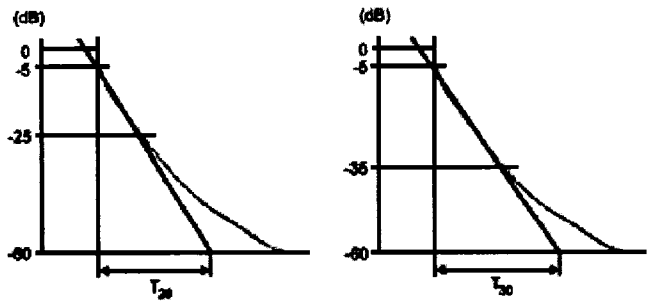

Fig. 2.7: Illustration of the sound decay process using T_{20} and T_{30} (Brüel & Kjaer Type-7841).

The reverberation time in a room can also be estimated using Sabine theory or Eyring theory upon consideration of room geometry and material properties (Fischetti, 2003; Beranek, 2002; Irwin & Graf, 1979).

2.2.4.5.1 Sabine's theory

The Sabine formula, introduced early in the 20th century, for estimating the reverberation time (RT) is given as (Fischetti, 2003):

$$RT = \frac{0.16V}{A} = \frac{0.16V}{S\bar{\alpha}} \quad [s] \qquad (20)$$

where:

V = volume of the room in m^3

$A = S\bar{\alpha}$ =Sabine room absorption in m^2 from equation (18).

According to equation (20), RT depends on the room geometry (V,S) and average absorption coefficient $\bar{\alpha}$. Since $\bar{\alpha}$ depends on frequency, so does RT. Sabine's theory is founded on the assumption that the field is uniformly reverberant in the room. In order that sound energy has the time to be regularly distributed in the room, it is necessary that absorption be comparatively weak. Thus, the Sabine's theory gives less valid results as the room is becoming less reverberant. In practice, the Sabine's formula is used when the average absorption coefficient in the room, $\bar{\alpha}$, is lower or equal than 0.2 (Fischetti, 2003).

2.2.4.5.2 Eyring's theory

Eyring's equation was established in 1930 (Fischetti, 2003). Eyring's method consists of following the path of a sound ray through the room and calculating the energy absorbed during each reflection (Fischetti, 2003).

The Eyring's formula for estimating the reverberation time (*RT*) is:

$$RT = \frac{-0.16V}{S\ln(1-\bar{\alpha})} \quad [s] \qquad (21)$$

where:

V = volume of the room in m^3

S = total surface of the room in m^2

$\bar{\alpha}$ = average absorption coefficient of the room.

In a very reverberant environment, the average absorption coefficient of the room is very small ($\bar{\alpha} \rightarrow 0$). Since $\bar{\alpha}$ is positive, hence $\ln(1-\bar{\alpha}) \rightarrow 0^-$ (Fischetti, 2003). Therefore *RT* tends towards $\frac{0.16V}{S\bar{\alpha}}$, which is coherent with Sabine's formula. Conversely, when $\bar{\alpha} \rightarrow 1$, $\ln(1-\bar{\alpha})$ tends towards minus infinity and hence $RT \rightarrow 0$. This result is logical since the room absorbs all the reverberant energy, while Sabine's formula gives an aberrant higher estimate (Fischetti, 2003).

Table 2.2 compares the Sabine and Eyring formulas for a room of dimensions 25m×15m×10m, (V=3750 m^3, S=1550 m^2).

Average absorption coefficient $\bar{\alpha}$	*RT* Sabine [s]	*RT* Eyring [s]	Relative difference *RT* Sabine versus *RT* Eyring
0.1	3.87	3.67	5%
0.2	1.93	1.73	10%
0.4	0.97	0.76	21%
0.8	0.48	0.24	50%

Table 2.2: Difference between Eyring and Sabine formulas for calculating *RT* [From Fischetti, (2003)].

As shown in Table 2.2, the Sabine's formula overrates the reverberation time compared to Eyring's formula. For $\bar{\alpha} \leq 0.2$, Sabine can be used. Otherwise, Eyring gives more acceptable results (Fischetti, 2003).

2.2.5 Sum of direct and reverberant fields

In a typical room, the total sound field is the sum of the direct (section **2.2.3**) and reverberant fields (section **2.2.4**). From Irwin & Graf (1979), the steady-state time and space-average energy density δ_t in the room is given by:

$$\delta_t = \frac{4W}{\bar{\alpha} cS} \quad [\mathrm{J/m^3}] \qquad (22)$$

where c is the sound velocity [m/s], W is the power of the sound source [W], $\bar{\alpha}$ is average absorption coefficient, and S is the total surface of the room [$\mathrm{m^2}$].

The time average of the energy density of the direct sound (spherical spreading only) depends on the distance r from the source as follows (Irwin & Graf 1979):

$$\delta_d = \frac{W}{4\pi r^2 c} \quad [\mathrm{J/m^3}]. \qquad (23)$$

The total direct energy, E_d, in the room is obtained by integrating the direct energy density, δ_d, over the equivalent spherical volume of the room and is given by (Irwin & Graf, 1979):

$$E_d = \frac{4WV}{cS} \quad [\mathrm{J}]. \qquad (24)$$

The reverberant energy in the room ($\delta_r V$) due to all reflections is obtained by subtracting the direct energy E_d from the total energy $\delta_t V$ as follows (Irwin & Graf, 1979):

$$\delta_r V = \delta_t V - E_d \quad [\mathrm{J}]. \qquad (25)$$

Expanding and simplifying yields:

$$\delta_r V = \frac{4WV}{cS}\left(\frac{1-\bar{\alpha}}{\bar{\alpha}}\right) \quad [\mathrm{J}]. \qquad (26)$$

Defining the room constant R as follows:

$$R = \frac{S\bar{\alpha}}{1-\bar{\alpha}} \qquad (27)$$

and substituting for R in equation (26) yields:

$$\delta_r V = \frac{4WV}{cR} \quad [\mathrm{J}]. \qquad (28)$$

Using equations (23) and (28) we can now determine the total energy density δ_t at any position in the room as follows:

$$\delta_t = \delta_d + \delta_r \qquad [J/m^3]. \qquad (29)$$

Upon expansion, equation (29) becomes:

$$\delta_t = \frac{W}{4\pi r^2 c} + \frac{4W}{cR} \qquad [J/m^3]. \qquad (30)$$

However, the total energy density at any point in the room is related to the local sound pressure as follows (Irwin & Graf, 1979):

$$\delta_t = \frac{p^2}{\rho_0 c^2} \qquad [J/m^3] \qquad (31)$$

where ρ_0 is the static gas density (1.18 kg/m^3) and p^2 is the root mean square sound pressure [Pa].

Substituting equation (31) into equation (30) and introducing the source directivity factor Q, we obtain (Irwin & Graf, 1979):

$$p^2 = \frac{WQ\rho_0 c}{4\pi r^2} + \frac{4W\rho_0 c}{R} \qquad [Pa]. \qquad (32)$$

Using equations (1) and (3), the sound pressure level L_p at a distance r from the source is then given by:

$$L_p = L_w + 10\log\left(\frac{Q}{4\pi r^2} + \frac{4}{R}\right) \qquad [dB] \qquad (33)$$

where L_w is the source sound power level.

	Direct sound (DS)	Reverberant sound (RS)	DS and RS Using Eyring
Intensity as a function of sound pressure [$Pa^2m^2s_{/Kg}$]	$I_d = \frac{p_d^{\,2}}{\rho_0 c}$	$I_r = \frac{p^2{}_r}{4\rho_0 c}$	$I_t = \frac{p^2{}_d}{\rho_0 c} + \frac{p^2{}_r}{4\rho_0 c}$
Intensity as a function of the source power [W/m^2]	$I_d = \frac{WQ}{4\pi r^2}$	$I_r = \frac{W}{R}$ $R = \frac{S\alpha}{1-\alpha}$	$I_t = \frac{WQ}{4\pi r^2} + \frac{W}{R}$
Pressure level as a function of the power level [dB]	$L_{pd} = L_w + 10\log\frac{Q}{4\pi r^2}$	$L_{pr} = L_w + 10\log\left(\frac{4}{R}\right)$	$L_{pt} = L_w + 10\log\left(\frac{Q}{4\pi r^2} + \frac{4}{R}\right)$

Table 2.3: Summary of the direct and reverberant field equations using Eyring's theory. The Sabine's equations are identical except the room constant R is replaced by the room absorption A (Fischetti, 2003).

A summary of the previous formulas for the direct and the reverberant field for both Sabine and Eyring theory are presented in Table 2.3.

2.3 Mirror image method

In this section, the basic principles of the mirror image method for calculating the sound field in a room are briefly presented. Determining the room's impulse response by computations and measurements is also reviewed.

2.3.1 General outline of the mirror image method

An overview of the mirror image method is presented in this section. Further details can be found in the literature (Kahrs & Brandenburg, 1998; Allen & Berkley, 1978) .

The mirror image method consists of modeling reflections as if they originated from virtual surfaces behind room boundaries. This method assumes that the sound wavelength is small compared to the dimensions of the reflecting surfaces (Kahrs & Brandenburg, 1998). As a result, the sound wave can be represented by a ray similar to the ray of light that reflects off a mirror specularly (Kahrs & Brandenburg, 1998). Figure 2.8 shows a single wall reflection using the ray tracing model. The real source is at point *M*. The sound ray leaves the source at point *M* and is reflected off the wall towards the receiver at point *N*. Geometrically, the sound ray is being reflected as if it was coming straight from *M'*. *M'* is called the virtual source or the image of *M* and is symmetric to *M* with respect to the wall.

The virtual source *M'* in Figure 2.8 is a first order source since the sound ray gets reflected only once. Multiple reflections of the sound ray would correspond to a higher order of virtual sources.

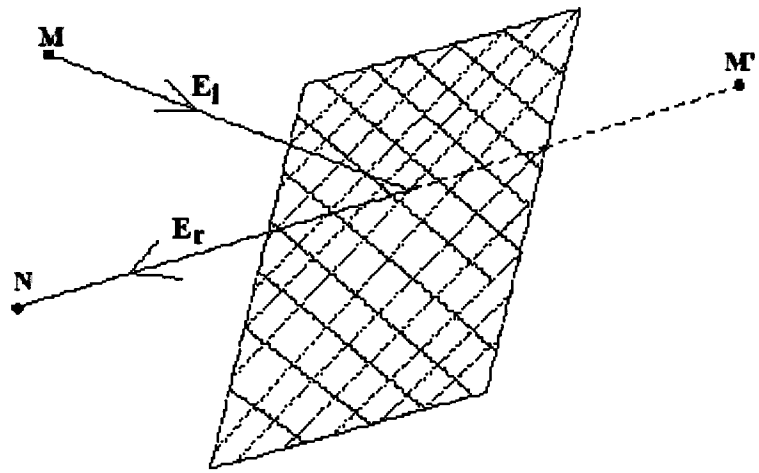

Fig. 2.8: First order wall reflection and corresponding virtual image source.

A second order wall reflection is shown in Figure 2.9. *M"* is a second order virtual source since the sound ray it models represents a reflected wave reaching receiver *N* after two wall reflections at point *P* (wall 1) and *Q* (wall 2). This process can be expanded to higher orders of wall reflections by creating additional virtual sources at larger and larger distances from *N* according to the geometry of the room. In addition to locating virtual sources in space, the energy loss at each wall reflection due to absorption must also be accounted for with the mirror image method. Solutions for rectangular and arbitrary room sizes have been reported (Borish, 1984; L'Espérance, 2000).

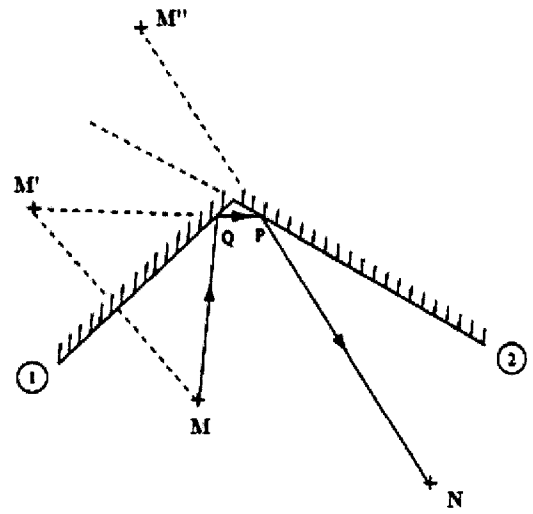

Fig. 2.9: Second order wall reflection and corresponding virtual image sources [From Fischetti (2003)].

2.3.2 Impulse response method

The transmission of sound from a source to a receiver point, such as source M and receiver N in Figure 2.9 can be described as an impulse response function (Fischetti, 2003).

2.3.2.1 Basic concept

An impulse or an impact noise is a short and intense sound emitted by a source (Beranek & Ver, 1992). For an omnidirectional source, the impulse is spread in all directions. In a room a listener first receives the direct sound wave followed by a succession of the first reflections (R1, R2, R3, etc.) as shown in Figure 2.10. The multitude of waves reflected by the walls, ceiling, and other objects in the room constitute the reverberated sound. The complete series of reflections (including the direct field) at a certain position in the room is what we call the impulse response, and is specific to each source/receiver configuration. Therefore, the impulse response depends on the source and receiver positions. Once the impulse response is found, it is easy to determine the received signal for any signal emitted from the source. If the source is directional, the measured impulse response also incorporates source directivity effects.

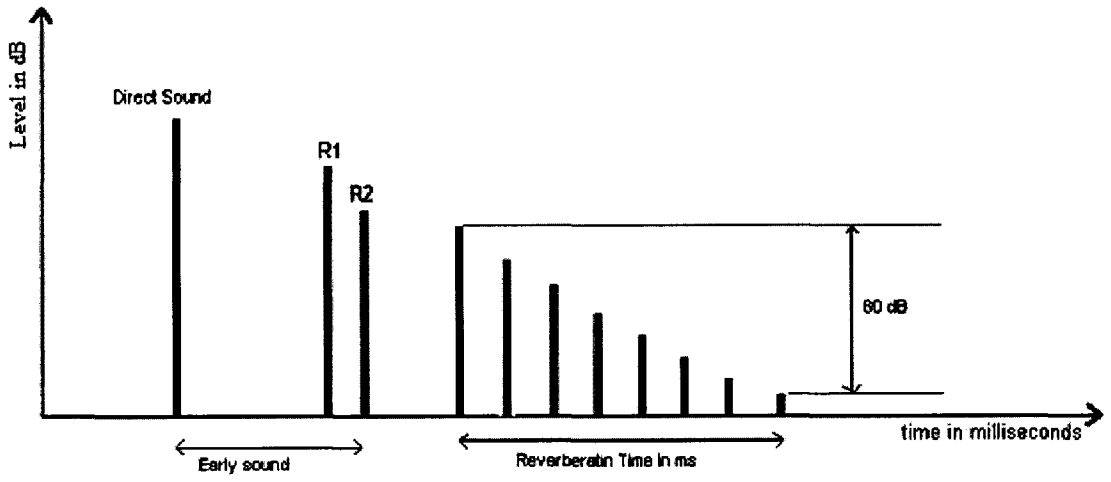

Fig. 2.10: Illustration of the reflection model in an enclosed area.

Consider a source emitting a signal $x(t)$ at a specific position in a room, the received $y(t)$ signal at another point in the room is determined by using the convolution between $x(t)$ and the impulse response of the room $h(t)$ between these two points (Fischetti, 2003):

$$y(t) = x(t) * h(t). \qquad (34)$$

Conversely, if we apply a signal *x(t)* and measure the sound pressure signal *y(t)* at a certain point in the room, deconvolution techniques can be used to obtain the impulse response *h(t)*. By repeating this process for many different positions of the source and receiver, we can determine the impulse response in the entire room.

2.3.2.2 Computation of the room impulse response using the mirror image technique

Using geometric models of the room, the room impulse response can be predicted as a set of attenuated and delayed impulses (Kahrs & Brandenburg, 1998). The room impulse response at the listener or workstation position can be approximated by using a high order of reflections. A very high order of reflections would cover the late reverberation field. The late reverberation is described as a dense collection of echoes traveling in all directions, in other words a diffuse sound field. Computationally, the contributions from all the virtual sources are summed. Each image or virtual source contributes a delayed impulse (echo), whose time delay is equal to the distance between the source and the listener divided by the speed of sound (Kahrs & Brandenburg, 1998). This is shown in Figure 2.11. The echo amplitude is inversely proportional to the distance traveled to account for spherical expansions of the sound, and proportional to the product of the reflection coefficient of the surface(s) encountered (Kahrs & Brandenburg, 1998). A FIR (Finite Impulse Response) structure can be implemented as shown in Figure 2.11 with the set of delays m_i and gains a_i. In Figure 2.11, *R(z)* is a filter that renders the late reverberation.

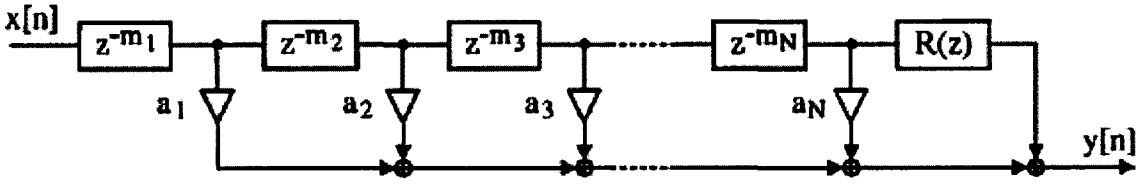

Fig. 2.11 FIR filter cascaded with reverberator *R(z)* to model early echoes and late reverberation [From Kahrs & Brandenburg (1998)].

2.3.2.3 Measured room impulse response

The room impulse response can be measured using different techniques. For example, the software tool Dirac (Brüel & Kjaer Type 7841) provides eight possible measurements

techniques which differ in excitation source and/or recording conditions. One of the techniques consists of generating a MLS (minimum length sequence) input stimuli. The stimulus is then fed to a loudspeaker sound source through a power amplifier. Dirac records the response through microphones that are fed into a soundcard on a computer. The impulse response between source and receiver is then obtained by deconvolving the MLS input stimuli from the received response.

Once obtained, the impulse response can be used to derive other relevant parameters and functions describing the acoustic behavior of the room. Such parameters include the reverberation time T_{60}, the early decay time and the frequency response (Brüel & Kjaer Type 7841). Similar to the impulse response, the frequency response is defined for a given position of the source and receiver. The frequency response can be obtained by applying the Fourier Transform to the impulse response, as shown in Figure 2.12.

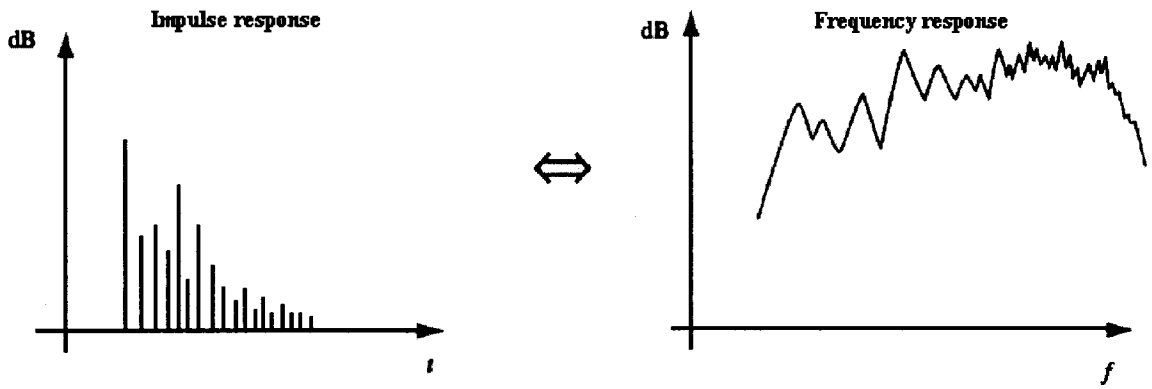

Fig. 2.12: Impulse and frequency response for one source/receiver configuration [From Fischetti (2003)].

2.4 Hybrid method

As shown in section **2.2**, the classical theory of room acoustics requires only the volume (V) and the interior surface area (S), without room geometrical modeling, to estimate the reverberant sound field, in addition to knowledge of the average absorption coefficient. The latter can be easily estimated through measurement of T_{60} (equation 21). However, computation of the direct field is problematic if sources are placed directly on walls, as Q changes as a function of wall placement.

As shown in section **2.3**, the mirror image method can be used to derive impulse response functions which are potentially more accurate for both direct and reverberant fields.

However, it can be computationally heavy for models requiring large orders of reflections and if there are a large number of source/receiver arrangements to simulate. Moreover, it requires an accurate geometrical model of the room including a detailed description of the distribution of acoustic absorption on walls and ceiling.

In the current research for finding the optimal power level, number and wall placement of alarm devices, the receiver or workstation locations are known but the source positions are not known a priori, and it is not convenient to calculate or measure impulse responses for all possible source-receiver locations in the room. Therefore, a method combining the mirror image technique and the classical room acoustics theory is established to compute the sound pressure level of the alarm devices. The proposed method assumes omnidirectional sources but accounts for wall-placement directivity effects by using a relatively low order of virtual sources to simulate early reverberation. Statistical room acoustics theory is used for late reverberation. The method is contrasted to other room simulation methods at the end of this chapter.

2.4.1 Basic approach

As shown in section **2.2.2.2**, the directivity effects produce the following Q values 2, 4, 8 depending on the source position near reflective surfaces (Figure 2.3). However, these values are only accurate if the surfaces are totally reflective and the source itself is omnidirectional. The following example shown in Figure 2.13 shows the problem in using this technique in practice.

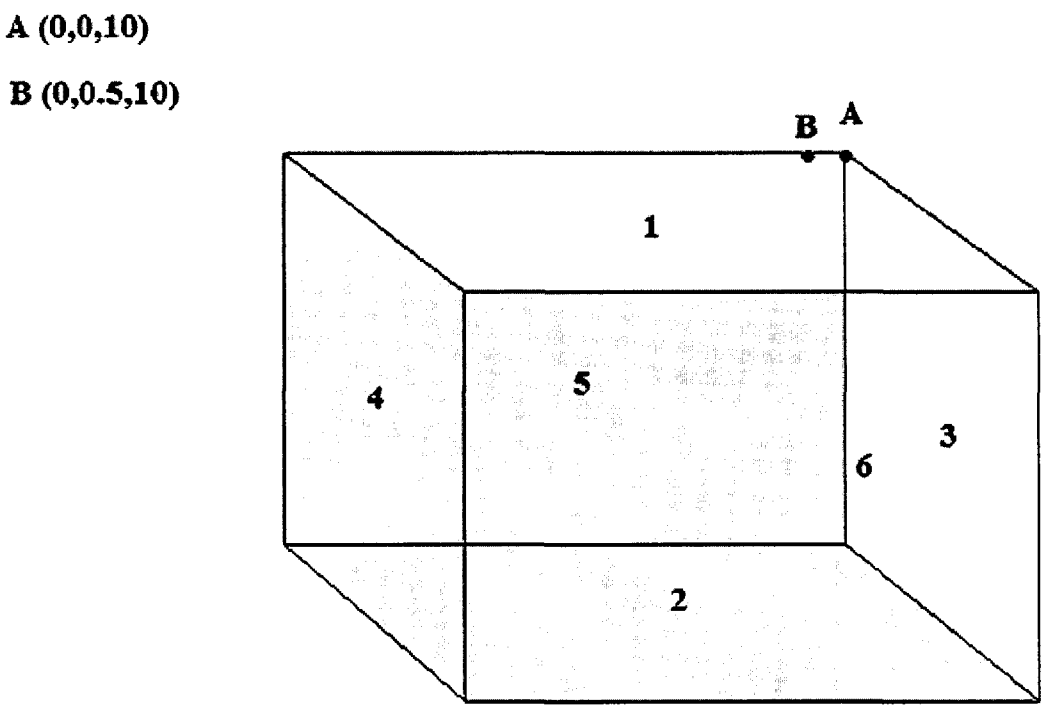

Fig. 2.13: Problem with the conventional method to compute the directivity in an enclosed area.

For source *A* (0,0,10), the directivity factor is 8 if and only if the surfaces 1,3, and 5 are totally reflective. In real work plants, the surfaces are not totally reflective; thus, the directivity is less than 8. For complete reflective surfaces, the directivity is considered equal to 8 since the source (point *A* in Figure 2.13) is placed in the corner of a 3 plane intersection (section **2.2.2.2**). In a large room, only the acoustic contribution from this corner (surfaces 1, 3, and 5) generally needs to be taken into account for sound level computation. For a small room, the contribution from the other surfaces (2, 4, and 6) may also need to be taken into consideration if the distance between source *A* and these surfaces is not large compared to the source-receiver distance. Hence, reflections over these additional surfaces may not be negligible.

For source *B* (0,0.5,10), the directivity factor is even more difficult to determine. It is between 4 and 8 according to the conventional way if the surfaces are totally reflective (section **2.2.2.2**). As shown in Figure 2.13, *B* is very close to the corner but not at the corner. Therefore, the position of the source *B* is neither at a three plane corner nor at a 2 plane corner. Hence, not only the contribution of the surfaces 1 and 5 should be taken

into account, but surface 3 also has a contribution in this case. Again, the contribution of the other surfaces (2, 4 and 6) may be not negligible in case of a small room.

Using the mirror image method, source placement effects can be accounted for as early reverberation terms. A minimum order of 3 is necessary to simulate directivity effects of a placement at a 3 plane intersection where $Q = 8$. The latter requires the following 8 ray paths: the direct wave (order 0), three single-surface reflections (order 1), three two-surface reflections (order 2) and one three-surface reflection (order 3). This technique ensures a better approximation of the directivity effects due to wall placement.

2.4.2 Early reverberation

The early reverberation components consist of the direct sound in addition the first few reflections. In this research, these will be simulated using mirror image method and a reflection order up to 3. The early reverberation concept can be easily examined by using a rectangular geometrical model. It can also be examined for irregularly shaped room (Borish, 1984; L'Espérance, 2000); however, it is more difficult and requires a large computational resources if many source-receiver arrangements are required.

In this research, the real room is considered as a rectangular volume surrounded by many virtual rooms of its same size. The number of peripheral rooms depends on the order of reflection. A first-order reflection model would require one room for each surface of the real room; thus, a total of 6 virtual rooms. A second-order reflection would require 30 virtual rooms. A third-order reflection would require 68 virtual rooms as we will see shortly. The average absorption coefficient $\bar{\alpha}$ is assumed uniform in the room and it is derived from the measured reverberation time T_{60}. The average room reflection coefficient β is assumed to be equal to $1-\bar{\alpha}$.

2.4.3 Virtual sources plane models

For a better view, planes instead of rooms are presented to show the virtual sources for each of the three orders (order 1, 2, and 3) used in this research.

For instance, the middle plane represents any plane between the ceiling and the ground of the room. As shown in Figure 2.14, the virtual sources of different orders are located in different rectangles identified by the power reflection coefficient β^n where n is the order

of reflection. Each rectangle represents a virtual room. For instance, if the sound ray is reflected twice, its virtual source should be placed in a rectangle identified by β^2.

As shown in Figure 2.14, source S_0 represents the free field and all the other peripheral sources represent the virtual sources, where each of them is an image of S_0 corresponding to a specific reflection configuration. An order 0 of reflection would correspond only to the source S_0. An order 1 of reflection would correspond to the contribution of the sources in the rectangles where the reflection coefficient is β. These sources are S_1, S_3, S_5, and S_7 of the middle plane (see Figure 2.14), and S_0 in the ground and ceiling plane level 1 (see Figure 2.15). An order 2 of reflections corresponds to the contribution of all the sources in Figures 2.14 to 2.17 where the reflection coefficient in rectangular virtual rooms is β^2. Accordingly, an order 3 of reflections corresponds to the contribution of all the sources in Figures 2.14 to 2.17 where the reflection coefficient is β^3.

In reality, the real source S_0 is located on a wall in this research, but for a better view it is dislocated as shown in Figure 2.14. The coordinates of all the virtual sources along with their order of reflections are presented in Table 2.4 assuming real source is at $(0,0,Z)$. The Z coordinate of these sources is Z since the middle plane corresponds to any plane between the ceiling and the ground of the room; therefore the coordinate is free: $Z \in [0,h]$ where h=height of the room.

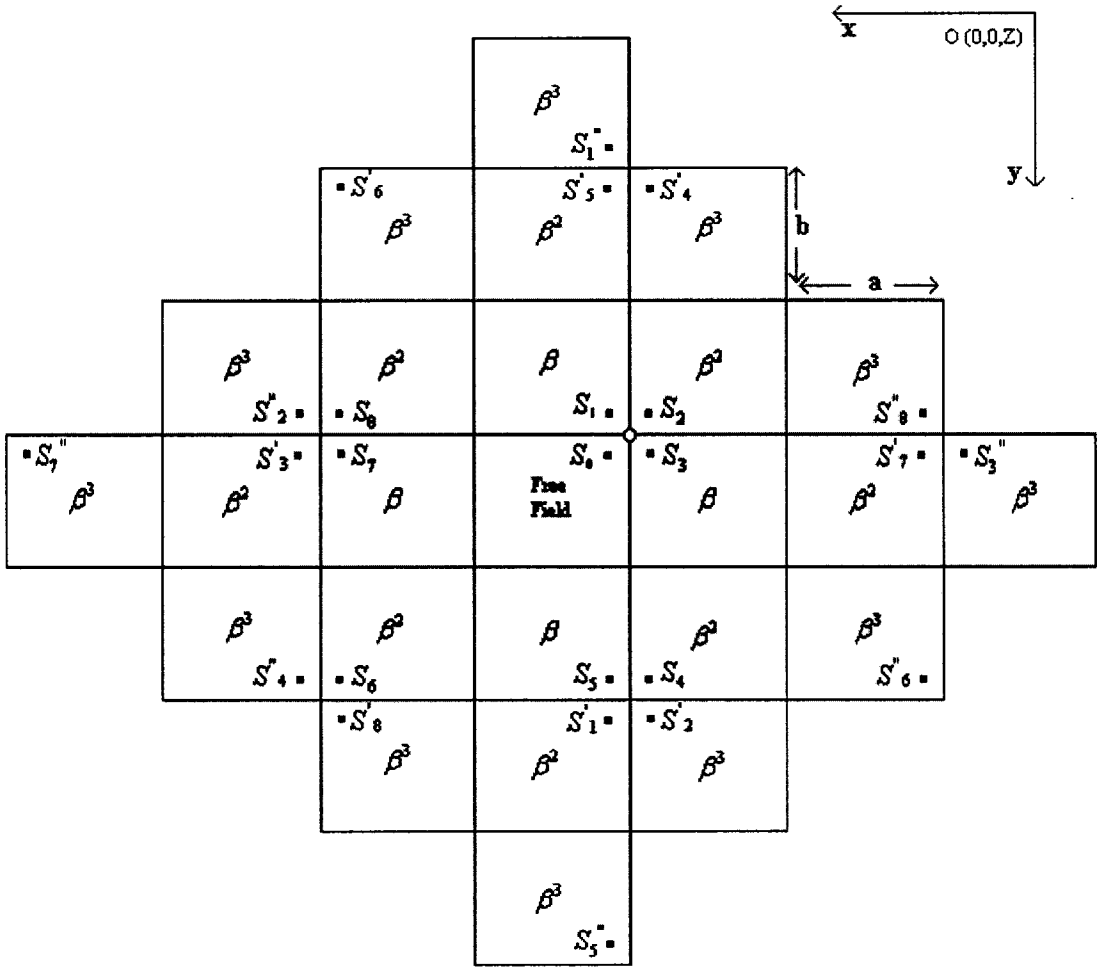

Fig. 2.14: Middle plane virtual sources configuration for order 0, 1, 2 and 3.

Above the real room, many levels of virtual rooms exist. Each level represents a cut of the surfaces of the virtual rooms above the real room. Since the maximum order of reflection used in this research is three, three planes of virtual rooms are presented, where each corresponds to a certain level of height (see Figures 2.15, 2.16 and 2.17).

The coordinates of all the virtual sources of ceiling level 1 (Figure 2.15) along with their order of reflections are presented in Table 2.5.

Source	X	Y	Z	Order N
S_0	0	0	Z	0
S_1	0	0	Z	1
S_2	0	0	Z	2
S_3	0	0	Z	1
S_4	0	2b	Z	2
S_5	0	2b	Z	1
S_6	2a	2b	Z	2
S_7	2a	0	Z	1
S_8	2a	0	Z	2
S'_1	0	2b	Z	2
S'_2	0	2b	Z	3
S'_3	2a	0	Z	2
S'_4	0	-2b	Z	3
S'_5	0	-2b	Z	2
S'_6	2a	-2b	Z	3
S'_7	-2a	0	Z	2
S'_8	2a	2b	Z	3
S''_1	0	-2b	Z	3
S''_2	2a	0	Z	3
S''_3	-2a	0	Z	3
S''_4	2a	2b	Z	3
S''_5	0	4b	Z	3
S''_6	-2a	2b	Z	3
S''_7	4a	0	Z	3
S''_8	-2a	0	Z	3

Table 2.4: Sources coordinates in the middle plane.

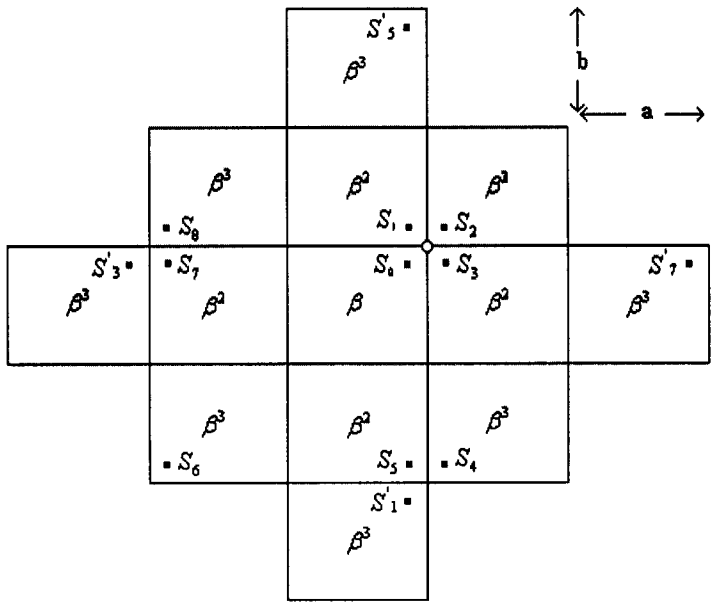

Fig. 2.15: Ceiling/ground plane level 1 virtual sources configuration for order 1, 2 and 3.

Source	X	Y	Z	Order N
S_0	0	0	2h-Z	1
S_1	0	0	2h-Z	2
S_2	0	0	2h-Z	3
S_3	0	0	2h-Z	2
S_4	0	2b	2h-Z	3
S_5	0	2b	2h-Z	2
S_6	2a	2b	2h-Z	3
S_7	2a	0	2h-Z	2
S_8	2a	0	2h-Z	3
S'_1	0	2b	2h-Z	3
S'_3	2a	0	2h-Z	3
S'_5	0	-2b	2h-Z	3
S'_7	-2a	0	2h-Z	3

Table 2.5: Virtual sources coordinates in the ceiling plane of level 1.

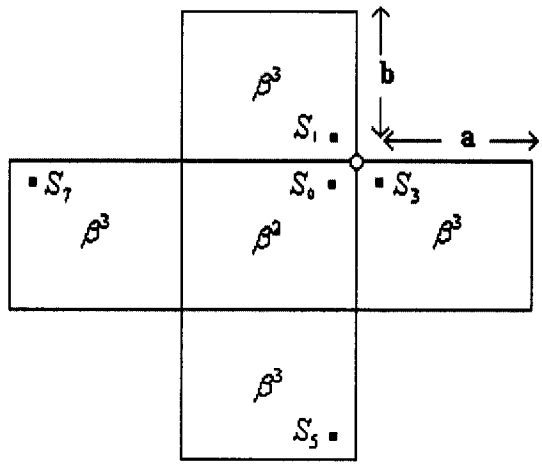

Fig. 2.16: Ceiling/ground plane level 2 virtual sources configuration for order 2 and 3.

The coordinates of all the virtual sources of the ceiling level 2 (Figure 2.16) along with their order of reflections are presented in Table 2.6.

Source	X	Y	Z	Order N
S_0	0	0	2h+Z	2
S_1	0	0	2h+Z	3
S_3	0	0	2h+Z	3
S_5	0	2b	2h+Z	3
S_7	2a	0	2h+Z	3

Table 2.6: Virtual sources coordinates for the ceiling plane of level 2.

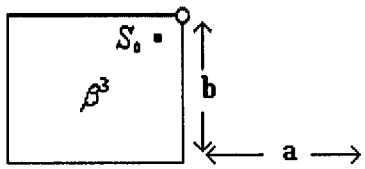

Fig. 2.17: Ceiling/ground plane level 3 virtual sources configuration for order 3.

The coordinates of all the virtual sources of ceiling level 3 (Figure 2.17) along with their order of reflections are presented in Table 2.7.

Source	X	Y	Z	Order N
S_0	0	0	4h-Z	3

Table 2.7: Virtual sources coordinates for the ceiling plane of level 3.

Similarly, for the virtual rooms below ground, three planes are presented where each corresponds to a certain level of height (see Figure 2.15, 2.16 and 2.17).
The coordinates of all the virtual sources of ground level 1 (Figure 2.15) along with their order of reflections are presented in Table 2.8.

Source	X	Y	Z	Order N
S_0	0	0	-Z	1
S_1	0	0	-Z	2
S_2	0	0	-Z	3
S_3	0	0	-Z	2
S_4	0	2b	-Z	3
S_5	0	2b	-Z	2
S_6	2a	2b	-Z	3
S_7	2a	0	-Z	2
S_7	2a	0	-Z	3
S'_1	0	2b	-Z	3
S'_3	2a	0	-Z	3
S'_5	0	-2b	-Z	3
S'_7	-2a	0	-Z	3

Table 2.8: Virtual sources coordinates in the ground plane of level 1.

The coordinates of all the virtual sources of ground level 2 (Figure 2.16) along with their order of reflections are presented in Table 2.9.

Source	X	Y	Z	Order N
S_0	0	0	-2h+Z	2
S_1	0	0	-2h+Z	3
S_3	0	0	-2h+Z	3
S_5	0	2b	-2h+Z	3
S_7	2a	0	-2h+Z	3

Table 2.9: Virtual sources coordinates for the ground plane of level 2.

The coordinates of all the virtual sources of ground level 3 (Figure 2.17) along with their order of reflections are presented in Table 2.10.

Source	X	Y	Z	Order N
S_0	0	0	-2h-Z	3

Table 2.10: Virtual sources coordinates for the ground plane of level 3.

2.4.4 Late reverberation

As shown in section **2.2.5,** the classical equation for calculating sound pressure in room (equation 33) includes a direct wave component and a general reverberation term R as follow:

$$R = \frac{\bar{\alpha} S}{1 - \bar{\alpha}}. \qquad (27)$$

This term is meant to include all reflection components (early + late). In this research, we are explicitly modeling the direct wave and early reflections; thus, equation (27) must be adapted.

As discussed before (section **2.2.5**), the total energy of the direct field in the room is (Irwin & Graf, 1979):

$$E_d = \frac{4WV}{cS} \qquad [J]. \qquad (35)$$

By extension, the energy of the first order of reflections is given by:

$$Er_1 = \frac{4WV}{cS}\beta \qquad [J] \qquad (36)$$

where β is the reflection coefficient. This is the total energy in the room arising from one surface reflection only. The energy of the second order of reflections is given by:

$$Er_2 = \frac{4WV}{cS}\beta^2 \qquad [J]. \qquad (37)$$

Generalizing, the energy of the n[th] order of reflections is given by:

$$Er_n = \frac{4WV}{cS}\beta^n \qquad \text{[J]}. \qquad (38)$$

The energy of the residual reverberant field beyond the n[th] order of reflections can now be obtained. This is obtained by subtracting the direct energy and the energy of all reflections up to the n[th] order of reflections from the total energy in the room. The latter is obtained by multiplying equation (22) by the volume V of the room.

Thus we have:

$$\begin{aligned}
\delta_r V &= \frac{4WV}{\bar{\alpha}cS} - \frac{4WV}{cS}[1+\beta+\beta^2+...+\beta^n] \\
\delta_r V &= \frac{4WV}{cS}[\frac{1}{1-\beta} - (1+\beta+\beta^2+...+\beta^n)] \\
\delta_r V &= \frac{4WV}{cS}[\frac{1-(1+\beta+\beta^2+...+\beta^n-(\beta+\beta^2+...+\beta^n+\beta^{n+1}))}{1-\beta}] \\
\delta_r V &= \frac{4WV}{cS}[\frac{\beta^{n+1}}{1-\beta}] \\
\delta_r V &= \frac{4WV}{cS}[\frac{(1-\bar{\alpha})^{n+1}}{\bar{\alpha}}] \\
\delta_r V &= \frac{4WV}{cR_n}
\end{aligned} \qquad \text{[J]} \qquad (39)$$

where:

R_n is the residual room constant after n[th] order of reflections; i.e.:

$$R_n = \frac{\bar{\alpha}S}{(1-\bar{\alpha})^{n+1}} \qquad [\text{m}^2]. \qquad (40)$$

For a zero order of reflection (direct field only), R_n reduces to the usual room constant (equation 27).

2.4.5 Total sound pressure level

At the receiver, the energy from the direct field, early reflected sound and residual reverberant field are added. The phase effects are being neglected.

For N order of reflections, the following equation is used:

$$L_p = L_w + 10\log(\frac{1}{4\pi r_{S_0}^{\ 2}} + \sum_{\forall n \le N} \frac{\beta^n}{4\pi r_{S_i}^{\ 2}} + \frac{4}{R_N}) \qquad \text{[dB]. (41)}$$

For instance, for N=1 (order 1 of reflection), the contribution of S_0, S_1, S_3, S_5 and S_7 in the middle plane (Figure 2.14), the contribution of S_0 in the ground plane level 1 (Figure 2.15), and the contribution S_0 in the ceiling plane level 1 (Figure 2.15) are added.

From equation (41), the sound pressure level would be:

$$L_p = L_w + 10\log(\frac{1}{4\pi r^2 S_0} + \frac{\beta}{4\pi r^2 S_1} + \frac{\beta}{4\pi r^2 S_3} + \frac{\beta}{4\pi r^2 S_5} + \frac{\beta}{4\pi r^2 S_7} + \frac{\beta}{4\pi r^2 S_{0G}} + \frac{\beta}{4\pi r^2 S_{0C}} + \frac{4}{R_1}) \qquad (43)$$

where:

R_1=Room constant for order 1 of reflection

$$R_1 = \frac{\bar{\alpha} S}{(1-\bar{\alpha})^2}.$$

In theory, a high order of reflections (e.g. n>10) would cover the reverberant field without the need for a statistical late reverberation term. However, this approach may not be realistic for several reasons:

1. An industrial room is not perfectly rectangular; therefore, sound rays would deviate from model predictions after colliding several times with the room boundaries;
2. The room contains objects and workers which are not modeled; as a result, sound rays may diverge from model predictions after a few reflections;
3. The current model assumes that the acoustic absorption is uniformly distributed over the room boundaries;
4. The computational load increases rapidly with the order of reflections simulated and can become excessive if the computation of a large number of source-receiver configurations is required.

The warning sound optimization problem targeted in this research (section 1.4) requires the computation of a large number of source-receiver configurations. Moreover, the number of sources and their positions are not known a-priori. For these reasons, a maximum order of three reflections is considered in this research. This ensures

computational efficiency while allowing wall-placement directivity effects to be considered.

In summary, the proposed method combines the advantages of the classical method (no detailed room modeling) and the mirror image method (higher accuracy especially for sources and receivers near walls). While limited to rectangular room sizes and omnidirectional sources, it can be used with only knowledge of the overall dimensions of the room and the reverberation time. The latter can be easily measured with standard sound measurement equipment and ensures that the sound absorption coefficient used in the model is "calibrated" to the actual room under study. This is in contrast to the simpler standardized method for sound level prediction in rooms (CSA Z107.52-M1983), which relies on very broad judgments of absorption (highly, partly or poorly absorbing) by the user and accounts only for first-order wall and ceiling effects, without residual reverberation. More advanced room simulation methods, such as L'Espérance (2000) for noise control engineering applications, are valid for arbitrary room sizes; however, they require a detailed geometrical model of the room and the specification of each sound absorption surface, which is more time consuming from the user point of view and more difficult to "calibrate" in the field since it relies on tabulated absorption coefficients instead of measurements. The proposed method is a compromise between accuracy, ease of use and the requirement for simulating a large number of source-receiver configurations in the current application for warning device installation.

Chapter 3: Design and implementation of "AlarmLocator"

The main goal of this research is to develop a method to facilitate the installation of acoustic warning devices in the workplace. This is accomplished with a tool referred to as "AlarmLocator" that simulates the process of sound propagation of auditory warning signals from the physical device location (on walls or ceiling) to the position of individual workers or workstations in the room. More specifically, this tool aims at determining the number of alarm devices to use, their optimal placement in the plant, and their sound power characteristics.

In this chapter, an outline of the warning sound optimization problem is presented. The algorithmic procedures and the design and implementation of the software tool are also discussed in details. Finally, case studies are presented.

3.1 The warning sound optimization problem

In this section, an outline of the warning sound optimization problem is described. The objective function, variables, and constraints of the optimization problem are also discussed. Basic algorithmic considerations and assumptions are exposed. A similar method to optimally install acoustic warning signals in the workplace by Nanthanvanij & Yenrades (1999) is also discussed.

3.1.1 The problem

In Figure 3.1, a hypothetical factory room illustrates the warning sound optimization problem. The room contains three workstations with some workers wearing hearing protector devices (HPDs). It can also be assumed that there is a background noise from the machinery equipment, which can mask warning sounds. The installation of acoustic warning devices thus requires knowledge of the background noise in the room, the hearing protector attenuation, and the hearing status of the workers to determine the audibility of warning sounds in the workplace.

Acoustic standard ISO 7731 (Danger signals for public and work areas) presents a set of guidelines to determine the sound level an alarm should produce at a given workstation. A software tool called "Detectsound" was also previously developed to determine

whether the sound pressure level of an acoustic warning signal satisfies the constraints for optimal detection and recognition by the attending workers at any given workstation (Zheng, 2003; Zheng et al., 2006). "Detectsound" is particularly useful when assessing the suitability of existing alarm systems, where the alarm sound level can be measured at each workstation. Unfortunately, these two tools do not provide a scientific method to guide installation of acoustic warning devices on wall or ceiling in a room in such a way that all workstation alarm levels fall within the optimal level with a minimum number of devices. The purpose of this research is to cover this requirement.

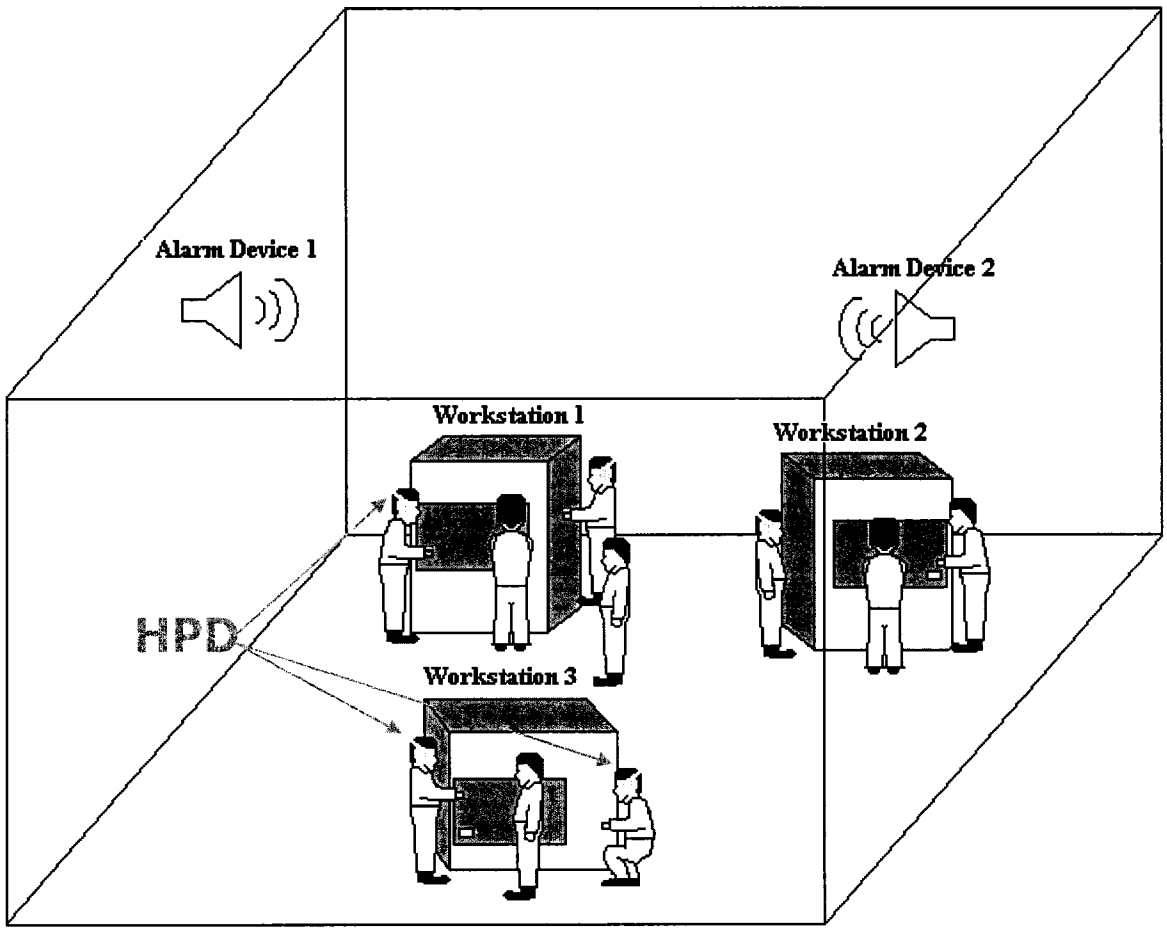

Fig. 3.1: Factory room having three workstations attended by workers, some wearing HPDs. Two warning devices are to be optimally located to ensure audibility of warning sounds by all workers.

3.1.2 Optimization problem

The warning device optimization problem can then be summarized as follows:

Objective optimization function:

- Minimize the number of warning devices required to meet the alarm sound level constraints at each workstation;
- Optimally locate the warning devices on walls; and
- Specify the optimal sound power level (L_w) of each alarm.

Constraints:

- The total warning signal sound level Lp_k produced by the aggregate of all warning devices shall be within the warning sound level conception window or targets specified by the psychoacoustic tool "Detectsound" for all workstations k. i.e Lp_k is within $[TL_{min}, TL_{max}]_k$ $(1 \leq k \leq N_S)$; where N_S is the number or workstations.
- The A-weighted sound level at any location in the room is limited to 118 dBA (ISO 7731).

Variables:

- Number of warning devices N_D ;
- Spatial coordinates (X_i, Y_i, Z_i) of the warning devices $(1 \leq i \leq N_D)$; and
- Power level L_{wi} of the alarms $(1 \leq i \leq N_D)$.

3.1.3 Search method

The optimization algorithm used in this research exhaustively seeks all possible alarm's positions on the walls around the room. Initially, one warning device D1 is considered in the factory room. The factory walls are assumed to be encircled by a virtual "spiral like" path which contains a number of nodes that constitute the legitimate set of locations where the warning devices can be placed, as shown in Figure 3.2. The warning device D1 is tested for all the nodes in the room going from the first node to the last. If no solution is found, another warning device D2 is added and the process of searching and testing is repeated. The search process stops once valid solutions are found with a given minimum number of devices.

3.1.4 Assumptions

This research deals with industrial plants that are essentially of rectangular form and assumes that the sound absorption is evenly distributed on the boundaries surfaces in the room. The corresponding average absorption coefficient $\overline{\alpha}$ is computed based on the

Eyring/Sabine theory and knowledge of the reverberation time in the room. This research also deals with warning devices that are assumed to be omnidirectional sources.

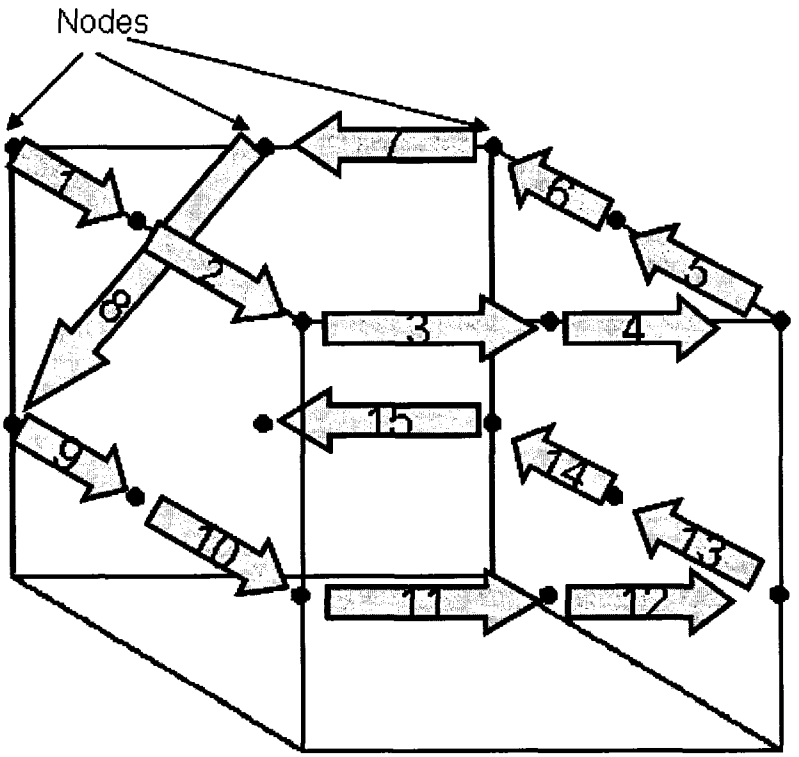

Fig. 3.2: Spiral path over which the acoustic alarm devices are tested. The black nodes represent the set of locations where the warning devices can be placed.

3.1.5 Other techniques to install acoustic warning devices

Some researchers (Nanthanvanij & Yenrades, 1999) have recently attempted to solve this problem by providing a set of analytical methods for predicting the optimum number, location, and sound power level of auditory warning devices for manufacturing facilities. However, their methods only considered the direct sound field propagation from alarm devices to workstations. In other words, they assumed that the room is an open area. Thus, the effects of sound reflection from walls, ceiling, floor and solid obstacles in the work plant were ignored. In typical facilities, this assumption is unrealistic once the distance between alarm devices and workers is more than a few meters. In practice, industrial work plants are often very reverberant, so that reflected sound waves can contribute considerably to the overall sound level at the receiver. In addition, their

methods do not directly account for the effects of hearing loss (or hearing status in general) or the use of hearing protectors.

This research presents a more realistic solution to the problem of installing acoustic warning devices in noisy work plants. Both the direct field from the alarm devices and the reverberant field due to walls, ceiling, floor and other reflections are considered. The solution is based on knowledge of the room acoustic characteristics in the work area, such as the reverberation time and room layout, the sound power characteristics of warning devices, and the distance between each warning device to each workstation. The new tool can be integrated with psychoacoustic tool "Detectsound" (Zheng, 2003; Zheng et al. 2006) to provide a solution targeted to the individual workers in the plant, which accounts for the effects of hearing loss and HPD use.

3.2 Algorithmic procedures

3.2.1 Initial algorithm for "AlarmLocator"

A first algorithm was designed in the early stages of the research and published as Al Osman et al. (2006). It is based on the room acoustics equation (33) and considers the directivity effects due to wall source placements presented in section **2.2.5.** Accordingly, the directivity factor Q is made equal to 2, 4 or 8 if the sound source is placed on a hemispherical plane, corner of two planes or a corner of three planes, respectively, as previously shown in Figure 2.3.

3.2.1.1 Algorithm

Initially, we suppose that we only need one warning device D1 in the factory room. D1 is tested for all the nodes in the room going from the first node to the last as shown in Figure 3.2. After reaching the last node, the alarm returns to the first node, its power level is incremented, and again it gets tested at each node until it loops back to the initial node. The looping will continue until D1 reaches its maximum power level, and if no solution meeting the constraints is reached, another alarm device D2 is added while D1's power level is reset to its initial value. D1 and D2 are tested for all the possible configurations on the node grid. For instance, assuming a room containing 16 different nodes (16 different placements for alarms), then the number of possible configurations is 16x15 =

240. After testing all the configurations, the power level of D1 is increased. We keep on testing all the possible configurations and increasing D1 until it reaches its maximum power level, then D2's power level is increased, D1's power level is reset and the process is restarted. This process goes on until D2 reaches its maximum power level. If no practical solutions are found at this point, a third alarm is added and the whole process of looking for feasible solutions restarts.

The process of adding warning devices continues until at least one practical solution is achieved. A solution is obtained if the combined sound pressure level computed from all the alarm devices satisfies the design constraints imposed by Detectsound at each workstation.

3.2.1.2 Inputs

The inputs for this version of "AlarmLocator" are as follows:

Inputs:

- The room geometry parameters (width, length and height of the room);
- Reverberation time measured or estimated;
- Classical room acoustics formulation (Sabine or Eyring);
- Alarm options parameters (minimum and maximum power level, power level step size, maximum number of alarms, minimum alarm height, and horizontal and vertical node step size along walls);
- Workstations number N_s and their spatial coordinates; and
- Warning signal level targets at each workstation from Detectsound $[TL_{max}, TL_{min}]_k$ $(1 \leq k \leq N_s)$.

3.2.1.3 Sound pressure level computation

The classical room acoustics theory exposed in section **2.2** is used for version 1 of "AlarmLocator". Using Eyring's theory, the sound pressure level L_p at a distance r from a given alarm device source is given by equation (33):

$$Lp = Lw + 10\log\left(\frac{Q}{4\pi r^2} + \frac{4}{R}\right) \text{ [dB].}$$

If Sabine formulation is used, the absorption of the room A replaces the room constant R in equation (33). Assuming there are a total of N_D simultaneous alarm devices being

tested in the work plant, the combined sound pressure level at a given workstation k is obtained as follows:

$$Lp_k = \sum_{i=1}^{N_D} 10^{(Lp_{ik}/10)} \quad \text{[dB]} \qquad (44)$$

where:

Lp_k = total sound pressure level at workstation k from all alarms devices [dB]
Lp_{ik} = sound pressure level contribution of alarm source i at workstation k [dB]
N_D = number of alarms devices in the work plant.

Equation (44) assumes a summation of acoustic energy from all alarm devices at any given point in the room, so it is representative of the spatial average of the sound level near a workstation.

3.2.1.4 Drawbacks

As discussed in section **2.4.1,** the prediction of the directivity factor Q as 2, 4 or 8 is inaccurate when the surrounding surfaces of the source are not totally reflective and poses practical problems for certain positions of the source as shown in Figure 2.13. As a result, a simple method to compute the wall directivity effects was developed by introducing the concepts from the mirror image method (section **2.3)**. Moreover, the initial algorithm can only accommodate for a single alarm frequency component at a time. A multi-frequency algorithm accommodating up to five frequency components concurrently is presented in section **3.2.2.**

3.2.2 Multi-frequency algorithm using a hybrid method

A hybrid method that combines the mirror image method (section **2.3**) and the classical room acoustics theory (section **2.2**) is used to compute the sound pressure level due to acoustic warning devices in the room. An updated version of "AlarmLocator" has been developed based on this simulation method (section **2.4**). This version is also expanded to achieve multi-frequency alarm solutions.

3.2.2.1 Algorithm

This algorithm is an updated version of the algorithm presented in section **3.2.1**. This version provides solutions for multiple frequencies. It accounts for up to five different alarm frequencies presented separately or simultaneously. For each frequency, the average absorption coefficient $\bar{\alpha}$ in the room is estimated from reverberation time measurements at the corresponding one or third octave band.

A procedure similar to the optimization algorithm in section **3.2.1.1** is used for the multi-frequency version. Once again, we assume that only one warning device D1 is needed in the room. The interior walls are subdivided into a grid layout where the nodes represent the set of possible positions where a warning device can be installed (Figure 3.3).

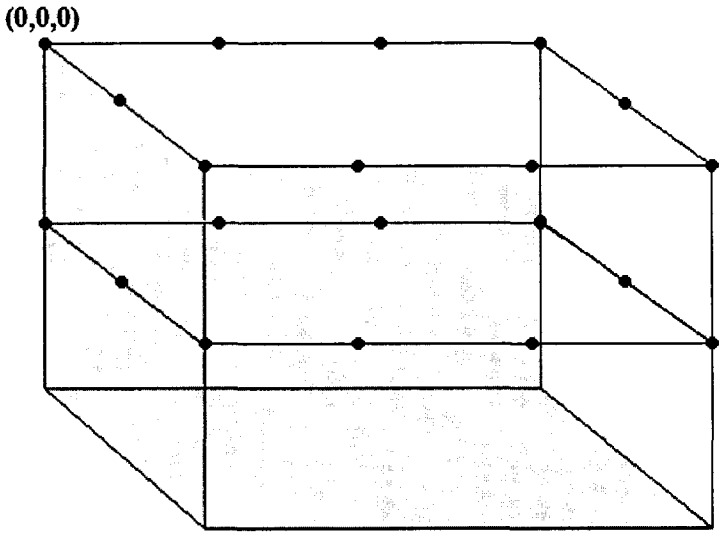

Fig. 3.3: Alarm grid layout in the factory room.

Originally, D1 travels along the grid around the room in a spiral like fashion from the ceiling down to the minimum height specified by the user while looking for a valid solution at each node. Moreover, the sound power level of the acoustic warning signal is incremented by a power level step size over a practical range at each node to search for all possible solutions. This is shown in Figure 3.4. The maximum power level that could be reached is limited to 120 dB unless the user chooses a different upper limit.

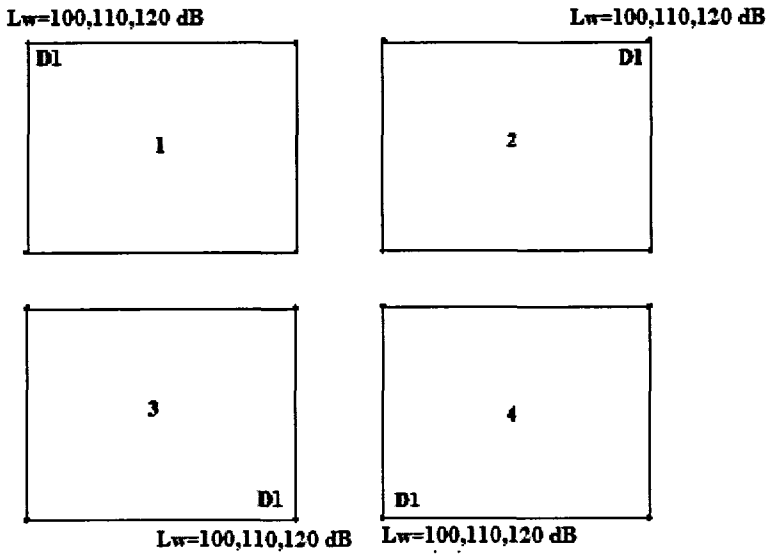

Fig. 3.4: Alarm device D1 routing in a spiral fashion around the grid layout of the factory room. The alarm device D1 power level is incremented over all the possible levels at each node until a solution is found or the maximum power level is reached. The minimum and maximum power levels of the alarms are chosen to be 100 dB and 120 dB in this example (power level step size is 10 dB).

If the acoustic warning device has circulated over the entire grid layout and no solution is found, another warning device D2 is added. D2 is then fixed at the starting position (Figure 3.5) while D1 travels along the coiled path. At each grid node reached by device D1, the current configuration of warning devices is tested for a valid solution by varying the power level of D1 over a realistic range at each node (Figure 3.5). Once the power level L_{wD1} reaches the maximum power level, we reset L_{wD1} to its initial value and increment Lw_{D2} by a power level step size (Figure 3.5, second panel). Lw_{D1} is then varied over a realistic range and tested for each configuration (Figure 3.5, second panel). If no solution is found, L_{wD2} is incremented again and the same procedure is repeated until L_{wD2} has reached the maximum power level (See Figure 3.5, third panel). Then we reset the power level for D2 and the alarm device D1 is moved one step towards the next node (Figure 3.5, fourth panel). The same process continues until D1 loops the entire grid layout of the room. Note that a test for a possible solution is performed every time a new configuration is generated by either moving an alarm or incrementing its power level.

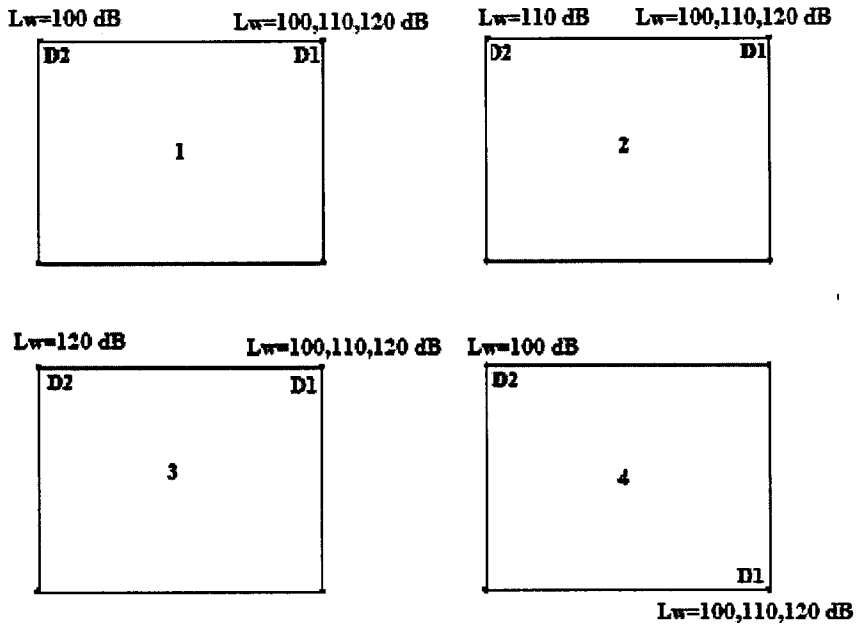

Fig. 3.5: Alarm devices D2 and D1 routing in a spiral fashion around the grid layout of the factory room. The alarm device D1 is moved one step towards the next node when the power level of the alarm device D2 has reached the maximum threshold.

Next, the two alarm devices will each move one step towards to the next node on the grid. The alarm device D1 new loop is now updated while the alarm device D2 maintains its initial looping coordinates as shown in the first panel in Figure 3.6. Once again, D1 is incremented over its range and tested for a feasible solution. Once L_{wD1} reaches its maximum power level threshold, L_{wD1} is reset and L_{wD2} is incremented by a power level step size. This keeps going until L_{wD2} attains the maximum power level, then D1 moves one step towards the next node. This is shown in the second and third panels of Figure 3.6. The same process continues until D1 reaches the next node as shown in fourth panel in Figure 3.6.

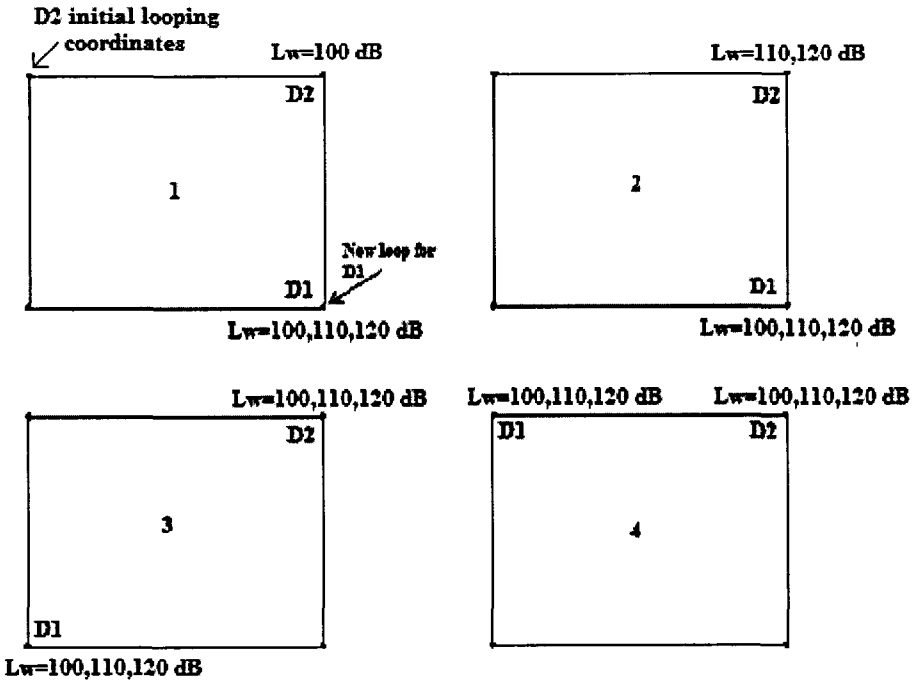

Fig. 3.6: Alarm devices D2 and D1 routing in a spiral fashion around the grid layout of the factory room. The alarm device D1 renews its looping coordinates as shown in the first panel.

If no solution is found, the two alarm devices D1 and D2 will each move then one step towards the next step as shown in Figure 3.7. The alarm device D1 new loop is now updated while the alarm device D2 still maintains its initial looping coordinates.

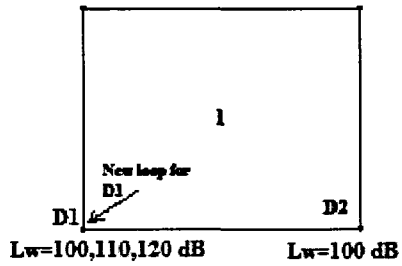

Fig. 3.7: Alarm devices D2 and D1 routing in a spiral fashion around the grid layout of the factory room. The alarm device D1 renews its looping coordinates.

The same process continues until the alarm device D2 loops. If no solution is found, then a new alarm D3 is added as shown in Figure 3.8.

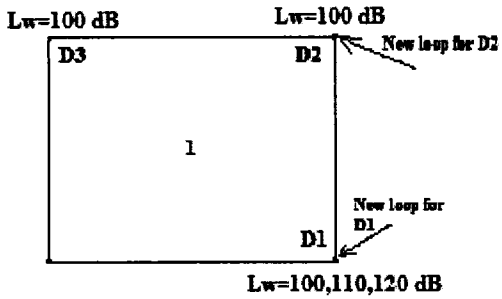

Fig. 3.8: Alarm device D3 is added to the configuration. Alarm devices D2 and D1 renew their looping coordinates.

This alarm routing would carry on until a solution is found with the least number of alarms N_D for the selected frequency. The algorithm then searches for all possible solutions with that number of alarms. The algorithm also exits if the maximum number of alarm devices has been reached. Next, solution coordinates are tested for the remaining frequencies to check if their sound pressure levels at each of the workstations can also satisfy the design window set by "Detectsound". Interim solutions that do not satisfy the requirements at any one of the selected frequencies are disregarded. As a result, final solutions consist in the same coordinates for all the selected frequencies, but the power levels may differ.

Finally, the tool can generate a map of the warning sound level distribution in the room for each solution. The implementation of the "AlarmLocator" model is illustrated in the flow chart depicted in Figure 3.9.

3.2.2.2 Inputs

The process starts by defining the required parameters for the computations. This includes:

- The room geometry parameters (width, length and height of the room);
- Reverberation time for the selected frequencies in the room or the corresponding acoustic average absorption coefficient in the room;
- Late reverberation theory (None, Sabine, Eyring) along with the order of early reflections (0,1,2 or 3) to consider;
- Alarm options parameters (minimum and maximum power level, power level step size, maximum number of alarms, minimum height, and horizontal and vertical node step size along walls);

- Workstations number and their spatial coordinates; and
- Warning signal level targets at each workstation from Detectsound $[TL_{max}, TL_{min}]_k$ $(1 \leq k \leq N_S)$.

3.2.2.3 Sound pressure level computation

As mentioned earlier, a hybrid method that combines the mirror image method and the classical room acoustics theory is used to compute the sound pressure level of the acoustic warning devices (section **2.4).** The sound pressure level for N order of early reflections using Eyring residual reverberation is shown in equation (41).

3.3 "AlarmLocator" software

In this section, several aspects of the software tool "AlarmLocator" will be illustrated. Each block in Figure 3.9 will be represented by its graphical interface window and will be accompanied with a detailed step by step analysis.

3.3.1 Flow chart

Figure 3.9 reveals the process of "AlarmLocator" from entering the input parameters to obtaining the optimum number, location and power level for acoustic warning devices.

3.3.2 Entry of room geometry parameters

The room geometry is described by the width, length and height of the room. The unit used is meter. Values can be integers or floats. An identification name for the room can be specified as well (Figure 3.10). Given these parameters, the total surface of the interior surfaces S and the volume of the room V can be computed.

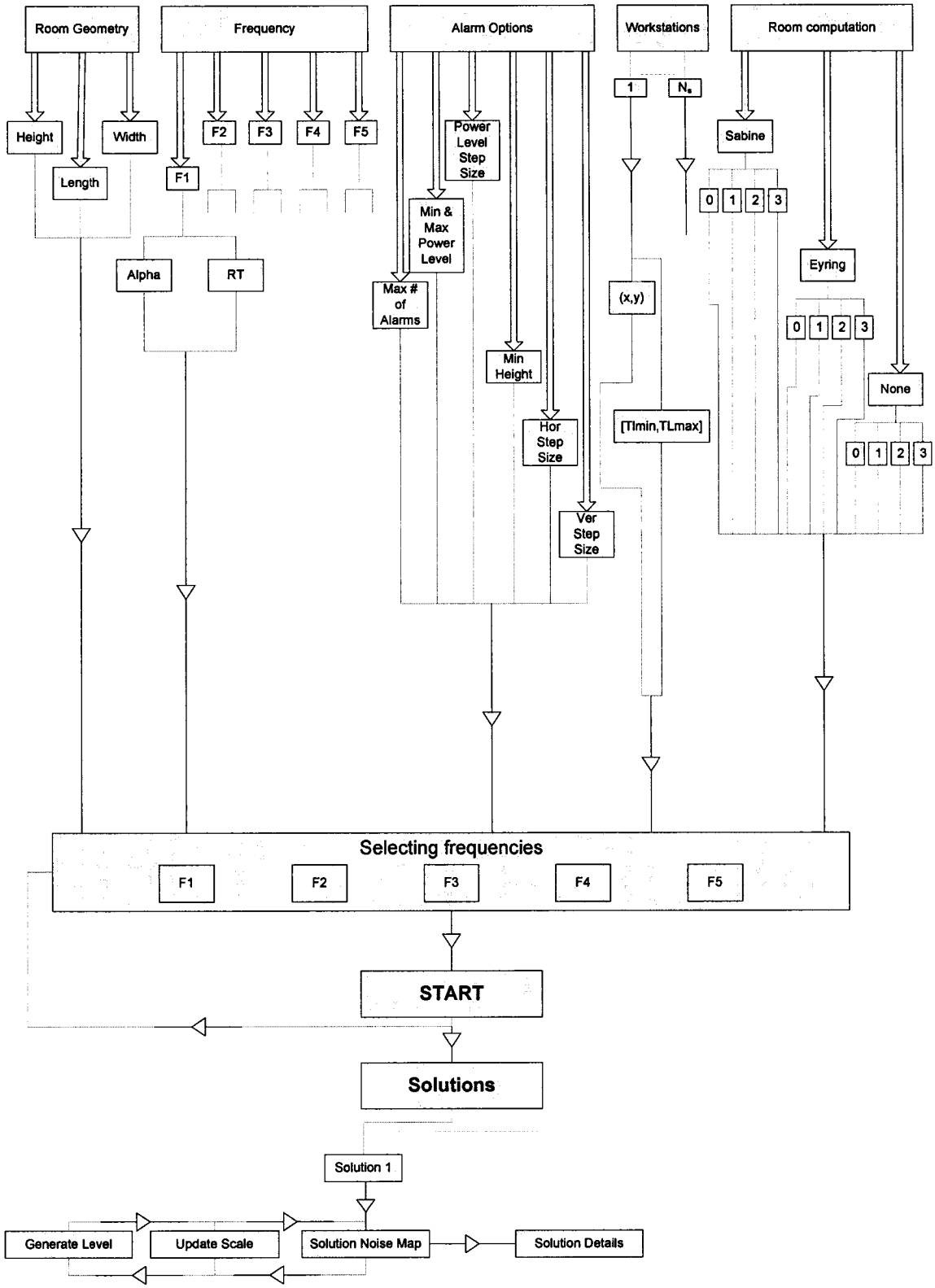

Fig. 3.9: Flow chart of "AlarmLocator".

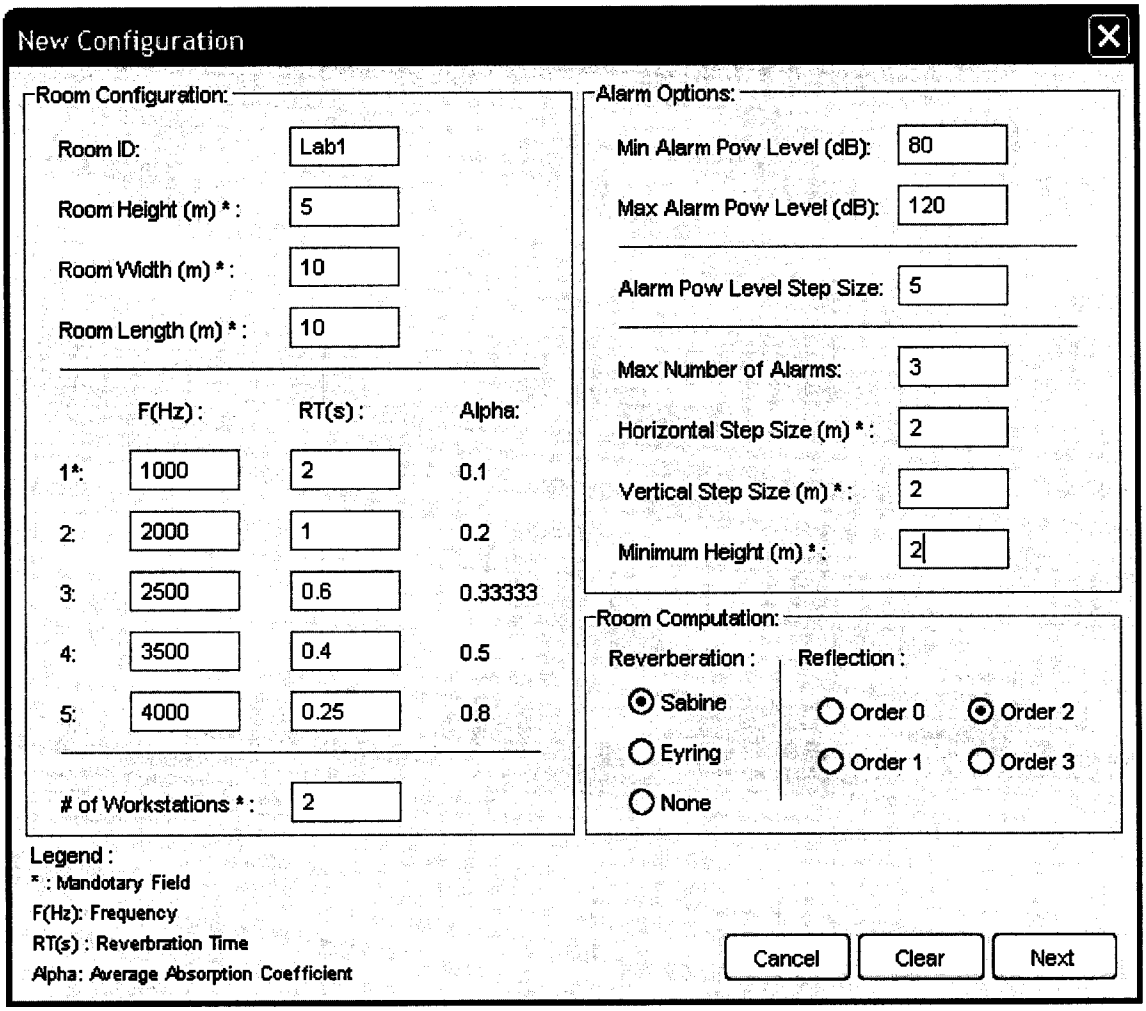

Fig. 3.10: Main graphical user interface for "AlarmLocator" for entering the input parameters (room configuration, number of workstations, alarm options and room computations).

3.3.3 Entry of reverberation time

The reverberation time is an input parameter in the simulation software. It could be measured (section **2.3.2.3)** or estimated (section **2.2.4.5.2**) using various techniques. The room average absorption coefficient $\bar{\alpha}$ can be calculated once the reverberation time is known. This has been taken into consideration in "AlarmLocator" to determine the room constant according to equation (40).

Since the reverberation time depends on frequency, a choice of up to five frequencies can be selected in which each frequency has its own reverberation time specification and calculated average absorption coefficient as shown in Figure 3.10.

3.3.4 Entry of alarm options parameters

The default minimum power level of the alarm devices is set to 80 dB. The maximum power level is set according to guidelines from ISO 7731 to ensure that the A-weighted sound level at any location in the room is limited to 118 dBA. The default maximum and minimum power levels can be changed by the user in the window interface as shown in Figure 3.10. As described in section **3.2**, the alarm device is incremented by a given power level step to scan over possible solutions. The default power level step size is set to 5 dB and can be changed by the user as shown in Figure 3.10.

Alarm devices jump from node to node to scan for solutions. The horizontal step size is the distance traveled by an alarm in one step when it is moving in the same plane; while the vertical step size is considered when the alarm device is moving one level down or up to the next plane. Both the horizontal and vertical step sizes are not set to any default value since they depend on room dimensions. They must be entered by the user as shown in Figure 3.10. The default minimum height where an alarm can be placed is set to 1.5 m above the ground (approximately the ear's level). The default minimum height can be modified by the user as shown in Figure 3.10.

The default maximum number of alarms that can be placed in the room is set to the number of possible nodes on the grid layout of the room in a horizontal plane. A lower maximum number of alarms can also be entered by the user as shown in Figure 3.10.

3.3.5 Entry of room computation parameters

As described in section **2.4**, the sound pressure level at each workstation is computed using a modified mirror image method consisting of up to three orders of reflections for the early reverberation. Therefore, the order of reflections should be specified by the user. Order 0 considers only the direct wave from the source(s). Order 1 considers the direct wave and virtual sources involving one surface reflection. Similarly, Order 2 and 3 considers direct wave and virtual sources involving up to 2 or 3 surface reflections. The average reflection coefficient β is determined as $(1-\overline{\alpha})$. For the residual reverberation term, three choices are presented, Sabine, Eyring, or None (Figure 3.10). The "None" option represents no residual reverberation term.

3.3.6 Entry of workstations parameters

The number of workstations must specified by the user as shown in Figure 3.10. Once the button "Next" in Figure 3.10 is pressed, an interface where the parameters of the first workstation can be entered appears. The interface eventually leads the user to enter the parameters for all the workstations.

Figure 3.11 shows a sample of the interface for this window. The minimum and maximum target levels represent the design window provided by the psychoacoustic tool Detectsound (Zheng et al., 2006). The aggregate sound pressure level of all the alarms present in the room should satisfy these constraints (see section **3.2.1** for more details). A similar window appears for each workstation in the room. The name and the spatial coordinates of the workstations are specified by the user as shown in Figure 3.11.

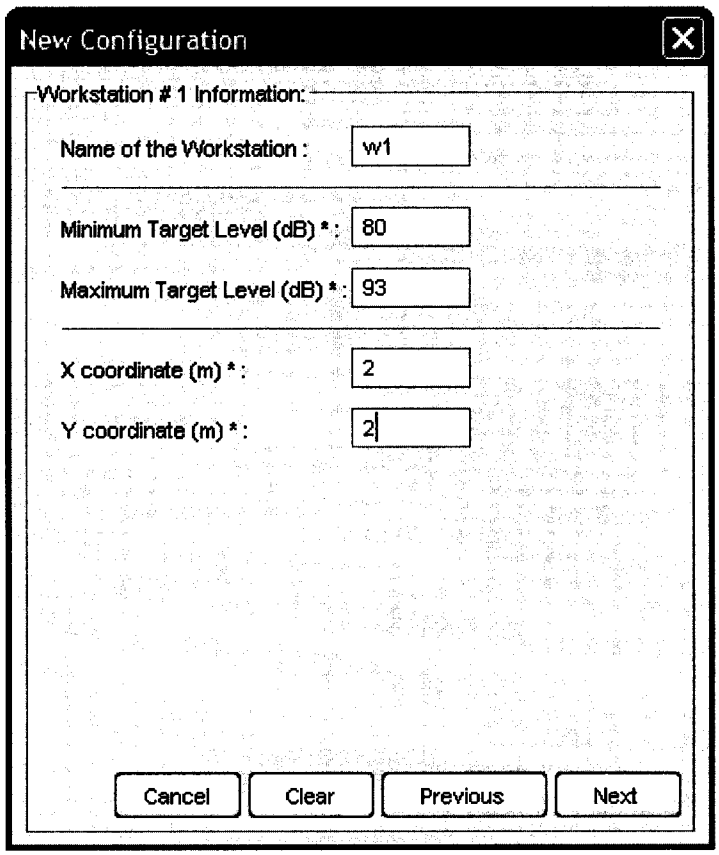

Fig. 3.11: Graphical user interface for entering the parameters for a workstation.

After completing the configuration of all the workstations, the user is directed to a window where all the parameters entered for the room and the workstations are shown on

the left side of the screen (Figure 3.12). The user may check if all the parameters are correctly entered. Pressing the start button will prompt "AlarmLocator" to begin searching for solutions.

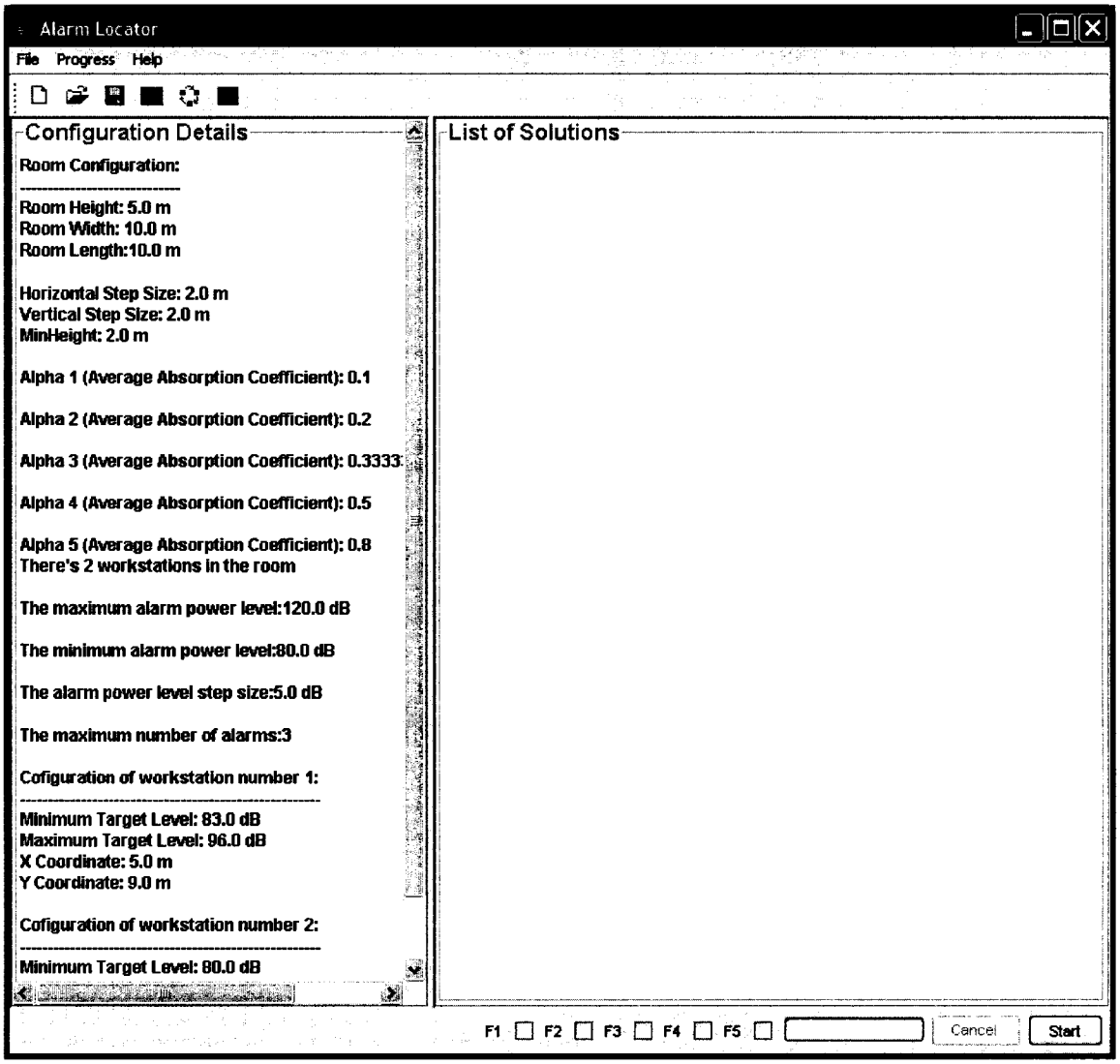

Fig. 3.12: The launch window for "AlarmLocator".

3.3.7 Solutions and results

3.3.7.1 Selecting frequencies

As shown at the bottom of Figure 3.12, the user has a choice of selecting up to five different alarm frequency components *F1*, *F2*, *F3*, *F4* and *F5*. For instance, if the user has selected all the five frequencies, "AlarmLocator" would provide solutions which

satisfy constraints for all the five frequencies simultaneously. A solution that satisfies all the frequencies should have the same number of alarms placed in the same coordinates (X,Y,Z), although the alarm's power levels could be different for each frequency.

3.3.7.2 Efficiency coefficient

Each solution presented by "AlarmLocator" satisfies the design target level from Detectsound $[TL_{min}, TL_{max}]$ at each workstation. Solutions consist of the coordinates (X,Y,Z) and the power level of the alarm device in addition to the efficiency coefficient. A solution with a sound pressure level (close to TL_{max}) is acceptable but not ideal. Similarly, a solution with a sound pressure level (close to TL_{min}) is also acceptable but not ideal. The best solution would ideally consist of a sound pressure level in the mid range of $[TL_{min}, TL_{max}]$. The efficiency is calculated as the deviation in dB from the Detectsound window as follows:

$$Efficiency = \left| \frac{TL_{\max k} + TL_{\min k}}{2} - Lp_k \right| \quad [\text{dB}] \quad (45)$$

where:

Lp_k= the aggregate sound pressure level from all the alarms at the workstation k.

The lower the efficiency value, the more effective the solution is considered. Once the efficiency coefficient at each workstation is computed, the average efficiency coefficient for a solution is obtained by averaging all the efficiency coefficients at each workstation in the workplace over all selected frequencies.

3.3.7.3 Results

The solutions are ordered according to their average efficiency coefficient in an ascending order and placed in the right panel of the main graphical user interface of "AlarmLocator", as shown in Figure 3.12. As described in section **3.2**, the algorithm provides all possible solutions in the room for the particular minimum number of devices. The reverberation time (or average absorption coefficient) are frequency dependent; therefore, the power level is also frequency dependent. Each solution provided by "AlarmLocator" for a multi-frequency configuration consists of the same coordinates

(X,Y,Z) but the alarm power level may vary from one frequency component of the alarm to another.

3.3.7.4 Warning sound level distribution

The distribution of warning sound level in the workplace can be generated for each solution at any desired height (Z coordinate) in the room by selecting one of the solutions provided by "AlarmLocator". The alarm sound map graphical user interface is shown in Figure 3.13.

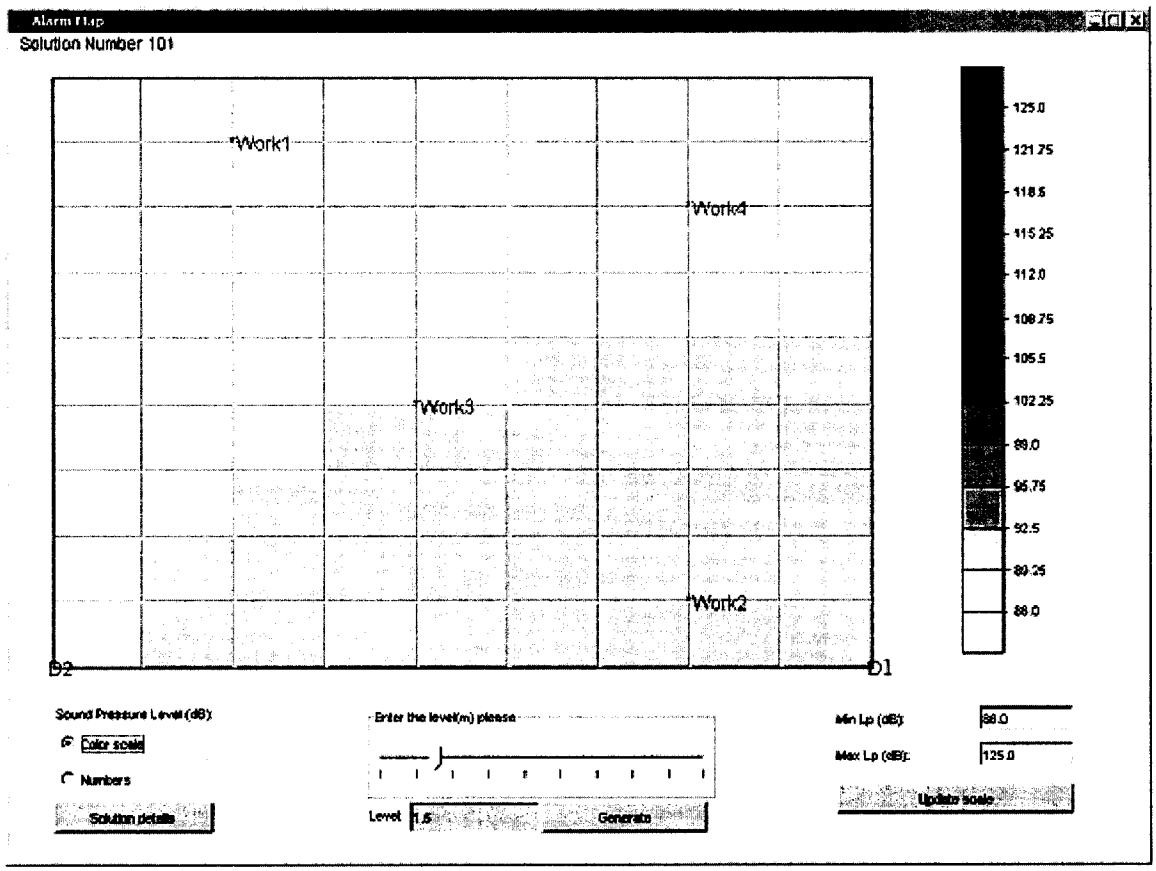

Fig. 3.13: Warning sound level distribution (dB) in the room using the default "Color" option. There are four workstations and two alarm devices.

The warning sound level distribution indicates the sound pressure level from the aggregate of all alarms in the solution. As shown in Figure 3.13, the sound map is divided into squares where each square represents 1 m^2 of the dimensions of the room. Each square is attributed to the sound pressure level of all the alarm devices at its center coordinates. The workstations are shown in red in their relative coordinates with respect

to the room. On the right hand side of Figure 3.13, a legend of the sound pressure level is provided in dB. This legend has a range from below 86 dB to above 125 dB by default. The legend range can be varied by updating the minimum and maximum sound pressure level thresholds. The alarm map is generated by default at the ear's height (1.5 m). This height can be varied from 0 m (room ground's level) up to the room's ceiling level. On the left hand side of the Figure 3.13, two display options are provided: "Color scale" (default) or "Numbers". The "Color scale" option provides the user with a colored alarm sound map according to the legend on the right side of Figure 3.13. The "Numbers" option provides the user with a white colored map where the sound pressure level in the center of each square is listed as shown in Figure 3.14.

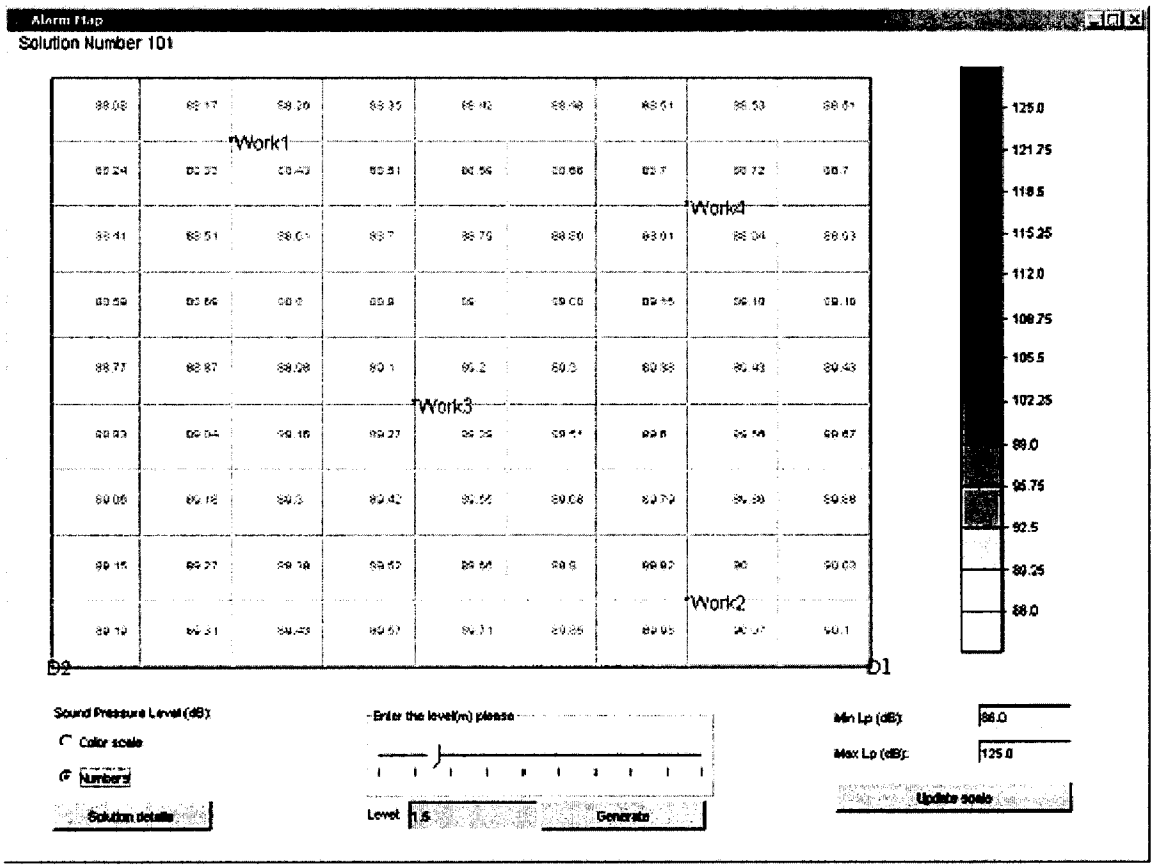

Fig. 3.14: Warning sound level distribution (dB) in the room using the "Numbers" option. There are four workstations and two alarm devices.

The warning sound level distribution (alarm map) provides the user with an overall view of the sound pressure level in the room at any desired height from the ground up to the ceiling. This assessment of the sound distribution may be helpful to determine any large variation in alarm level in the room. For instance, a high or low sound pressure level at certain locations in the workplace may affect the workers' audibility away from their intended workstations. Therefore, an alarm sound map is useful to assess additional situations.

3.3.7.5 Solution details

"Solution details" button in Figure 3.13 or 3.14 provides information about the solution for which the alarm map is currently displayed. This detailed information of the solution consists of the room identification, room height, room width, room length, frequency, reverberation time, room average absorption coefficient, order of early reflections along with the late reverberation equations used (Sabine or Eyring), horizontal and vertical step size, minimum height, alarm power level step size, alarms coordinates, alarms power levels, average efficiency, workstation's names, target levels and coordinates as shown in Figure 3.15. The aggregate sound pressure of all the alarms in the solution at each of the workstations is also provided.

Solutions details can be provided in an HTML format as well by clicking on the menu bar "File" (Figure 3.12) and choosing the "Generate HTML" item or by simply clicking at the fourth item in the tool bar shown in Figure 3.12.

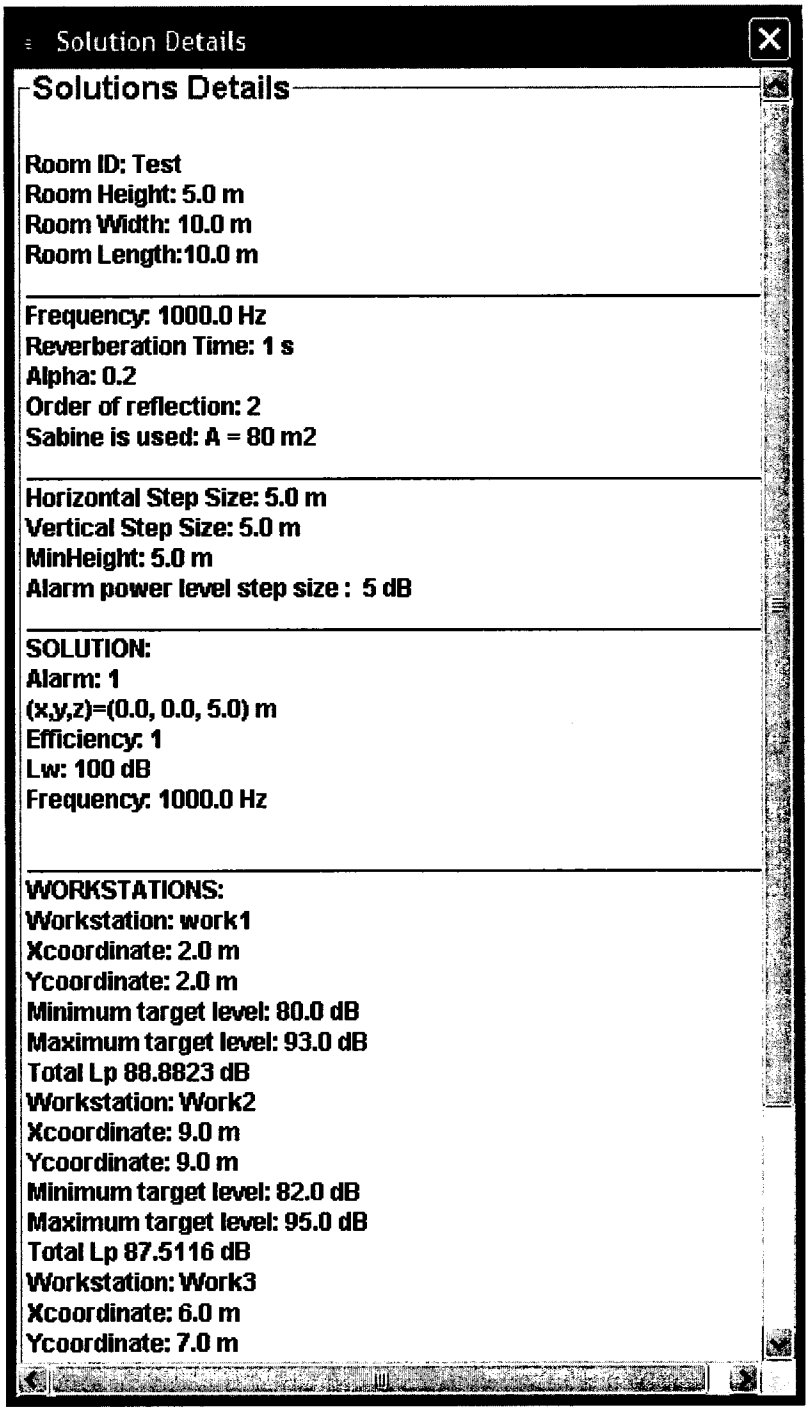

Fig. 3.15: Graphical user interface for listing of solution details. This window contains all the detailed information about the input parameters entered by the user in the main graphical user interface (Figure 3.10) and shows the detailed solutions parameters.

3.3.8 "TestingLocator"

The "TestingLocator" is another software tool designed in this research. This tool can be accessed through "AlarmLocator" and is useful for testing alarm configurations at

specific locations in a given room for debugging or verification purposes. For example, the user might use this tool for a given room layout to test a certain pattern of alarms settings for a particular configuration of workstations. The graphical user interface for this tool is similar to the graphical interface shown in Figure 3.10.

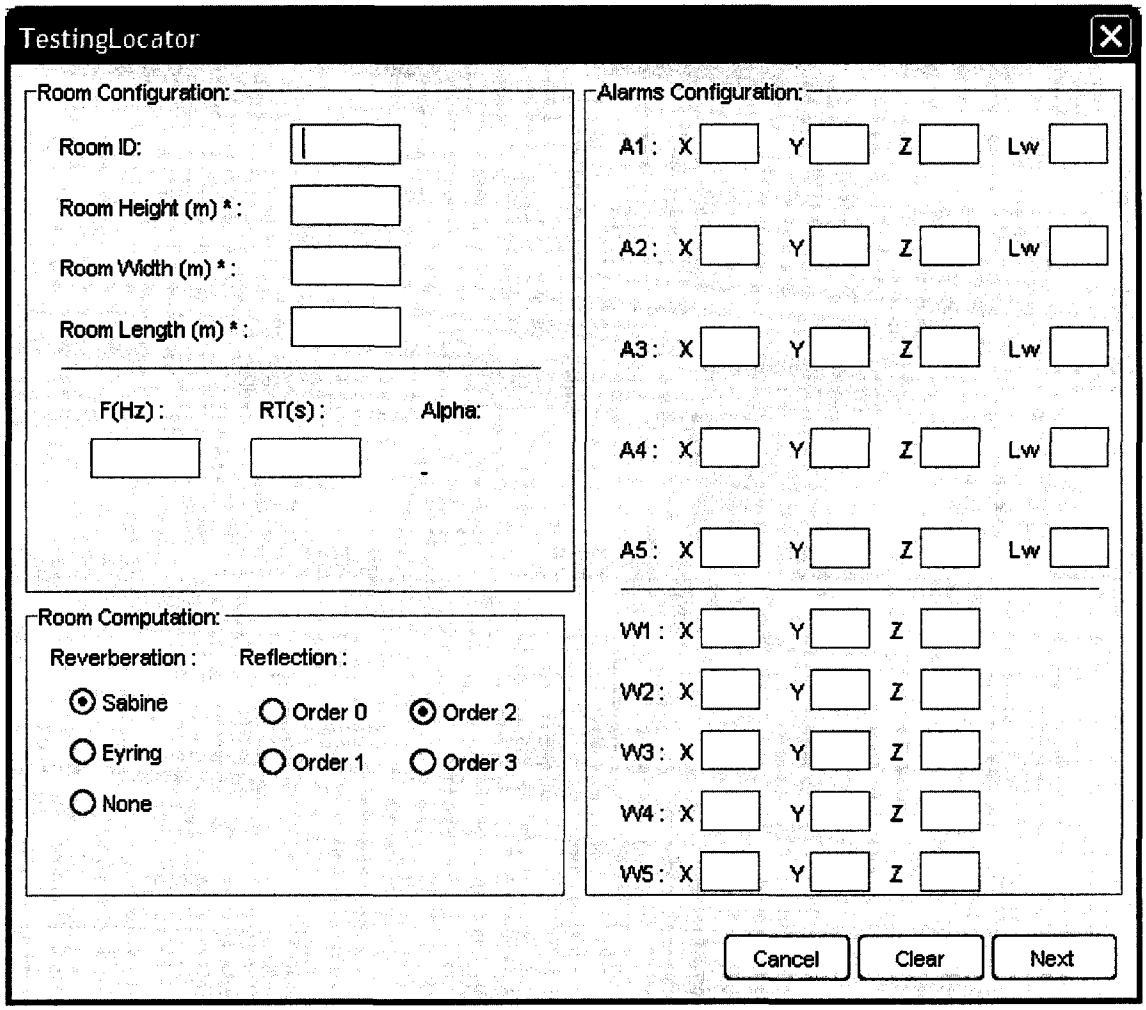

Fig. 3.16: Main graphical user interface for "TestingLocator".

The "TestingLocator" graphical interface is shown in Figure 3.16 and it consists of the following input parameters: the room configuration (room identification, room height, room width, room length), the frequency, the reverberation time and the room average absorption coefficient of the room, the number of workstations, the room computation theory (Sabine, Eyring, or None), along with the order of early reflections. A configuration from 1 up to 5 alarms may be used; the coordinates and power level of each

alarm must be specified. A maximum of 5 workstations may be used; the coordinates of the workstations must be specified as shown in Figure 3.16.

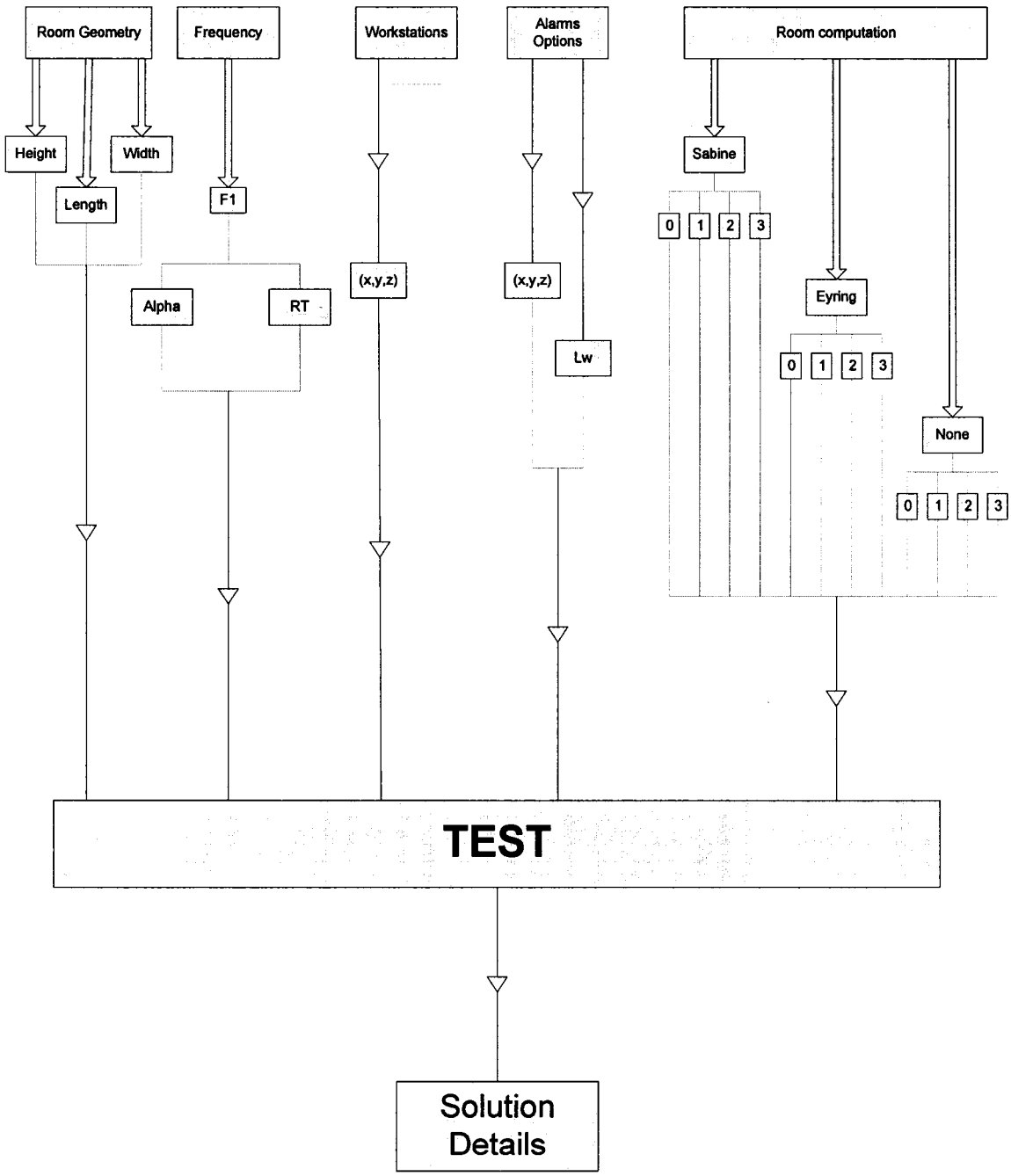

Fig. 3.17: Flow chart of "TestingLocator".

3.3.8.1 Algorithm for "TestingLocator"

The algorithm for this tool is shown in Figure 3.17. Once all the parameters have been entered in Figure 3.16, the aggregate sound pressure level of all the alarms introduced in the configuration is computed. The same formulas and techniques used for "AlarmLocator" are used once again for "TestingLocator". Once the user has entered all the desired parameters, the "Next" button is pressed and another window appears showing the sound pressure levels at each of the workstations.

The room identification, the frequency, the formulas used (Sabine, Eyring, or None) along with the order of early reflections, the name of the workstations and their coordinates, and the aggregate sound pressure level from all the alarms at each of the workstations are shown in the Testing result window. This is shown in Figure 3.18.

The user can create another testing configuration or can update the initial configuration simply by going back to the window of the "TestingLocator", making the possible changes and then clicking "Next" to see the results.

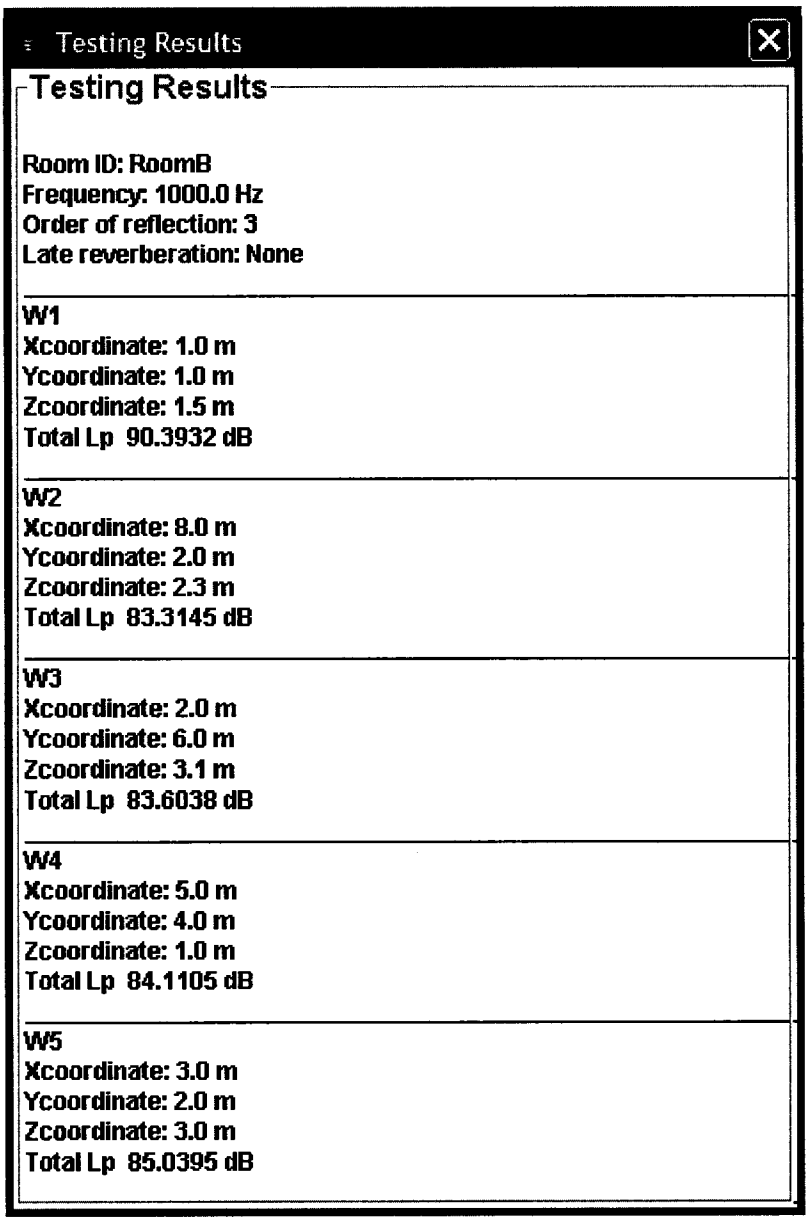

Fig. 3.18: Graphical user interface for presenting results of "TestingLocator".

3.4 Case studies

In this section, we present different hypothetical scenarios to demonstrate the use of software tool "AlarmLocator". Different late reverberation terms (Sabine, Eyring, or None) with different maximum order of early reflections (up to 3) are being considered. Five alarm frequencies are evaluated separately and then simultaneously. Input parameters that affect the outcome of "AlarmLocator" such as the power level step size, the minimum and maximum power levels of the alarm devices, the horizontal and vertical step size, and the minimum height of the alarm devices are also being presented.

3.4.1 Case study 1

The following case study demonstrates the use of "AlarmLocator" in a hypothetical work plant. Assume that the work area is 8m×15m×20m ($H \times W \times L$) and that it includes five workstations. The spatial coordinates and the target warning sound levels of the workstations are presented in Table 3.1. The workstations' target levels are assumed to be generated by "Detectsound" after an analysis of the noise field in the room and the hearing characteristic of the individual workers. In this case study, both Eyring and Sabine late reverberation formulation are being evaluated with a second order of early reflections.

Workstation Index k	X_k[m]	Y_k [m]	TL_{min} [dB]	TL_{max} [dB]
1	6.0	7.0	87.0	100.0
2	11.0	11.0	90.0	103.0
3	12.0	2.0	93.0	105.0
4	6.0	8.0	86.0	99.0
5	13.0	19.0	96.0	105.0

Table 3.1: The workstation coordinates and the minimum and maximum target levels in a hypothetical work plant. The Z coordinates (height) are assumed to be 1.5 m (ear level).

Frequency	Reverberation Time [sec]	Sabine Room Average Absorption Coefficient	Eyring Room Average Absorption Coefficient
F_1	2.0	0.17	0.15
F_2	1.0	0.33	0.28
F_3	0.7	0.47	0.38
F_4	0.5	0.662	0.48
F_5	0.35	0.95	0.61

Table 3.2: Reverberation time and corresponding average absorption coefficient at each frequency.

Five different frequencies are considered in this problem. Each frequency has its own reverberation time and average absorption coefficient. The room average absorption coefficient $\bar{\alpha}$ for both Sabine and Eyring is deducted from the reverberation time as shown in Table 3.2. Whenever the reverberation time T_{60} decreases, the average absorption coefficient $\bar{\alpha}$ increases since they are inversely proportional. A progression from a reverberant space where the reverberation time is 2 s to an absorbant space where

the reverberation time is 0.35 s is presented in this example depending on the frequency. The minimum power and maximum power levels of the alarms are set to 80 and 120 dB respectively. The power level step size is 5 dB; the horizontal and vertical step sizes are 5 m each; the minimum height is 5 m. Using "AlarmLocator", a set of optimum solutions for installing warning devices in a given room can be found. Each solution depicts the number, locations and power levels of the necessary warning device(s).

At first, the five frequencies are evaluated separately while using a second order of early reflections (default option). The five frequencies are then analysed simultaneously for the same order of early reflections.

3.4.1.1 Eyring late reverberation using a second order of early reflections

For frequency F_1, the reverberation time (T_{60}) is 2 s and the room average absorption ($\bar{\alpha}$) coefficient is equal to 0.15. Using "AlarmLocator", 12 possible solutions are established; all of them require one alarm device with a 115 dB power level. One possible solution is shown in Table 3.3; the rest of the solutions have the same power level but are located at different coordinates in the room. The warning sound level distribution for F_1 is shown in Figure 3.19. The efficiency of the solution is 2 dB.

Alarm Index i	X_i [m]	Y_i[m]	Z_i [m]	Power Level [dB]
1	5.0	20.0	8.0	115.0

Table 3.3: One possible solution for F_1 where T_{60} = 2.0 s using Eyring late reverberation with a second order of early reflections.

For F_2, T_{60} is 1.0 s and $\bar{\alpha}$ increases to 0.28. Five solutions are recognized by "AlarmLocator", demanding one alarm device (N_D=1). One possible solution is shown in Table 3.4; the rest of the solutions have the same power level but are placed at different positions in the room. The warning sound level distribution for F_2 is shown in Figure 3.20. The efficiency is 2 dB.

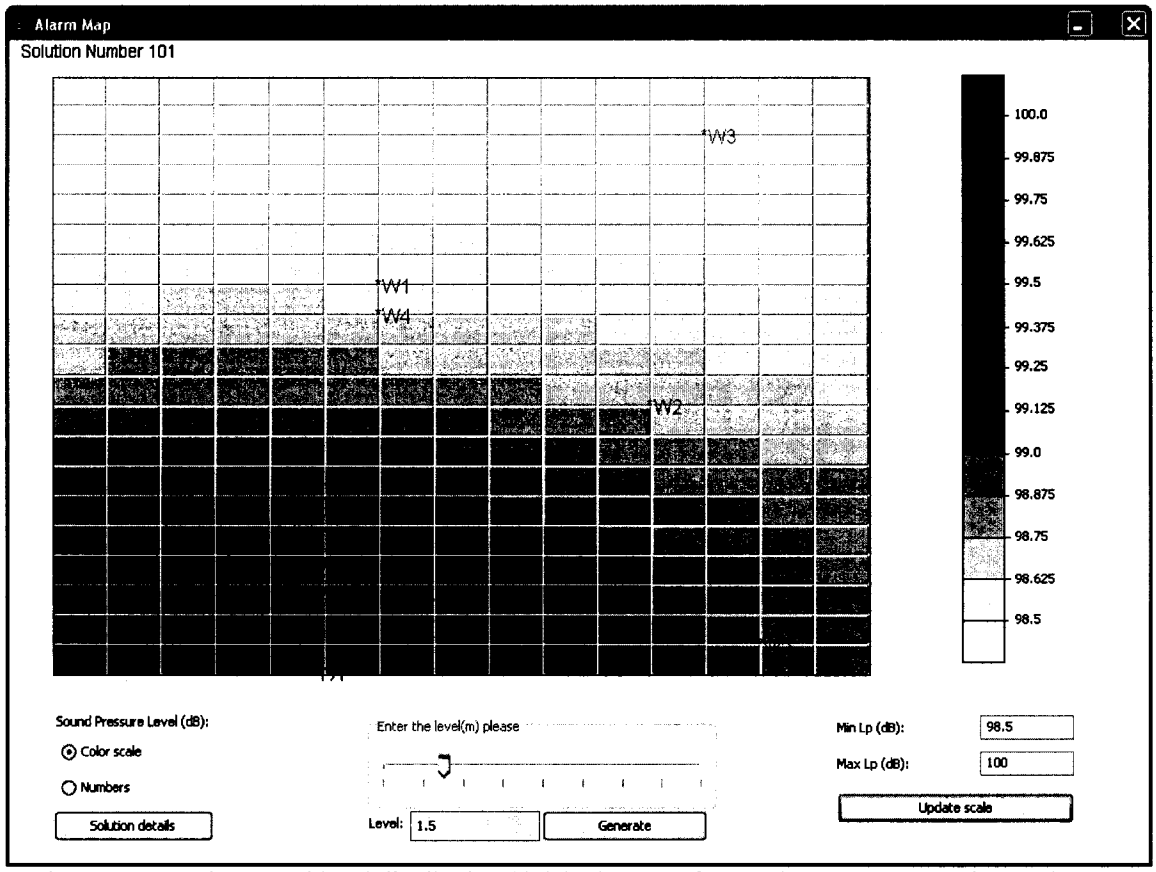

Fig. 3.19: Warning sound level distribution (dB) in the room for F_1 where T_{60} = 2.0 s using Eyring late reverberation with a second order of early reflections. Only one alarm devices *D1* is required.

Alarm Index i	X_i [m]	Y_i[m]	Z_i [m]	Power Level [dB]
1	5.0	20.0	8.0	115.0

Table 3.4: One possible solution for F_2 where T_{60} = 1.0 s using Eyring late reverberation with a second order of early reflections.

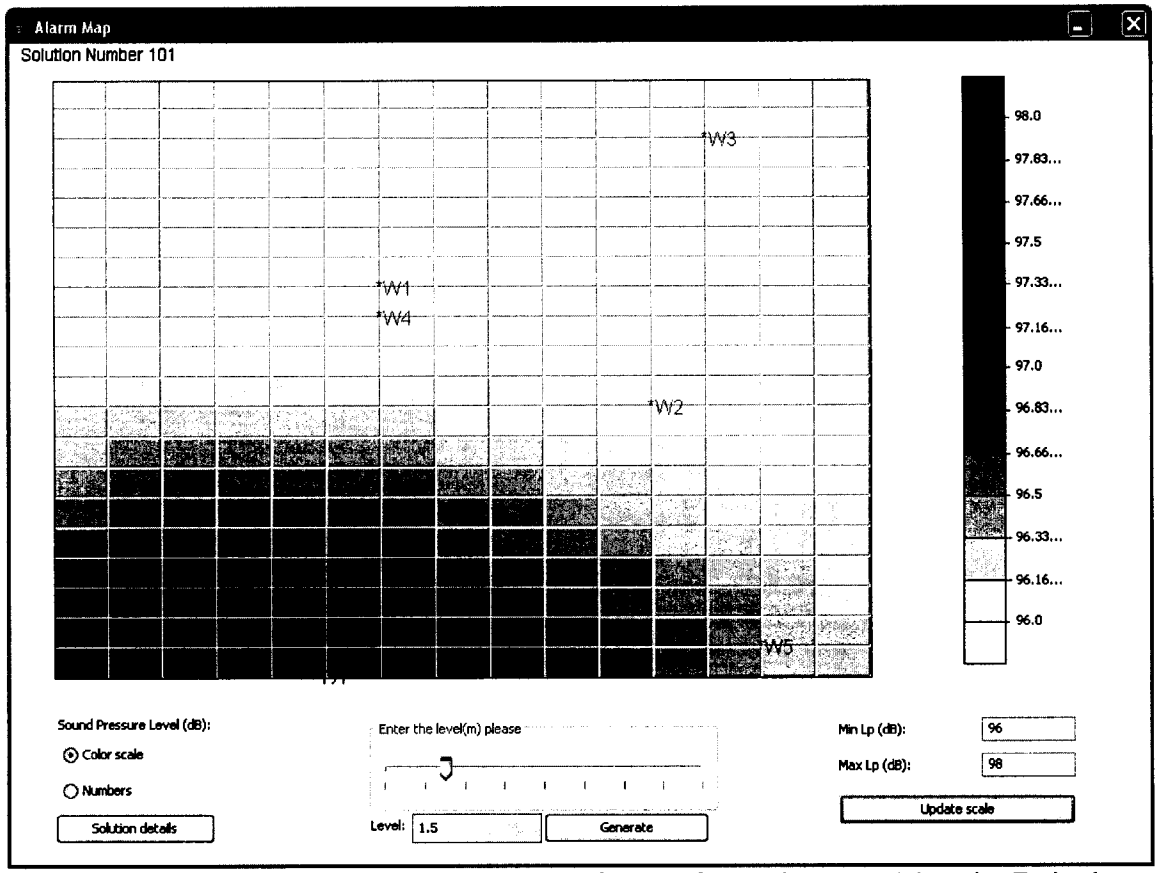

Fig. 3.20: Warning sound level distribution (dB) in the room for F_2 where T_{60} = 1.0 s using Eyring late reverberation with a second order of early reflections. Only one alarm device *D1* is required.

For F_3, T_{60} is 0.7 s and $\overline{\alpha}$ increases to 0.38. Only two solutions are found, demanding one alarm device (N_D=1). The efficiency of the solutions is 2 dB. One of the two possible solutions is shown in Table 3.5; the other solution has the same power level but is placed at a different position in the room. The warning sound level distribution for F_3 is shown in Figure 3.21.

Alarm Index i	X_i [m]	Y_i[m]	Z_i [m]	Power Level [dB]
1	10.0	20.0	8.0	115.0

Table 3.5: One possible solution for F_3 where T_{60} = 0.7 s using Eyring late reverberation with a second order of early reflections.

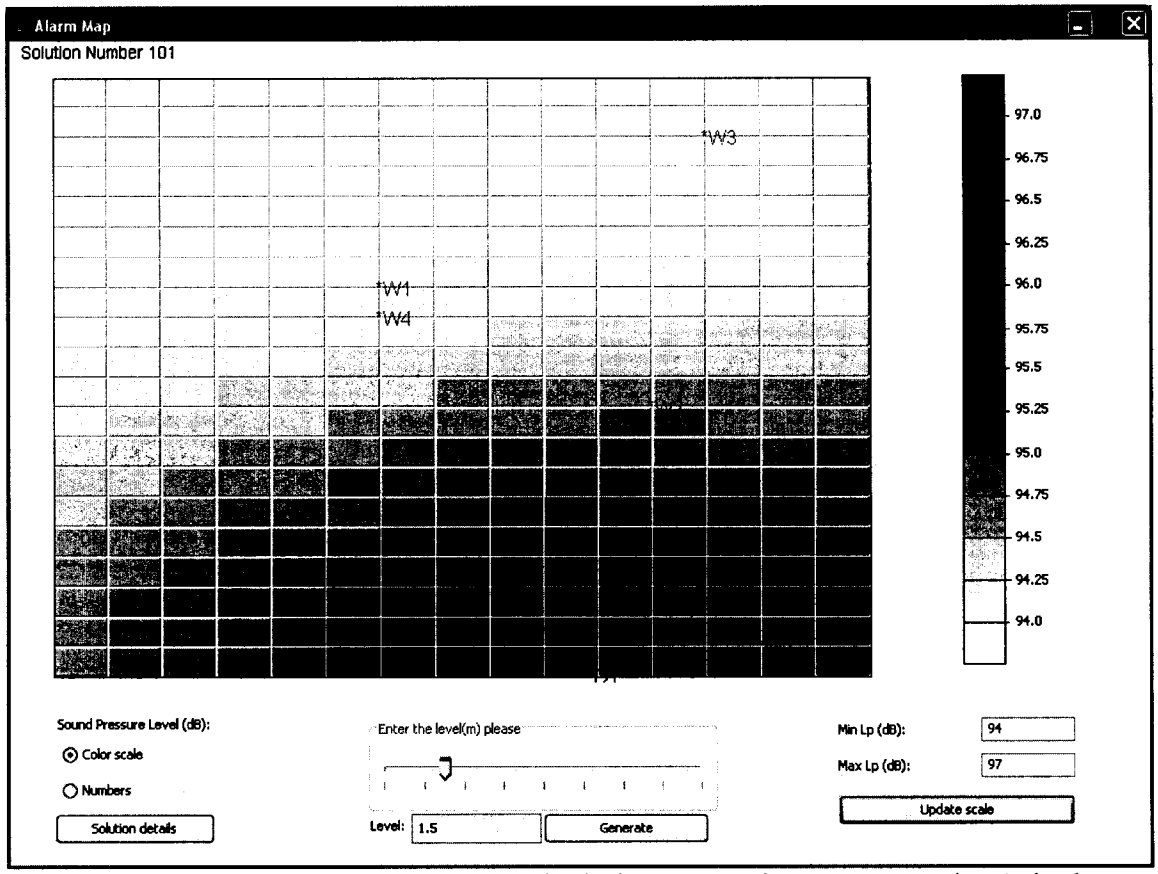

Fig. 3.21: Warning sound level distribution (dB) in the room F_3 where T_{60} = 0.7 s using Eyring late reverberation with a second order of early reflections. Only one alarm device *D1* is required.

For F_4, T_{60} is 0.5 s and $\overline{\alpha}$ increases to 0.48. No solution is found requiring only one alarm device. However, 96 solutions are found requiring two alarm devices. One possible solution is shown in Table 3.6, the rest of the solutions have the same power level but are placed at different positions in the room. The warning sound level distribution for F_4 is shown in Figure 3.22. The efficiency of this solution is 2 dB.

Alarm Index i	X_i [m]	Y_i[m]	Z_i [m]	Power Level [dB]
1	10.0	20.0	8.0	115.0
2	0.0	0.0	8.0	115.0

Table 3.6: One possible solution for F_4 where T_{60} = 0.5 s using Eyring late reverberation with a second order of early reflections.

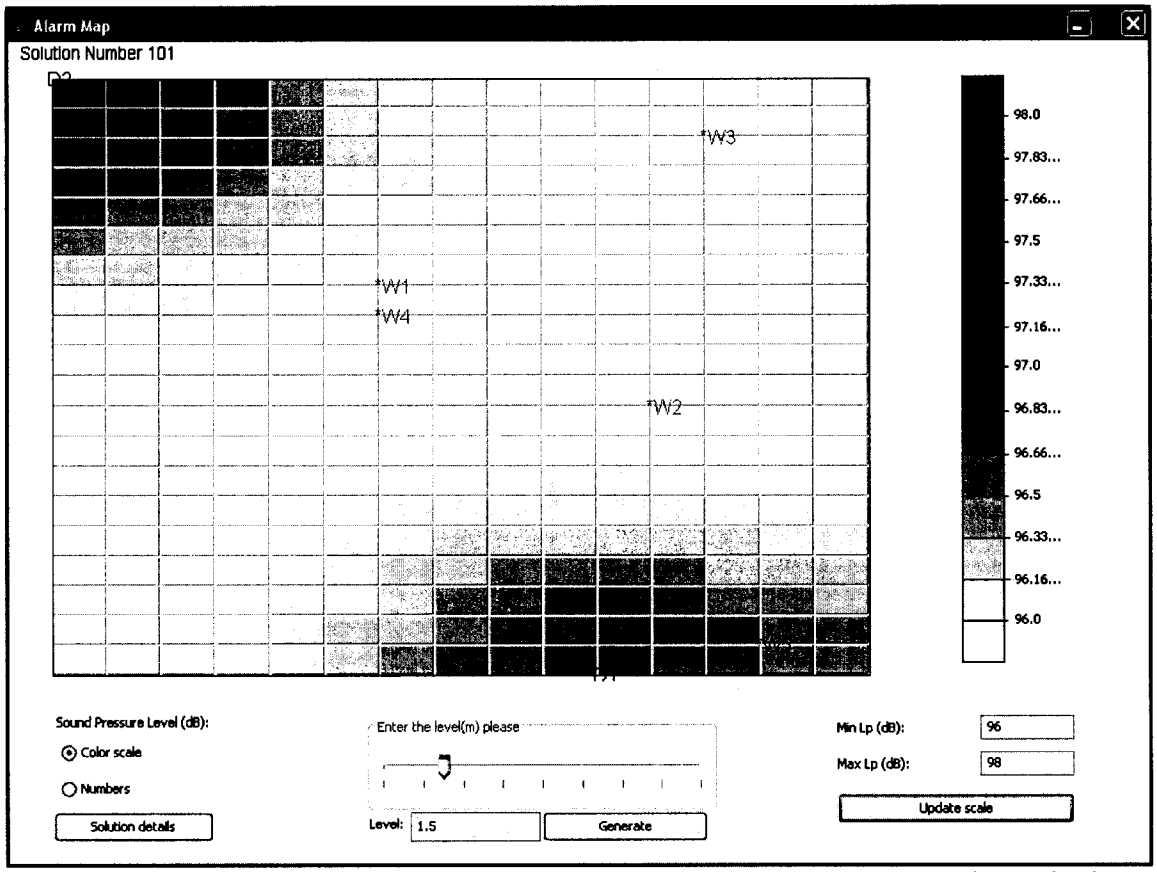

Fig. 3.22: Warning sound level distribution (dB) in the room for F_4 where T_{60} = 0.5 s using Eyring late reverberation with a second order of early reflections. Two alarm devices *D1* and *D2* are required.

For *F5*, T_{60} is 0.35 s and $\overline{\alpha}$ increases to 0.61. Seven possible solutions are detected by "AlarmLocator" necessitating two alarm devices. The efficiency is 2 dB. One possible solution is shown in Table 3.7, the rest of the solutions have the same power level but are placed at different positions in the room. The warning sound level distribution for F_5 is shown in Figure 3.23.

Alarm Index i	X_i [m]	Y_i[m]	Z_i [m]	Power Level [dB]
1	15.0	15.0	8.0	115.0
2	10.0	20.0	8.0	115.0

Table 3.7: One possible solution for F_5 where T_{60} = 0.35 s using Eyring late reverberation with a second order of early reflections.

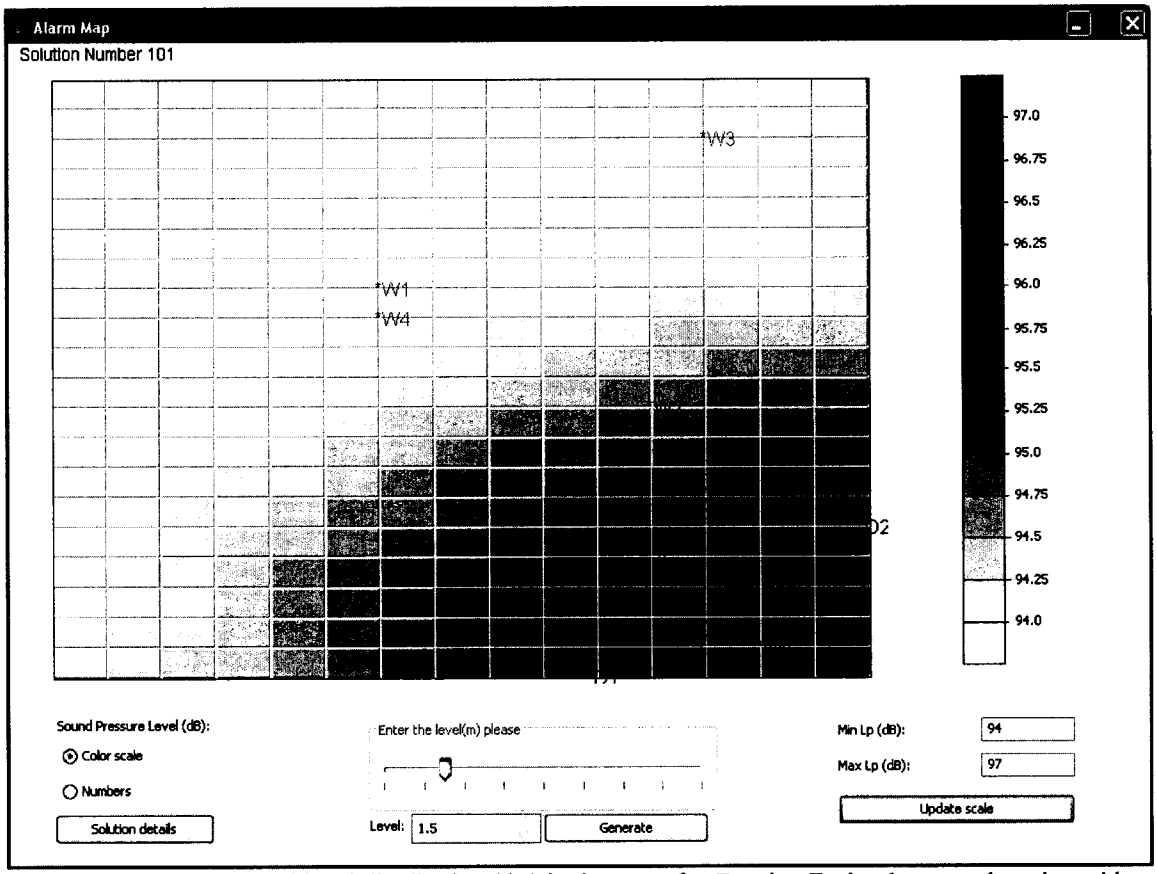

Fig. 3.23: Warning sound level distribution (dB) in the room for F_5 using Eyring late reverberation with a second order of early reflections. Three alarm devices D_1, $D2$, and $D3$ are required.

When selecting all the frequencies (F_1, F_2, F_3, F_4, and F_5) simultaneously, "AlarmLocator" finds seven solutions requiring two alarm devices. The efficiency for each solution is 2 dB. One of the solutions is shown in Table 3.8.

Alarm Index i	X_i [m]	Y_i[m]	Z_i [m]	Power Level [dB]
1	15.0	15.0	8.0	F1:110 F2:115 F3:115 F4:115 F5:115
2	10.0	20.0	8.0	F1:105 F2:105 F3:105 F4:110 F5:115

Table 3.8: One possible solution for F_1, F_2 F_3, F_4 and F_5 simultaneously using Eyring late reverberation with a second order of early reflections.

3.4.1.2 Sabine late reverberation using a second order of early reflections

Similar results to Eyring late reverberation formulation are obtained when Sabine formulation is used with the same order of early reflections, for F1, F2, F3, and F4. However, for F5, 1420 possible solutions are detected by "AlarmLocator" necessitating three alarm devices while Eyring necessitating only two alarm devices for the same frequency. The efficiency is 2 dB. One possible solution is shown in Table 3.9; the rest of the solutions have the same power level but are placed at different positions in the room. The warning sound level distribution for F5 is shown in Figure 3.24.

Alarm Index i	X_i [m]	Y_i[m]	Z_i [m]	Power Level [dB]
1	5.0	20.0	8.0	115.0
2	15.0	10.0	8.0	115.0
3	0.0	5.0	8.0	115.0

Table 3.9: One possible solution for F_5 where $T_{60} = 0.35$ s using Sabine late reverberation with a second order of early reflections.

Generally speaking, Eyring and Sabine solutions are quite similar. Difference may exist when the average absorption coefficient is very high, as expected in F_5.

When selecting all the frequencies (F_1, F_2, F_3, F_4, and F_5) simultaneously, "AlarmLocator" finds 1420 solutions requiring three alarm devices. The efficiency for each frequency is 2 dB. One of the solutions is shown in Table 3.10.

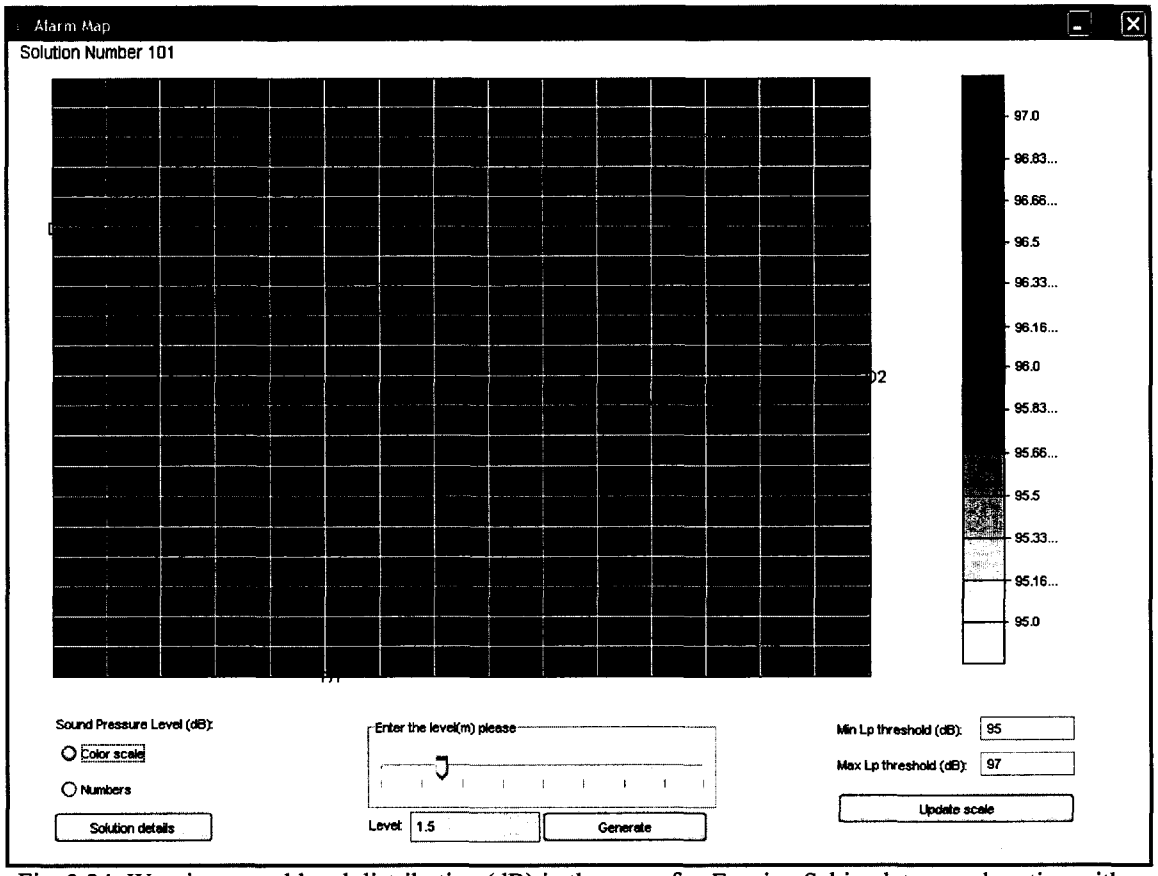

Fig. 3.24: Warning sound level distribution (dB) in the room for F_5 using Sabine late reverberation with a second order of early reflections. Three alarm devices D1, D2, and D3 are required.

Alarm Index i	X_i [m]	Y_i[m]	Z_i [m]	Power Level [dB]
1	10.0	20.0	8.0	F1:110 F2:100 F3:115 F4:115 F5:115
2	0.0	5.0	8.0	F1:105 F2:105 F3:110 F4:110 F5:115
3	0.0	0.0	8.0	F1:100 F2:115 F3:105 F4:110 F5:115

Table 3.10: One possible solution for F_1, $F2$ F_3, F_4 and F_5 simultaneously using Sabine late reverberation with a second order of early reflections.

3.4.2 Case study 2

In this case study, factors such as the minimum and maximum power levels, minimum height, power level step size, horizontal and vertical step size of the alarm device(s) are explored. The work area is 6m×18m×13m (*H×W×L*) and includes five workstations. The spatial coordinates and the target warning sound levels of the workstations are presented in Table 3.11. The workstations' target levels are again assumed to be generated by "Detectsound". The reverberation time in the room is assumed to have the values shown in Table 3.12. In this case study, Eyring late reverberation with a third order of early reflections is being evaluated.

Workstation Index k	X_k[m]	Y_k [m]	TL_{min} [dB]	TL_{max} [dB]
1	2.0	1.0	82.0	95.0
2	11.0	11.0	89.0	102.0
3	12.0	2.0	85.0	98.0
4	6.0	8.0	83.0	96.0
5	14.0	11.0	91.0	104.0

Table 3.11: The workstation coordinates and the minimum and maximum target levels in a hypothetical work plant. The *Z* coordinates (height) are assumed to be 1.5 m (ear level).

Frequency	Reverberation Time [sec]	Eyring Room Average Absorption Coefficient
F_1	1.6	0.15
F_2	0.7	0.32
F_3	0.5	0.41
F_4	0.3	0.59
F_5	0.11	0.91

Table 3.12: Reverberation time and corresponding average absorption coefficient at each frequency.

3.4.2.1 Reference condition

The power level step size is 5 dB, the horizontal and vertical step sizes are 5 m respectively, and the minimum height is 5 m. The minimum and maximum power levels are 80 dB and 120 dB respectively (default values).

For F_1, 11 possible solutions are established necessitating only one alarm device. One solution is shown in Table 3.13; the efficiency of the solution is 1 dB.

Alarm Index i	X_i [m]	Y_i[m]	Z_i [m]	Power Level [dB]
1	10.0	13.0	6.0	110.0

Table 3.13: One possible solution for F_1 where T_{60} = 1.6 s using Eyring late reverberation with a third order of early reflections.

For F_2, 12 possible solutions are established necessitating only one alarm device. One solution is shown in Table 3.14; the efficiency of the solution is 1 dB.

Alarm Index i	X_i [m]	Y_i[m]	Z_i [m]	Power Level [dB]
1	18.0	13.0	6.0	110.0

Table 3.14: One possible solution for F_2 where T_{60} = 0.7 s using Eyring late reverberation with a third order of early reflections.

For F_3, 13 possible solutions are established necessitating only one alarm device. One solution is shown in Table 3.15; the efficiency of the solution is 3 dB.

Alarm Index i	X_i [m]	Y_i[m]	Z_i [m]	Power Level [dB]
1	18.0	13.0	6.0	115.0

Table 3.15: One possible solution for F_3 where T_{60} = 0.5 s using Eyring late reverberation with a third order of early reflections.

For F_4, four possible solutions are established necessitating only one alarm device. One solution is shown in Table 3.16; the efficiency of the solution is 1 dB.

Alarm Index i	X_i [m]	Y_i[m]	Z_i [m]	Power Level [dB]
1	10.0	13.0	6.0	115.0

Table 3.16: One possible solution for F_4 where T_{60} = 0.3 s using Eyring late reverberation with a third order of early reflections.

For F_5, 49 possible solutions are established requiring two alarm devices. One solution is shown in Table 3.17; the efficiency of the solution is 3 dB. The warning sound level distribution in dB is shown in Figure 3.25.

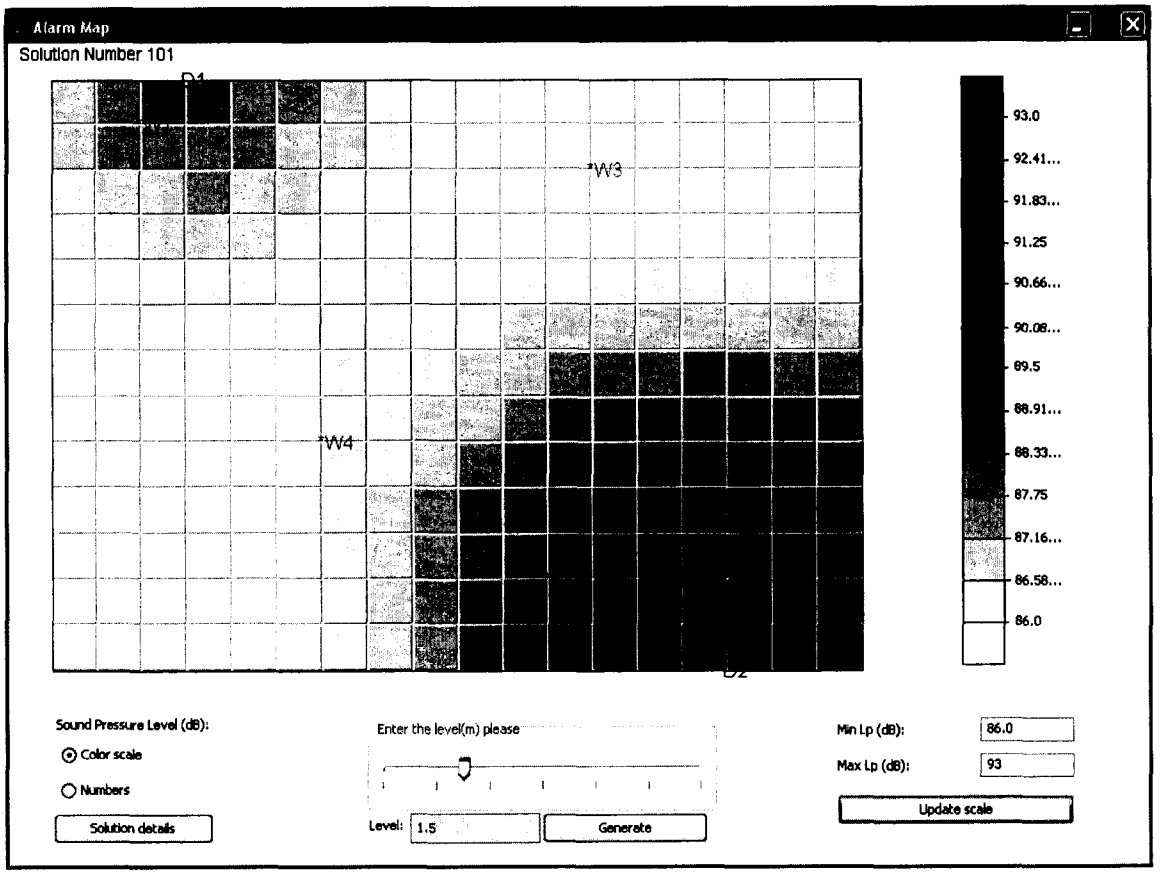

Fig. 3.25: Warning sound level distribution (dB) in the room for F_5 using Eyring late reverberation with a third order of early reflections. Two alarm devices *D1* and *D2* are required.

Alarm Index i	X_i [m]	Y_i[m]	Z_i [m]	Power Level [dB]
1	3.0	0.0	6.0	110.0
2	15.0	13.0	6.0	115.0

Table 3.17: One possible solution for F_5 where T_{60} = 0.11 s using Eyring late reverberation with a third order of early reflections.

3.4.2.2 Effect of power level step size

The power level step size is now set to 1 dB; however the horizontal and vertical step sizes and the minimum height maintain their values in section **3.4.2.1.** The minimum and maximum power levels maintain their default values. Results in this case are quite similar to section **3.4.2.1** for the frequencies F_1, F_2, F_3 and F_4; but some of the solutions require less power level. However, for F_5, 10 possible solutions are established requiring only one alarm device instead of two alarm devices in section **3.4.2.1**. One solution is shown in Table 3.18; the efficiency of the solution is 2 dB. The warning sound level distribution in dB is shown in Figure 3.26.

Alarm Index i	X_i [m]	Y_i[m]	Z_i [m]	Power Level [dB]
1	10.0	13.0	6.0	118.0

Table 3.18: One possible solution for F_5 where $T_{60} = 0.11$ s using Eyring late reverberation with a third order of early reflections.

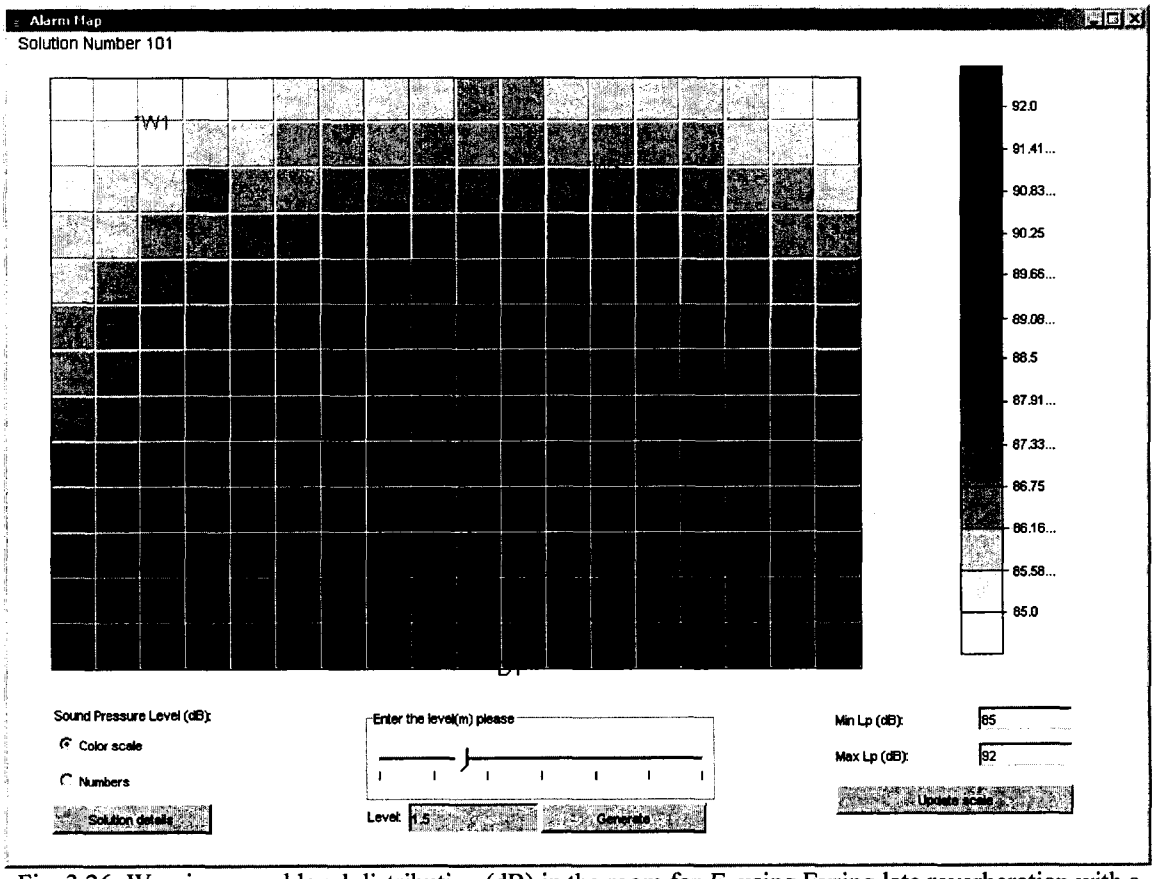

Fig. 3.26: Warning sound level distribution (dB) in the room for F_5 using Eyring late reverberation with a third order of early reflections. Only one alarm device *D1* is required.

3.4.2.3 Effect of grid size

In this case, the power level step size is set to 1 dB; the horizontal and vertical step sizes and the minimum height are now set to 1 m, 1 m, and 1.5 m respectively. The minimum and maximum power levels maintain their default values.

Results in this case are quite similar to section **3.4.2.1** for the frequencies F_1, F_2, F_3 and F_4; but much more solutions are found due to the finer node grid. Some of the solutions require less power level. For instance, for F_5, 270 solutions are found requiring one alarm device. One solution is shown in Table 3.19; the efficiency of the solution is 1 dB.

Alarm Index i	X_i [m]	Y_i[m]	Z_i [m]	Power Level [dB]
1	15.0	13.0	6.0	116.0

Table 3.19: One possible solution for F_5 where T_{60} = 0.11 s using Eyring late reverberation with a third order of early reflections.

3.4.2.4 Effect of power level range

Similar to section **3.4.2.1**, the power level step size is set to 5 dB; the horizontal and vertical step sizes and the minimum height are now set to 5 m, 5 m, and 5 m respectively. However, the minimum and maximum power levels are now set to 95 dB and 108 dB respectively. Generally speaking, when the maximum and/or minimum power levels are limited, we may need more alarm devices since some of the solutions may be skipped. For our case, the results for all the frequencies F_1, F_2, F_3, F_4 and F_5 are different from section **3.4.2.1**. For instance, for F_1, 275 possible solutions are established requiring two alarm devices. One solution is shown in Table 3.20; the efficiency is 1 dB.

Alarm Index i	X_i [m]	Y_i[m]	Z_i [m]	Power Level [dB]
1	18.0	13.0	6.0	105.0
2	15.0	13.0	6.0	105.0

Table 3.20: One possible solution for F_1 where T_{60} = 1.6 s using Eyring late reverberation with a third order of early reflections.

3.4.3 Discussion

The results are quite similar for the scenarios presented in sections **3.4.1.1** and **3.4.1.2** for the frequencies F1, F2, F3 and F4 for Eyring versus Sabine late reverberation with a second order of early reflections. However, for F5, the reverberation time is 0.35 s and the average absorption coefficient $\overline{\alpha}$ for Sabine and Eyring late reverberation terms are 0.95 and 0.61 respectively. In this case, a difference is found. Using Sabine, a solution with three alarm devices has been detected by "AlarmLocator". On the other hand, using Eyring a solution with only two alarm devices has been generated by "AlarmLocator". Generally speaking, in order to have a noticeable difference in the results between Sabine and Eyring, the power level step size should be small (typically smaller than 2 dB) and/or the horizontal and vertical step size should be small compared to the room's dimensions. Otherwise, a noticeable difference would occur only when the reverberation time is really small (high absorption coefficient).

Nevertheless, increasing the room average absorption coefficient $\bar{\alpha}$ does not always result in increasing the power level of the alarm device(s) or adding an extra device. The workstation's target levels acts as constraints for the alarm's power level L_w. When $\bar{\alpha}$ increases, L_w should also increase, but the aggregate sound power level coming from all the alarms should still satisfy the target levels at each of the workstations. For instance, if the workstations have the same target levels everywhere in the workplace, then there's a requirement for increasing L_w when $\bar{\alpha}$ increases; when L_w reaches the maximum power level, an alarm is added. In reality, the target levels for the workstations are dissimilar. Therefore, increasing $\bar{\alpha}$ may not always lead to increasing L_w or adding another alarm device. The workstation's coordinates is another major factor that can affect the nature of the solutions. A solution may be practical for a certain spatial arrangement of some workstations and not feasible when these same workstations are arranged differently in the same workplace.

The minimum and maximum power levels are quite important parameters. The wider the window range between the minimum and maximum power levels, the more possible solutions can be found, and the opposite is true. The power level step size, the horizontal and vertical step sizes of the alarm device are also crucial factors in the solution generation process of "AlarmLocator". By setting the horizontal and vertical step size of the alarm device to small values with respect to the room's dimensions, much more processing overhead is incurred while the results produced are more efficient and more solutions are provided. The minimum height of the alarm device is set to 1.5 m (average ear's level) by default. However, generally speaking, alarm devices are typically installed at a certain distance close to the ceiling. Therefore, the user has the choice of simply using the default value or selecting the desired height, which will affect the possible number of valid solution.

Essentially, it is a trade off between processing time and efficiency. A power level step size in the range of (0, 2] dB will result in more accurate solutions but, on the other hand, will require excess processing time. This is shown in case study 2 in section **3.4.2**. By setting only the power level step size to 1 dB in section **3.4.2.2** and by maintaining the other input parameters (horizontal and vertical step sizes of the alarm device, minimum height, and maximum and minimum power level), a difference in the solution space is

depicted compared to a power level step size of 5 dB in section **3.4.2.1**. For instance, only one alarm device (L_w=118 dB) is then required for F_5 in section **3.4.2.2,** as shown in Table 3.17, comparing to two alarm devices (L_{w1}=115 dB and L_{w2}=110 dB) in section **3.4.2.1,** as shown in Table 3.18. In section **3.4.2.3,** by setting the power level step size to 1 dB, the horizontal and vertical step size to 1 m each, the minimum height to 1.5 m and by maintaining the maximum and minimum power level to their default value, a large difference in the solution space is depicted due to the fine grid size. Number of solutions increase tremendously compared to sections **3.4.2.1** and **3.4.2.2.** The user would have more choices on installing alarm devices. Finally, in section **3.4.2.4**, by minimizing the range between the maximum and minimum power levels to 13 dB comparing to 40 dB in the reference condition (section **3.4.2.1**), the solution space is reduced. For instance, for F_1 in section **3.4.2.4,** only solutions with two alarm devices can be generated by "AlarmLocator"; however, several solutions exist with only one alarm device in the reference condition (section **3.4.2.1**).

Currently, a brute force algorithm is implemented in "AlarmLocator". The algorithm exhaustively scans all possible solutions in the room to obtain the optimum number, location and power level of warning devices. As discussed above, various step and grid sizes must be specified by the user. Additional optimization methods may possibly be implemented that require less user intervention. For example, the algorithm could again scan the room for all possible locations, but an optimization algorithm would now be applied at each node of the virtual "spiral like" path (Figure 3.3) to find the exact optimal power level of warning devices, unconstrained by a power level step size. Other sophisticated optimization algorithms could also be employed such as the conjugate gradient method (White, 2004; Miller, 2000) or the steepest descent method (Jensen, 1995) to spatially locate the warning devices, uncontrained by a grid step size. However, the latter methods require several iterations and this could require heavy processing since the tool accounts for many variables.

The design window at each workstation generated by "Detectsound" is a major constraint for the solution provided by "AlarmLocator". "AlarmLocator" assumes static movement in the workplace; workers are expected to maintain their positions at the workstations. To deal with this issue, "AlarmLocator" currently generates a warning sound level

distribution for the solution in the room. This overall view of sound level distribution is useful for the user to assess the sound level near or away his workstation. Also, because of rotation of staff, workers with different hearing status may sometimes be assigned to the same workstation. In this case, the common range in target levels meeting the requirements for all workers at each workstation would be fed into "AlarmLocator" (Zheng, 2003).

The solution provided by "AlarmLocator", consisting of the optimum number, location, and power level of warning devices satisfies the design window provided by "Detectsound". However, unfortunate cases may occur when solution provides optimal coordinates of warning devices at locations where other objects (panels, flashing light, etc.) are already mounted in the room. In this case, "TestingLocator" can be employed to explore other feasible solutions on walls in the neighborhood of the original solution. Ultimately, specifying a solutions area, rather than a finite point location, would be a desirable feature in future implementation of "AlarmLocator" to facilitate its use in practice.

Chapter 4. Validation

This chapter presents a detailed field validation of "AlarmLocator" in a classroom at the University of Ottawa. Using sound measurement equipment, it was verified that "AlarmLocator" could provide realistic solutions for the installation of warning devices. Given that "AlarmLocator" and "TestingLocator" employ the same sound propagation algorithm, and therefore use identical formulas to compute sound pressure levels, "AlarmLocator" was validated by using "TestingLocator".

4.1 General procedure

The experimental validation consists of the following steps. First, the input parameters of "TestingLocator" are specified. These include the room geometry (H×W×L) to obtain the volume and the total surfaces of the room, and the reverberation time. The latter can be obtained using two approaches: (1) calculated predictions based on the absorption coefficients for the different surface elements in the room using tabulated data of acoustical materials or (2) acoustical measurements using specialized equipment (section **4.2**). The power level of the source(s) is also a required parameter for "TestingLocator" and it is must be determined (section **4.3**). In addition, "TestingLocator" requires the coordinates of the sources and workstations in the room. The sound propagation for a variety of source and workstation configurations can than be simulated with "TestingLocator". The results are compared to sound pressure level measurements at each workstation in the real room (section **4.4**).

4.2 Room specifications

In this section, the room dimensions are specified and the absorption coefficients of various surface elements in the room are described. The reverberation time in the room is then determined by computations and by measurements.

4.2.1 Description

The room selected is classroom 3031 in Roger Guidon Hall at the University of Ottawa. The room is almost rectangular apart from an irregular corner, as shown Figure 4.1. The

walls are made of Gypsum board with the following additional architectural features on the different sides:

Side A:

- 0.91m×2.12m (W×L) metal door
- 5.735m×1.22m (W×L) acoustic panel, 1.22 m above the ground
- Post with a circumference of 1.46 m

Side B includes:

- 5.78m×1.22m (W×L) acoustic panel, 1.22 m above the ground

Side C includes:

- 1.07m×1.22m (W×L) acoustic panel, 1.22 m above the ground.

Side D includes:

- 7.12m×1.22m (W×L) acoustic panel, 1.22 m above the ground.

Side E includes:

- 3.67m×1.23m (W×L) white board, 0.9 m above the ground.

The ground floor of the room consists of carpet on concrete while the ceiling is made of acoustical tile materials.

By assuming the room to be rectangular, thereby ignoring the irregular corner, the room dimensions become: 2.66m×7.90m×6.58m (H×W×L), as shown in Figure 4.2. The post was also ignored, and the metal door was assumed to be part of the wall and sharing its properties.

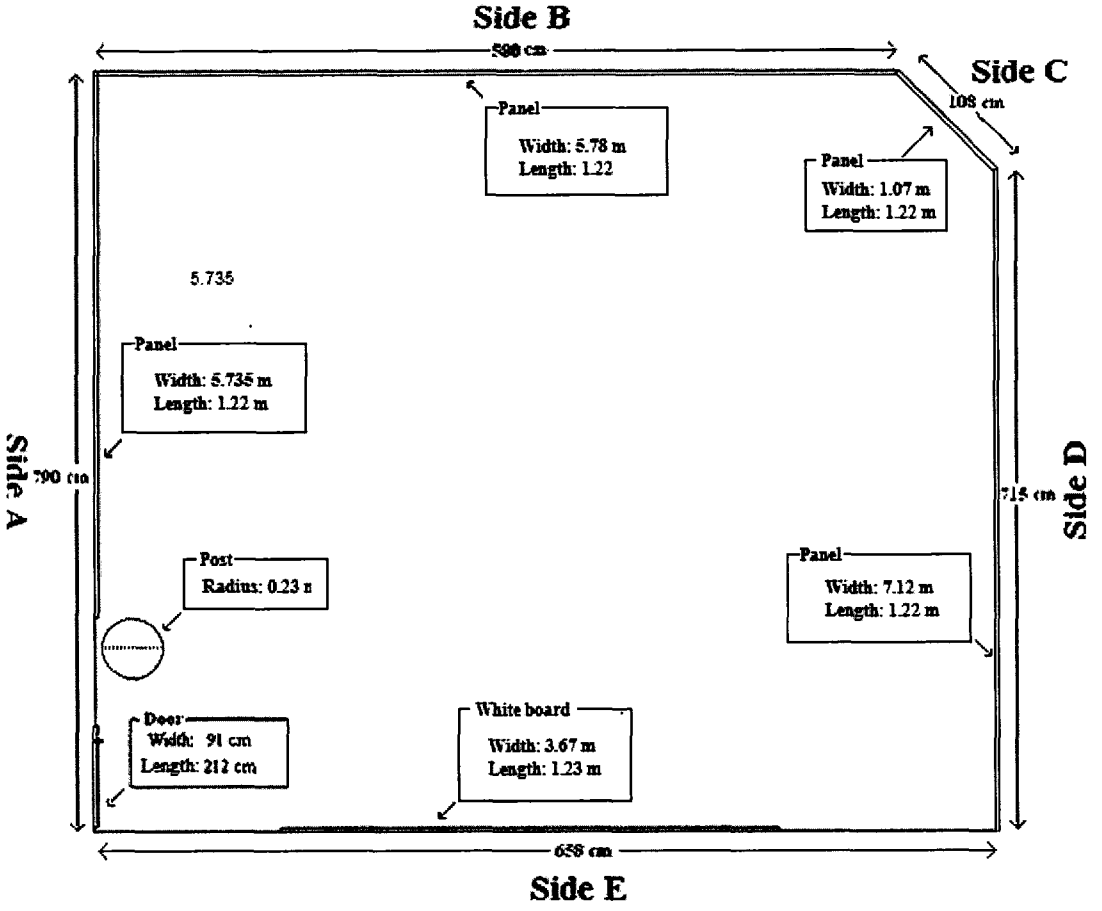

Fig. 4.1: Room layout.

4.2.2 Reverberation time computation

The materials used in the room and the tabulated absorption coefficients at octave frequencies between 250 and 4000 Hz are listed in Table 4.1.

The average absorption coefficient $\bar{\alpha}$ of the room was calculated using equation (19):

$$\bar{\alpha} = \frac{1}{S_{tot}}(\alpha_1 S_1 + \alpha_2 S_2 + \alpha_3 S_3 + ... + \alpha_n S_n)$$

where $\alpha_{1\text{-}5}$, $S_{1\text{-}5}$ and S_{tot} are illustrated in Table 4.1.

The reverberation time was computed using Eyring's formulation (21):

$$TR = \frac{-0.16V}{S\ln(1-\bar{\alpha})}$$

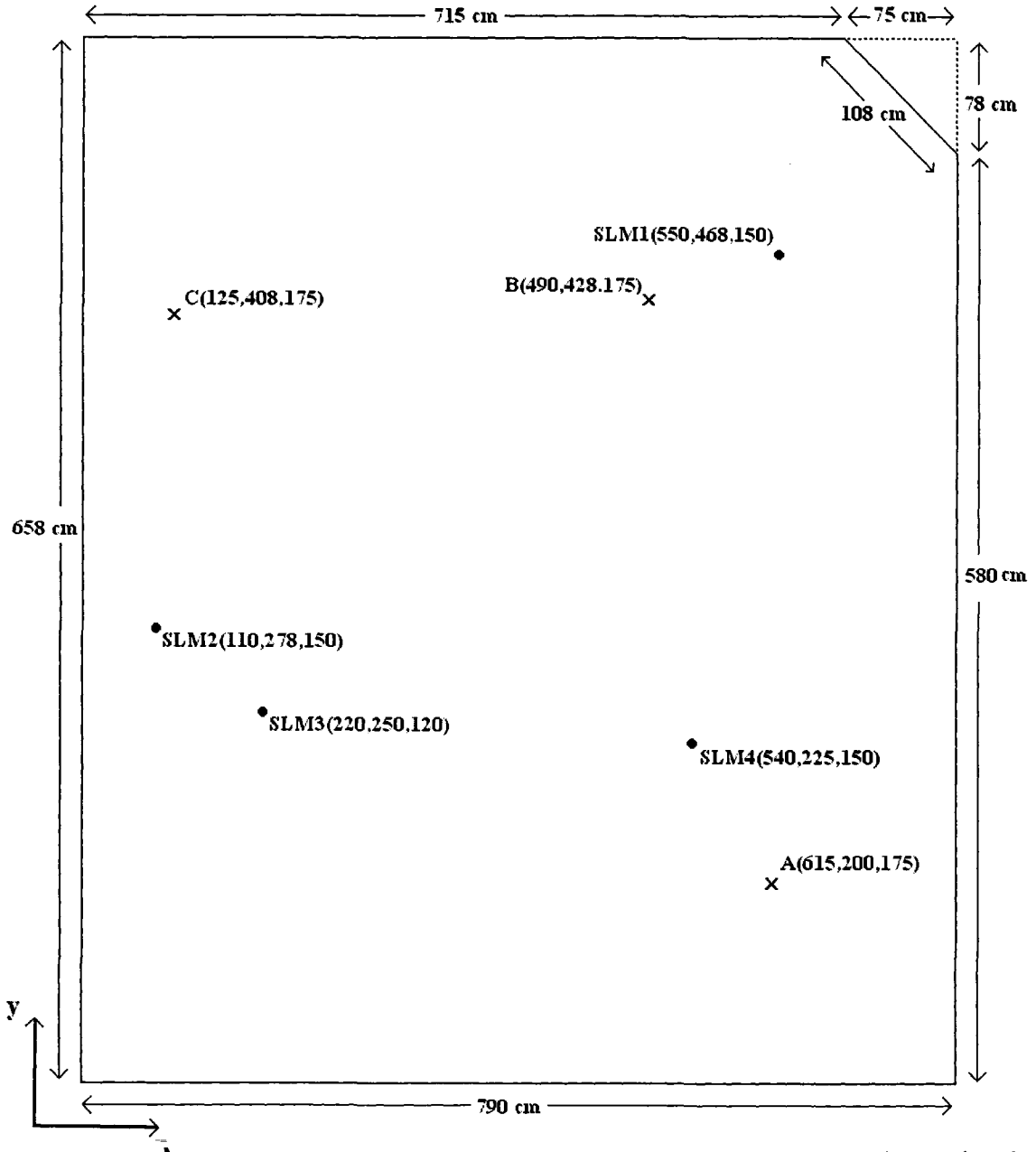

Fig. 4.2: Room layout with source (A, B, C) and workstation (SLM1-4) coordinates used for reverberation time measurements.

The total room surface and volume are 180.62 m^2 and 138.27 m^3 respectively. Reverberation times and absorption coefficients are listed in Table 4.2.

Element	Material type used	Absorption coefficient	Total surface [m^2]
1.Wall	Gypsum board, ½ in. thick	F_1: 0.10 F_2: 0.05 F_3: 0.04 F_4: 0.07 F_5: 0.09	48.11
2.White board	Standard glass window	F_1: 0.25 F_2: 0.18 F_3: 0.12 F_4: 0.07 F_5: 0.04	4.51
3.Panel	Fiberglass, 1½ in. thick	F_1: 0.91 F_2: 0.80 F_3: 0.89 F_4: 0.62 F_5: 0.47	24.04
4.Carpet	Carpet on concrete	F_1: 0.06 F_2: 0.14 F_3: 0.37 F_4: 0.60 F_5: 0.65	51.98
5.Ceiling	Acoustical tiles	F_1: 0.45 F_2: 0.81 F_3: 0.97 F_4: 0.93 F_5: 0.82	51.98
S_{tot}			180.62

Table 4.1: Absorption coefficients of room materials (F_1:250, F_2:500, F_3:1000, F_4:2000, and F_5: 4000 Hz) [From (Irwin & Graf) 1979].

Frequency [Hz]	Reverberation time [s]	Average absorption coefficient
F_1=250	0.34	0.30
F_2=500	0.24	0.40
F_3=1000	0.17	0.52
F_4=2000	0.16	0.54
F_5=4000	0.17	0.51

Table 4.2: Predicted reverberation times and average absorption coefficients.

Equipment
Brüel and Kjaer 2250 hand-held analyser
Brüel and Kjaer 7841 Dirac Room Acoustic Software
Brüel and Kjaer 7816 Acoustic Determinator
IBM portable computer with an embedded sound card
Brüel and Kjaer 1405 noise generator
Brüel and Kjaer 2716 power amplifier
Brüel and Kjaer 4295 omnidirectional source

Table 4.3 Sound generating and measuring equipment used during the validation process.

4.2.3 Reverberation time measurements

Reverberation times were also measured using Dirac Room Acoustic software, a hand-held sound analyser, a Power amplifier and an omnidirectional sound source. The equipment used is listed in Table 4.3. The experimental set-up is illustrated in Figure 4.3.

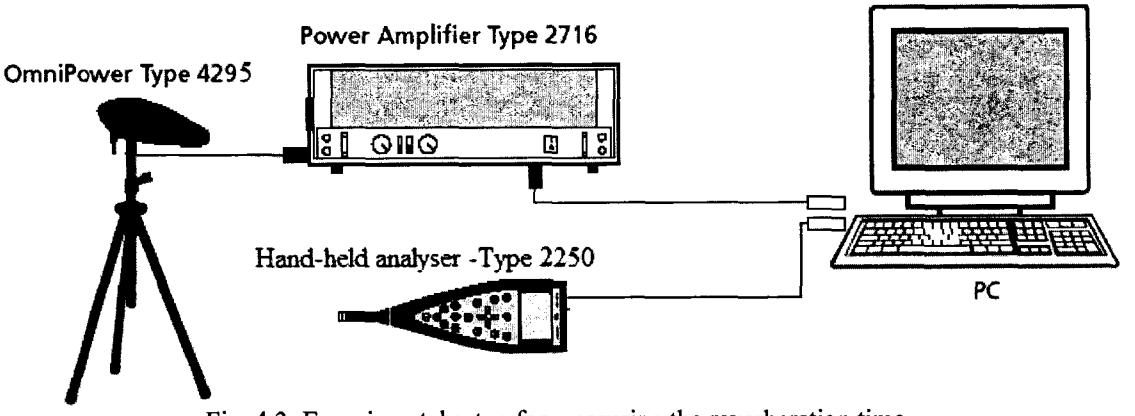

Fig. 4.3: Experimental setup for measuring the reverberation time.

The software tool Dirac is installed on a portable computer with a sound card. Using Dirac, a MLS (minimum length sequence) is generated and amplified by the power amplifier connected to the omnidirectional source. The sound level meter (hand-held analyzer), which is connected to the input of the sound card, and the omnidirectional source are placed at various locations in the room as shown in Figure 4.2. There are 3 possible source positions (A, B, and *C*) and 4 receiver positions (SLM1, SLM2, SLM3, and SLM4). For each source-receiver configuration, the space reverberation time (based on T_{30}) is computed over 36 sweeps for a MLS lasting 0.68 s, and then averaged. The

average reverberation time at each frequency is presented in Table 4.4 over different source-receiver configurations. Although many alternative locations exist for the sound source and sound level meter, the average reverberation time over all configurations (last row in Table 4.3) is used for the simulations with "TestingLocator" (section **4.4**).

The reverberation time measured with Dirac can be compared to those calculated based on Eyring's theory (equation 21) in Table 4.5. Although the measured and predicted reverberation times from calculation follow the same trends, predicted reverberation times are smaller than measured reverberation times. The differences may be attributed to 1) failure to consider many objects (tables, chairs, closets, and computers) during the computation of reverberation time using equation (21), and 2) the use of approximate tabulated values for the absorption coefficient of room materials (Table 4.1). The two sets of reverberation times are used in section 4.4 for making sound pressure level predictions.

T60 [s]	250 [Hz]	500 [Hz]	1000 [Hz]	2000 [Hz]	4000 [Hz]
A-SLM1	0.586	0.376	0.252	0.254	0.268
A-SLM2	0.546	0.37	0.247	0.241	0.255
A-SLM3	0.537	0.36	0.242	0.245	0.25
B-SLM3	0.468	0.398	0.254	0.226	0.249
B-SLM4	0.438	0.326	0.259	0.237	0.26
C-SLM4	0.469	0.348	0.227	0.221	0.26
AVG	0.507333	0.363	0.246833	0.237333	0.257

Table 4.4: Reverberation times for the various source and receiver configurations displayed in Figure 4.2.

Frequency [Hz]	Predicted T_{60} [s]	Average measured T_{60} [s]	Difference between average predicted and measured T_{60} [s]
F1=250 Hz	0.33	0.51	-0.18
F2=500 Hz	0.24	0.36	-0.12
F3=1000 Hz	0.17	0.25	-0.08
F4=2000 Hz	0.16	0.24	-0.08
F5=4000 Hz	0.17	0.26	-0.09

Table 4.5: Measured vs. predicted reverberation times in the room.

4.3 Sound Power Level computation

Knowledge of the sound power level generated by the omnidirectional source is required for the experimental validation of "AlarmLocator" using "TestingLocator". For this

validation, Brüel and Kjaer Type 4295 omnidirectional source is used. However, the manufacturer's specifications do no rate the actual sound power level for a given electrical signal. The experimental setup for determining the source's sound power level is shown in Figure 4.4. A white noise generator with 20-kHz upper frequency limit is connected to the power amplifier, which is in turn connected to the omnidirectional source. The sound level meter is connected to the input of the sound card of the portable computer.

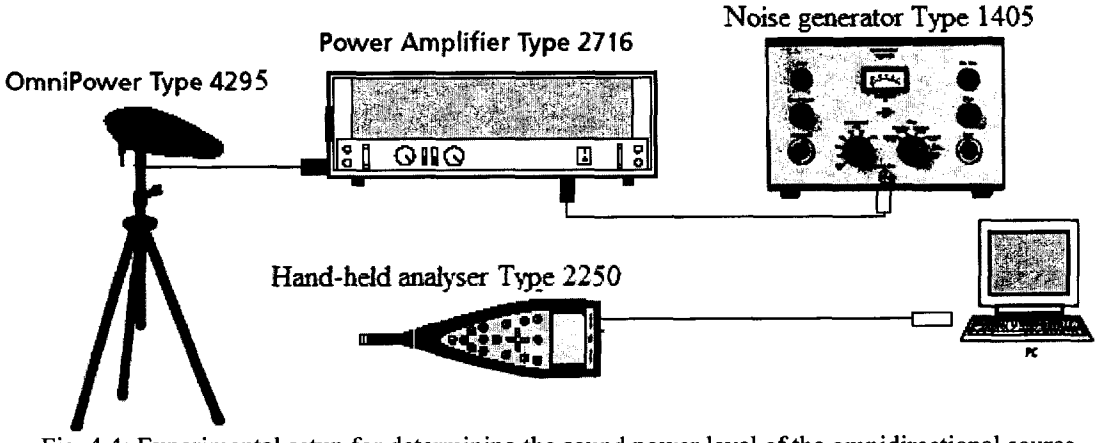

Fig. 4.4: Experimental setup for determining the sound power level of the omnidirectional source

Method II of the Acoustic Determinator software (Brüel and Kjaer 7816) is used to compute the sound power level of the source. This method determines the sound power level in a given sound direction and is usually used when the size of the source is considerably smaller than the measuring distance. The measuring distance should satisfy the following restrictions:

$R < 0.5\ Hb$;

$Hb + 0.05\ R \leq Hm \leq Hb + 0.2\ R$,

where:

R = distance between source and receiver

Hb = height of the source and

Hm = height of the receiver.

For distances less than 20 m, neglecting atmospheric absorption, Acoustic Determinator uses the following formula to compute the source's power level:

$$Lw = Lp + 10\log 4\pi R^2.$$

Sound pressure level measurements were carried out at 8 positions around the source at a distance R=0.5 m and at a height of Hm=1.4 m. The source height Hb was 1.35 m. Measured sound pressure levels and the sound power levels computed with Acoustic Determinator are found in Table 4.6. For each frequency, the average sound power level across the various locations was also computed (last row of Table 4.6).

	F1=250		F2=500		F3=1000		F4=2000		F5=4000	
	Lp[dB]	Lw[dB]	Lp[dB]	Lw[dB]	Lp[dB]	Lw[dB]	Lp[dB]	Lw[dB]	Lp[dB]	Lw[dB]
Pos1	84.2	89.2	78.9	83.9	77.4	82.4	81.9	86.9	82	87
Pos2	83.9	88.9	78.3	83.3	77.4	82.4	82.3	87.3	82	87
Pos3	83.8	88.8	79.7	84.7	77.8	82.8	82.1	87.1	81.8	86.8
Pos4	84	89	78.6	83.6	77.5	82.5	82.5	87.5	82	87
Pos5	84.9	89.9	79.7	84.7	78.8	83.8	85.5	90.5	88.9	93.9
Pos6	84.9	89.9	79	84	78.2	83.2	84.2	89.2	86.4	91.4
Pos7	83.5	88.5	78.5	83.5	76.8	81.8	81.3	86.3	80.2	85.2
Pos8	83.7	88.7	78.1	83.1	76.7	81.7	81	86	79.9	84.9
AVG		**89.1**		**83.8**		**82.5**		**87.6**		**87.9**

Table 4.6: Sound pressure level measured at 0.5 m from the omnidirectional source and corresponding sound power level computed using Acoustic Determinator.

4.4 Evaluation of "TestingLocator"

4.4.1 Measurements

The various source and workstation configurations used for this validation are shown in Figure 4.5. There are 5 source positions and 5 workstations. Only one source was operated at any given time. The sound power levels are listed in Table 4.6. Using the sound level meter, sound pressure levels at each workstation was measured using one octave band using the same measurement set up as is Figure 4.4. Results are listed in Table 4.7.

Sources	1/1Oct Hz	Workstations				
		W1	W2	W3	W4	W5
Source1	F1:250	78.6	79.2	76.2	75.7	76.4
	F2:500	69.4	71.8	67.2	67.1	65.9
	F3:1000	63.8	65.8	61.7	61.4	60.9
	F4:2000	72.7	70.9	70.4	67.2	69.5
	F5:4000	73.9	73.7	71.7	67.6	69.1
Source2	F1:250	77.8	78.3	78	80.9	78.1
	F2:500	68	70.3	69.9	70.1	69.4
	F3:1000	62.2	61.9	63.5	64	60.4
	F4:2000	72.1	70	68	68.8	67.8
	F5:4000	70	73.8	71.8	73.2	70.4
Source3	F1:250	76.1	76.6	76.3	81.3	78.9
	F2:500	67.5	66.2	70.9	73.9	70.6
	F3:1000	64	62.6	66.4	72.8	67.8
	F4:2000	68.8	68.7	72.6	79.1	73.2
	F5:4000	70.7	71.1	73.4	77.6	75.1
Source4	F1:250	79.2	80	83.1	83.1	82.8
	F2:500	72.7	71.8	74	73.2	76.7
	F3:1000	62.8	62.2	66	64.4	69.2
	F4:2000	67	68.4	68.3	71.5	72.5
	F5:4000	67.9	70.9	71.8	73.3	78.6
Source5	F1:250	79.9	80.8	78.9	76.8	78.6
	F2:500	69.4	71.2	68.8	65.7	67.3
	F3:1000	64.2	62.3	61.2	59.7	61
	F4:2000	74.7	73.7	69.7	67.6	73.6
	F5:4000	73.8	73.9	72	69.4	70

Table 4.7: Sound pressure level measurements (dB SPL) for each source-workstation configuration and in the real room.

4.4.2 Simulations

Simulations for the various source-workstation configurations (Figure 4.5) using "TestingLocator" were carried out for various settings of the late reverberation term (Eyring and None) and order of early reflections (0, 1, 2, and 3). The difference in sound pressure level predicted by "TestingLocator" and that measured using the sound level meter (Table 4.7) is found in Tables 4.8-4.11 for None late reverberation for orders 0 to 3, and in Table 4.12-4.15 for Eyring late reverberation for orders 0 to 3. For each frequency, the average difference for all the 25 arrangements (5 sources, 5 workstations) is presented. The average across all frequencies for 125 arrangements (5 sources, 5

workstations, 5 frequencies) is also computed. The measured reverberation time data (Table 4.4) is used for these predictions.

Finally, sound level predictions were also obtained based on the reverberation time data calculated from the various absorptive surface elements in the room (Table 4.2). Table 4.16 shows the difference in sound pressure level for Eyring with order 2 of early reflections and the measured values from the sound level meter for 125 configurations (5 sources, 5 workstations, 5 frequencies).

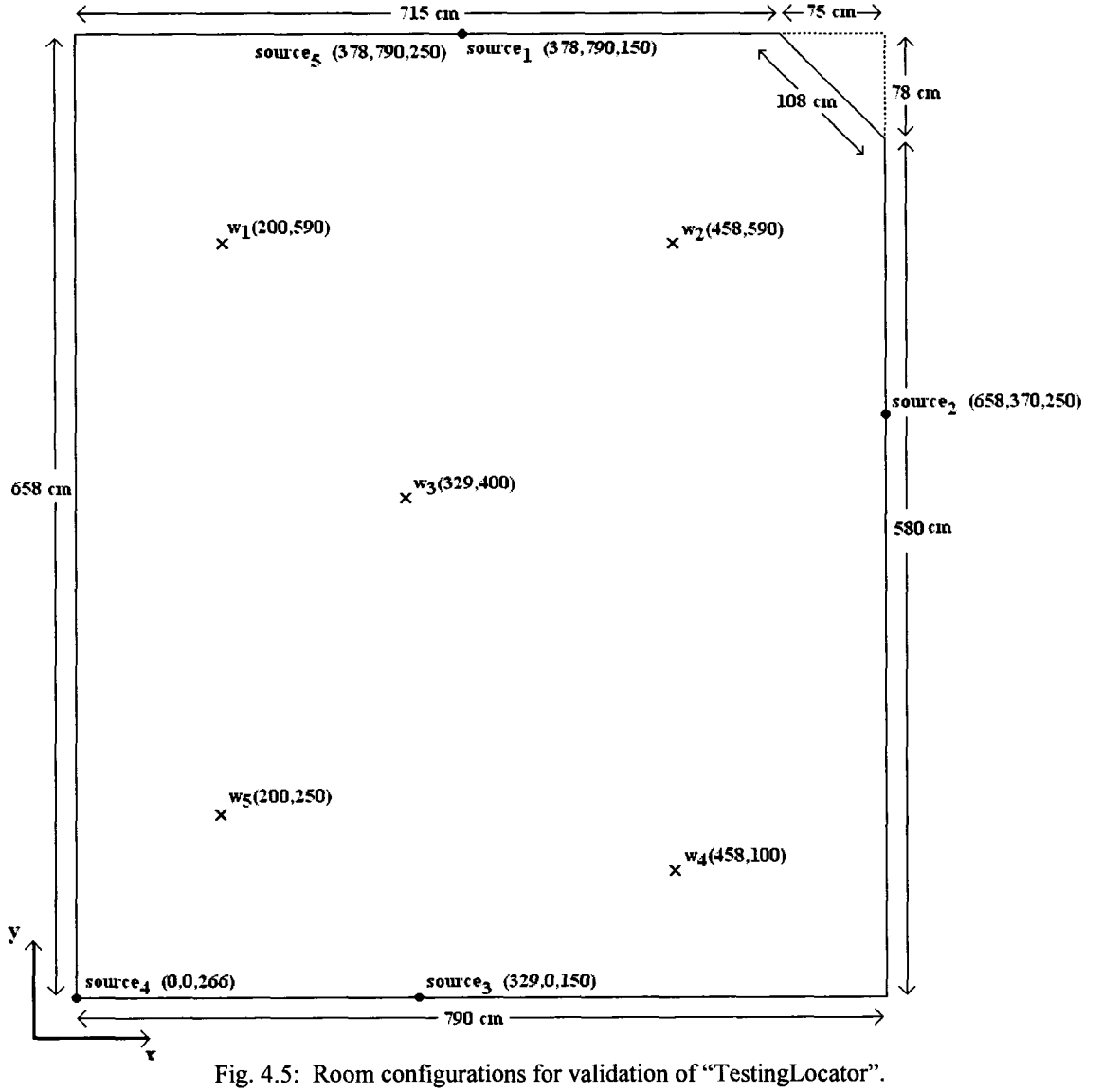

Fig. 4.5: Room configurations for validation of "TestingLocator".

	AVE [dB]	STDEV [dB]	N
F1=250 Hz	- 12.91	3.49	25
F2=500 Hz	- 9.31	3.48	25
F3=1000 Hz	- 4.34	2.88	25
F4=2000 Hz	- 6.22	2.52	25
F5=4000 Hz	- 7.44	2.11	25
ALL F	- 8.04	4.12	125

Table 4.8: Difference in sound pressure level between the solutions provided by "TestingLocator" for None with a zero order of early reflections and the measured values from the sound level meter for 125 configurations (5 sources, 5 workstations, 5 frequencies).

	AVE [dB]	STDEV [dB]	N
F1=250 Hz	- 6.94	3.61	25
F2=500 Hz	- 3.54	3.50	25
F3=1000 Hz	0.97	3.16	25
F4=2000 Hz	- 0.96	2.53	25
F5=4000 Hz	- 2.06	2.29	25
ALL F	- 2.51	4.03	125

Table 4.8: Difference in sound pressure level between the solutions provided by "TestingLocator" for None with a first order of early reflections and the measured values from the sound level meter for 125 configurations (5 sources, 5 workstations, 5 frequencies).

	AVE [dB]	STDEV [dB]	N
F1=250 Hz	- 4.27	2.77	25
F2=500 Hz	- 1.22	3.08	25
F3=1000 Hz	2.98	2.90	25
F4=2000 Hz	0.99	2.30	25
F5=4000 Hz	- 0.04	2.03	25
ALL F	- 0.31	3.56	125

Table 4.10: Difference in sound pressure level between the solutions provided by "TestingLocator" for None with a second order of early reflections and the measured values from the sound level meter for 125 configurations (5 sources, 5 workstations, 5 frequencies).

	AVE [dB]	STDEV [dB]	N
F1=250 Hz	- 2.94	2.44	25
F2=500 Hz	- 0.08	2.85	25
F3=1000 Hz	3.49	3.20	25
F4=2000 Hz	1.86	2.22	25
F5=4000 Hz	0.91	1.94	25
ALL F	0.65	3.32	125

Table 4.11: Difference in sound pressure level between the solutions provided by "TestingLocator" for None with a third order of early reflections and the measured values from the sound level meter for 125 configurations (5 sources, 5 workstations, 5 frequencies).

	AVE [dB]	STDEV [dB]	N
F1=250 Hz	- 0.30	2.12	25
F2=500 Hz	2.28	2.78	25
F3=1000 Hz	4.99	2.62	25
F4=2000 Hz	2.92	2.44	25
F5=4000 Hz	2.08	2.27	25
ALL F	2.39	2.96	125

Table 4.12: Difference in sound pressure level between the solutions provided by "TestingLocator" for Eyring with a zero order of early reflections and the measured values from the sound level meter for 125 configurations (5 sources, 5 workstations, 5 frequencies).

	AVE [dB]	STDEV [dB]	N
F1=250 Hz	- 0.32	2.19	25
F2=500 Hz	1.67	2.68	25
F3=1000 Hz	4.88	2.65	25
F4=2000 Hz	2.78	2.23	25
F5=4000 Hz	1.96	2.01	25
ALL F	2.20	2.88	125

Table 4.13: Difference in sound pressure level between the solutions provided by "TestingLocator" for Eyring with a first order of early reflections and the measured values from the sound level meter for 125 configurations (5 sources, 5 workstations, 5 frequencies).

	AVE [dB]	STDEV [dB]	N
F1=250 Hz	- 0.26	2.18	25
F2=500 Hz	1.71	2.71	25
F3=1000 Hz	4.90	2.68	25
F4=2000 Hz	2.82	2.20	25
F5=4000 Hz	2.00	1.96	25
ALL F	2.23	2.87	125

Table 4.14: Difference in sound pressure level between the solutions provided by "TestingLocator" for Eyring with a second order of early reflections and the measured values from the sound level meter for 125 configurations (5 sources, 5 workstations, 5 frequencies).

	AVE [dB]	STDEV [dB]	N
F1=250 Hz	- 0.24	2.17	25
F2=500 Hz	1.75	2.69	25
F3=1000 Hz	4.93	2.67	25
F4=2000 Hz	2.85	2.19	25
F5=4000 Hz	2.02	1.95	25
ALL F	2.26	2.86	125

Table 4.15: Differences in sound pressure level between the solutions provided by "TestingLocator" for Eyring with a third order of early reflections and the measured values from the sound level meter for 125 configurations (5 sources, 5 workstations, 5 frequencies).

	AVE	STDEV	N
F1=250 Hz	-2.34	2.29	25
F2=500 Hz	-0.31	2.81	25
F3=1000 Hz	2.90	2.75	25
F4=2000 Hz	0.70	2.19	25
F5=4000 Hz	-0.20	1.95	25
ALL F	0.15	2.93	125

Table 4.16: Differences in sound pressure level between the solutions provided by "TestingLocator" for Eyring with a second order of early reflections using the predicted reverberation times (Table 4.2) and the measured values from the sound level meter for 125 configurations (5 sources, 5 workstations, 5 frequencies).

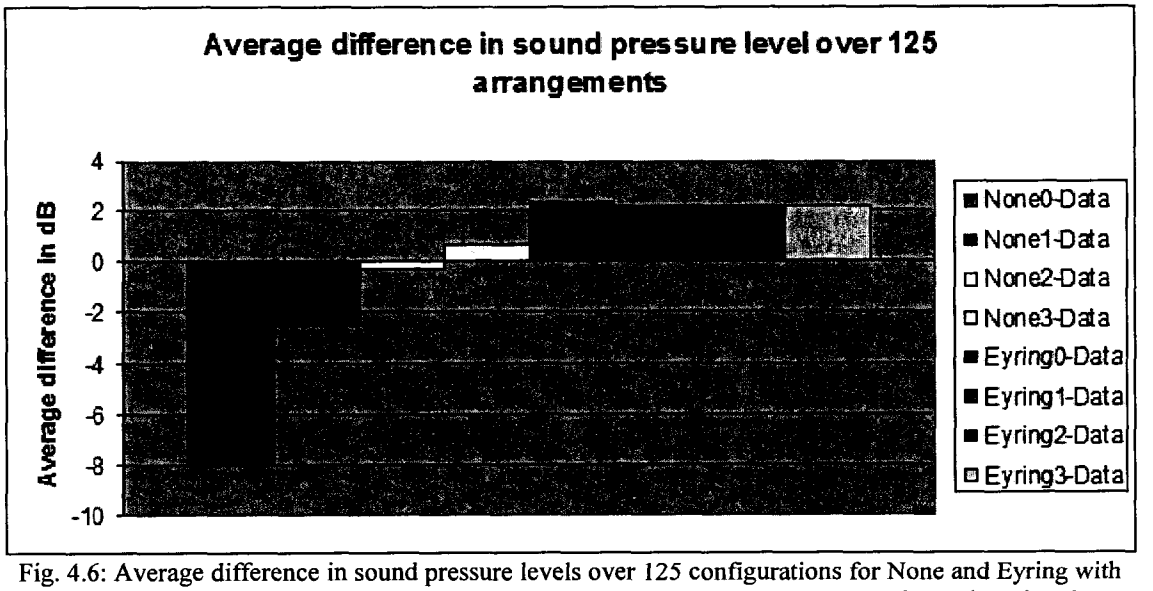

Fig. 4.6: Average difference in sound pressure levels over 125 configurations for None and Eyring with zero, first, second and third order of reflections based on simulations with measured reverberation times.

4.2.3 Discussion

The average difference in sound pressure levels over 125 configurations is displayed in Figure 4.6 for None and Eyring late reverberation terms with zero, first, second and third order of early reflections based on simulations with measured reverberation times.

As shown in Figure 4.6, when None with zero order of reflections is employed, an 8.04 dB underestimation occurs, which decreases to 0.31 dB by increasing the order of reflections to two. There is a slight overestimation of 0.65 dB for None with third order of reflections. When Eyring is used, an overestimation is noted for all orders of reflections, up to 2.39 dB for order 0. On the other hand, the standard deviation of error is lower with Eyring (2.86 - 2.96 dB) than None (3.32 – 4.12 dB) for all orders of reflections. The standard deviation values in Tables 4.8-4.15 express the dependence of the error on the position of the sources and workstations in the room. This spatial dependence is expected given the assumption of uniform sound absorption in the room using "AlarmLocator" or "TestingLocator", while the actual room under study has both highly reflective and highly absorbing surface elements (Table 4.1). The frequency content of the source is also a key factor. Indeed, simulations have demonstrated that the average error is significantly smaller when using a 250-Hz sound rather than 1000-Hz.

As shown in Table 4.16, "TestingLocator" solutions appear to be more precise when the predicted reverberation time data is used rather than the measured reverberation time data. For example, when using the predicted reverberation time, the error with Eyring late reverberation with a second order of early reflections is only 0.15 dB ± 2.93 dB compared to 2.23 dB ± 2.87 dB. Therefore, this tool needs to be validated over a wider range of different rooms in order to determine the best strategy to use to specify acoustic absorption in the room.

Overall, using Eyring late reverberation, the errors in estimation are relatively small compared to the "Detectsound" design window $[TL_{min}, TL_{max}]$ (13 dB) at each workstation. Typically, solutions from "AlarmLocator" are listed according to their efficiency deviations (in dB) from a target sound pressure level in the mid range of the window $[TL_{min}, TL_{max}]$. Therefore, the errors in estimation would not generally affect the decision outcome for alarm specifications; the sound pressure level at the workstation

would still be inside the design window, provided solutions with efficiency values better than 2-3 dB can be generated.

Chapter 5. Conclusions

In this thesis, a new software tool, referred to as "AlarmLocator", automates the process of installing auditory warning devices in a given setting, in terms of the characteristics of the devices to use and their optimal location in the plant. The software tool, when use in combination with psychoacoustic model "Detectsound" (Zheng, 2003; Zheng et al., 2006), produces a solution to two practical installation problems: (1) selecting a suitable number of warning devices and acoustic power for a given work area, and (2) specifying the location of the devices in the plant in such a way that the signals emitted are clearly audible by all workers at all workstations. Thus, a solution to the problem of installing warning devices is provided in a format that can be easily understood and used in the workplace.

"AlarmLocator" accounts for the sound propagation of auditory warning signals from the physical device location (on walls) to the position of individual workers or workstations. In contrast to prior work (Nanthavanij & Yenrades, 1999), both the direct and reverberant fields from the alarm devices are considered. "AlarmLocator" provides solutions for multiple frequencies. It accounts for up to five different alarm frequencies presented separately or simultaneously. An associated tool, "TestingLocator" has been created as an option in "AlarmLocator". This tool is useful for testing alarm configurations at specific locations in a given room for debugging or verification purposes.

A simple hybrid method, combining the mirror image technique and the classical room acoustics theory was used in this research to compute the sound pressure level generated by acoustic alarm devices. The former technique accounts for wall-placement directivity effects by using a relatively low order of virtual sources to simulate early reverberation. The classical theory of room acoustics is adapted to incorporate the late reverberation. The method only requires specification of the overall room dimensions and the estimated or measured reverberation time; however, it is currently limited to rectangular-shaped rooms. It can be easily calibrated to the actual room under study; that is the average absorption coefficient used in the model can be based on an actual measurement in the real room instead of being calculated from database acoustical materials.

An exhaustive scanning algorithm is employed in this research to check all possible solutions. The result is the optimum number, location and power level of acoustic warning devices. The proposed method is a compromise between accuracy, ease of use and the requirement for simulating a large number of source-receiver configurations in the warning device optimization process. Currently, spatial grid and power level step sizes must be specified by the user and this may require a certain amount of testing and experimentation with the software for each particular case. Future implementations may consider optimization methods that automatically find solutions without the need to specify grid and/or step sizes.

This sound level prediction method was validated in room 3031 of Roger Guidon Hall, University of Ottawa, to verify that "AlarmLocator" could provide realistic solutions of optimal installation of acoustic warning devices in the workplace. The validation illustrates the effectiveness of "AlarmLocator". An average error over 125 arrangements (source, receiver, frequency) of 2.2 dB was found (standard deviation of 2.9 dB) when acoustic absorption was based on measured reverberation time while the average error was 0.15 dB (standard deviation of 2.9 dB) when based on predicted reverberation time. In either case, the error is considered small compared to the size of the "Detectsound" design window (13 dB) at each workstation. Such an error in estimation does not affect the decision outcome; the sound pressure level at the workstation would still be inside the design window, unless the efficiency of the solution is poor. This tool needs to be validated in rooms of different sizes and absorption characteristics to assure its acoustic accuracy. For best installation, when a solution is generated from "AlarmLocator", verification by sound measurement equipments is preferably required to ensure efficiency of the audibility of warning devices at the desired workstations in the workplace.

"AlarmLocator" coupled with "Detectsound" thus provide an optimized solution to the complex problem of efficiently installing warning devices in a noisy work plant. To date, acoustic warning signals have been installed using intuitive techniques with little considerations to the issues contributing to an efficient use. In this research, a method for predicting the number, location and power level of warning devices is available to help stakeholders in occupational health and safety make informed decisions regarding the purchase and installation of warning devices. It could help decrease the risk of accidents

due to failure to react to danger situations, and prevent auditory trauma and startle reflex reactions resulting from overly loud signals. This work will also contribute to new knowledge and insight into the optimal design and operation of warning devices in the workplace, which will be directly relevant to device manufacturers and standardization organizations. It is hoped that the general modeling framework offered by "Detectsound" and "AlarmLocator" will lead to more valid and accurate solutions for the installations.

In the future, the "AlarmLocator" model can be further improved by considering rooms with irregular boundaries shapes (L'Espérance, (2000); Borish, (1984)). Since the algorithm for "AlarmLocator" assumes the warning devices to be omnidirectional sources, "AlarmLocator" can also be expanded to include directional sources in the future. In the meantime, it is recommended to verify final solutions provided by "AlarmLocator" with sound level measurement equipments once alarm devices are installed in a real environment. Finally, it also needs to be tested with "Detectsound" in subjective experiments in real workplaces to ensure that the solutions are not only acoustically accurate but warning sound levels are judged to be clearly audible by listeners (Annex B ISO 7731).

References

1. ANSI S1.6-1984 (R2006). American National Standard Preferred Frequencies, Frequency Levels, and Band Numbers for Acoustical Measurements
2. Allen, J.B., Berkley, D.A., (1978). Image method for efficiently small room acoustics. Acoustics Research Department, Bell Loboratories, Murrat Hill, New Jersey.
3. Al Osman, R., Giguère, C. & Laroche, C., (2006). "Optimal installation of acoustic warning devices in the workplace", IEA 16th World Congress on Ergonomics, Maastricht, Netherlands.
4. Berglund, B., Lindvall, T., Schwela, D.H., Goh, K.-T. (EDs) (2000). Guidelines for Community Noise (Institute of Environmental Epideiology, Singapore and World Health Organisation, Geneva), 138pp.
5. Beranek, L., Vér L.I., (1992). Noise and vibration control engineering principles and applications. United States of America.
6. Beranek, L., (2004). Concert halls and opera houses. United States of America.
7. Borish, J., (1984). "Expansion of the image model to arbitrary polyhedra". J. Acoust. Soc. Am., 75(6), 1827-1836.
8. Brüel & Kjaer., (1988). Measurements in Buildings Acoustics. Denmark.
9. CSA Z107.52 (M1983). "Recommended Practice for the Prediction of Sound Pressure Levels in Large Rooms Containing Sound Sources." Canadian Standards Association, Rexdale, ON.
10. CSA Z94.2-02 (2002). "Hearing Protection Devices – Performance, Selection, Care, and Use," Canadian Standards Association, Toronto, ON.
11. Fischetti, A., (2003). Initiation à l'acoustique. Belin, Paris.
12. Foreman, J.E.K., (1990). Sound analysis and noise control. United States of America.
13. Ghering, W.L., (1978). Reference data for acoustic noise control. United States of America.

14. Giguère, C., Laroche, C., Zheng, Y., and Sabourin, C., (2003). A warning sound perception model software. 8th Int. Congress on Noise as a Public Health Problem, Rotterdam, Netherlands, pp. 80-81.
15. Harris, C.M., (1979). Handbook of noise control. United States of America.
16. Hétu, R., and Tran Quoc, H., (1994). "Validation of masked threshold predictions among people with sensorineural hearing loss," Canadian Acoustics, 22(3), 83-84.
17. Irwin, J.D., Graf, E.R., (1979). Industrial noise and vibration control. (Englewood Cliffs, New Jersey 07632).
18. ISO 10534-1., (1996). Acoustics -- Determination of sound absorption coefficient and impedance in impedance tubes -- Part 1: Method using standing wave ratio (International Organization for Standardization, Geneva).
19. ISO 10534-2., (1998). Acoustics -- Determination of sound absorption coefficient and impedance in impedance tubes -- Part 2: Transfer-function method (International Organization for Standardization, Geneva).
20. ISO 354., (2003). Acoustics -- Measurement of sound absorption in a reverberation room (International Organization for Standardization, Geneva).
21. ISO 7731., (2003). Ergonomics -- Danger signals for public and work areas-Auditory danger signals (International Organization for Standardization, Geneva).
22. Jensen, J.L., (1995) Saddlepoint approximations. Oxford, New York.
23. Khars, M., Bradenburg, K., (1998). Applications of digital signal processing to audio and acoustics. United States of America.
24. Laroche, C., Hétu, R., L'Espérance, A. (1991b). "Des alarmes de recul qui tuent!," Travail et Santé, 7: 9-13.
25. Laroche, C., Josserand, B., Tran Quoc, H., Hétu, R., and Glasberg, B.R. (1992). "Frequency selectivity in workers with noise-induced hearing loss," Hearing Research 64: 61-72.
26. L'Espérance, A., (2000). Hybrid image/energy approach for acoustical predictions of industrial rooms. Canadian acoustical association. Sherbrooke, Canada.
27. Miller, R.E., (2000) Optimization: foundations and applications. New York, Wiley.

28. Nanthavanij, S., Yenrades, P., (1999). Predicting the optimum number, location, and signal sound level of auditory warning devices for manufacturing facilities. Int. J. of Industrial Ergonomics 24: 569-578.
29. Ostergaard, P.B., (2000). "Physics of sound and vibration," Chapter 2 in E.H. Berger, L.H. Royster, J.D. Royster, D.P. Driscoll, M. Layne (Eds.): The Noise Manual, Fifth Edition (American Industrial Hygiene Association, Fairfax VA).
30. Robinson, G.S., and Casali, J.G., (2000). "Speech communications and signal detection in noise," Chapter 14 in E.H. Berger, L.H., Royster, J.D., Royster, D.P., Driscoll, M., Layne (Eds.): The Noise Manual, Fifth Edition (American Industrial Hygiene Association, Fairfax VA).
31. Suter, A.H., (June 1989). The effects of hearing protectors on speech communication and the perception of warning signals (Technical Memorandum 2-89), U.S, Army Human Engineering Laboratory.
32. Suter, A., (2002). Hearing conservation Manual, Fouth Edition (Council for Accreditation in Occupational Hearing Conservation, Milwaukee USA), 312 pp.
33. Tran Quoc, H., Hétu, R., and Laroche, C. (1992). "Computerized assessment and prediction of the audibility of sound warning signals for normals and hearing-impaired individuals", in M. Matilla and W. Karwowski (eds.), Computer applications in ergonomics occupational safety and health (Elsevier, Amsterdam), pp. 105-112.
34. Ward, W.D., Royster, L.H. and Royster, J.D. (2000). "Anatomy and physiology of the ear: Normal and Damaged Hearing," Chapter 4 in E.H. Berger, L.H., Royster, J.D., Royster, D.P., Driscoll, M., Layne (Eds.): The Noise Manual, Fifth Edition (American Industrial Hygiene Association, Fairfax VA).
35. White, R.E., (2004) Computational mathematics: models, methods, and analysis with MATLAB and MPI. Boca Raton, Chapman & Hall/CRC.
36. Wilkins, P.A., and Acton, W.I., (1982). "Noise and Accidents - A Review", Ann. Occup. Hyg., 25, 249-260.
37. Zheng, Y., (2003) Development of new Detectsound: A Computerized Model for Adjusting the Level of Acoustic Warning Signalization in the Workplace. Master's Thesis in Systems Science, University of Ottawa

38. Zheng, Y., Giguère, C., Laroche C., et al., (2006). "A psychoacoustic model for specifying the level and spectrum of acoustic warning signals in the workplace". J. Occup. Environ. Hyg. (in press).